ANALYSIS OF THE CELL JUNCTION PROTEINS CASK AND CLAUDIN-5 IN SKELETAL AND CARDIAC MUSCLE

DISSERTATION

Presented in Partial Fulfillment of the Requirements for the Degree Doctor of Philosophy in the Graduate School of The Ohio State University

By

Jamie Lynn Sanford, B.S.

The Ohio State University

2005

Dissertation Committee:

Professor Jill A. Rafael-Fortney, Advisor

Professor Arthur Burghes

Professor Mark Parthun

Professor Christine Beattie

Approved by

_____

Advisor
Molecular, Cellular and Developmental Biology Graduate Program

ABSTRACT

Cell junctions are defined as specialized connections found between two adjacent cells or between a cell and the surrounding extracellular matrix. There are three basic types of cell junctions, known as occluding junctions, anchoring junctions and communicating junctions. These junctions are responsible for regulating diffusion, linking adjacent cells and transmitting electrical or chemical signals, respectively. In this dissertation, we examine the *in vivo* functions of two cell junction proteins, CASK (Ca^{2+}/calmodulin associated serine/threonine kinase) and Claudin-5. CASK is a member of the membrane associated guanylate kinase (MAGUK) family of proteins and is present in epithelial cells and central nervous system (CNS) synapses. Claudin-5 is a protein that has been most thoroughly characterized as a component of tight junctions, an occluding junction, at endothelial cells of the blood-brain barrier. This dissertation describes investigations of the CASK protein in skeletal muscle at the neuromuscular junction (NMJ) and Claudin-5 in cardiomyocytes

We show that the CASK protein is present in skeletal muscle and is specifically localized to the NMJ, as determined by both western and immunohistochemical analysis. Confocal microscopy analysis revealed that CASK is predominantly localized to the

primary gutter of the postsynaptic membrane at the NMJ. However, a small amount of CASK is also present presynaptically. In an effort to determine *in vivo* binding partners for CASK in skeletal muscle, we performed immunoprecipitations from total skeletal muscle protein homogenates. These immunoprecipitations revealed that CASK interacts with the Dlg protein, another MAGUK protein present at the NMJ. We next examined the expression and localization of the CASK protein in the C2C12 mouse myogenic cell line and found that CASK expression is developmentally regulated. In C2C12 myoblasts, CASK is localized almost exclusively to the nucleus. As myoblasts fuse to form multinucleated myotubes, CASK protein moves from the nucleus to the cytoplasm. Western analysis confirmed that this change in CASK protein localization is not accompanied by a change in CASK isoform expression. In order to assess possible mechanisms of CASK recruitment to acetylcholine receptor (AChR) complexes at the NMJ, we treated C2C12 myotubes with agrin and laminin, two trophic factors known to cluster AChRs. Interestingly, neither CASK, nor Dlg, is clustered with AChRs in response to treatment with either agrin or laminin. Finally, further delineation of the CASK protein function in skeletal muscle was achieved through the generation of two transgenic mouse models of the CASK protein in skeletal muscle, termed CASK F.L. and CASKΔ which overexpress a full-length version and a truncated version of the CASK protein, respectively. This study is the first to use transgenic mouse models to examine CASK protein function in skeletal muscle. Basic histological experiments, paired with

physiological experiments, revealed that overexpression of either the full-length or truncated CASK protein does not result in any gross morphological or functional abnormalities. As CASK is normally expressed at the NMJ, we also conducted a thorough examination of NMJ morphology and size in both lines of CASK transgenic mice. Immunofluorecence analysis revealed that the morphology and size of the NMJ are unaltered in both CASK F.L. and CASKΔ mice. However, immunlocalization studies of the CASK protein at the NMJ in both lines of transgenic mice revealed that overexpression of the full-length or truncated CASK protein results in a loss of CASK protein on the presynaptic side of the NMJ. We also examined whether Dlg protein expression or other CASK candidate interactors exhibit any localization changes in either line of transgenic mice. Immunofluorescent examination of Dlg, along with the candidate interactors Kir 2.2, Kir 2.3, ErbB4, syndecan-3 and NR2A, demonstrated that these proteins are not altered in CASK F.L. or CASKΔ mice.

This dissertation also details an examination of the Claudin-5 protein in cardiac muscle from wild-type mice and two mouse models of cardiomyopathy. We show via western and immunohistochemical analysis that the Claudin-5 protein is present in normal cardiac muscle and is specifically localized to the lateral membranes of cardiomyocytes. As remodeling of cell junction proteins has recently been associated with dilated cardiomyopathy, we also examined Claudin-5 localization and expression in *mdx* (dystrophin deficient) and dko (utrophin/dystrophin-deficient, double knockout)

mice. *Mdx* and dko mice are two mouse models of Duchenne muscular dystrophy that exhibit cardiomyopathy, in addition to their skeletal muscle pathology. We showed that Claudin-5 protein expression and localization is unaltered in hearts from *mdx* mice, as compared with hearts from normal mice. Conversely, Claudin-5 mRNA and protein levels are downregulated in dko hearts. Examination of other cell junction proteins present at the intercalated disc, including cadherins, catenins and ZO-1, are unaltered in the hearts of dko mice. Ultrastructural analysis demonstrated that the lateral membranes of dko mice exhibit an abnormal wavy appearance, while the lateral membranes of *mdx* mice appear normal. These experiments demonstrated that the cardiomyopathy of dko mice is associated with a breakdown of the lateral membranes of cardiomyocytes.

ACKNOWLEDGMENTS

It is virtually impossible to truly express my gratitude to all of those who have helped me throughout my time in graduate school, but I will start by thanking my advisor, Dr. Jill Rafael-Fortney, who has not only provided support in every aspect of my graduate career, but most importantly, has supported my decisions beyond those made in the lab, for that I am forever indebted. Of course, I would also like to thank all the members of the Rafael lab, for all of their help, on a daily basis. Having people to talk with during the day, about even the silliest of subjects, is a benefit of working in the lab that I am most grateful for, so thank you to Hilary, Don, Jess, Katie, Pat, Jon, and Tess. A special thanks to Jon Edwards, who provided me with more hands-on assistance than anyone by endlessly cutting sections. And to Wendy, what can I say, there are no words.

Thanks also to my committee members for their help and time.

I would also like to thank the people at Ohio State who have provided me with any technical assistance over the years, especially the Campus Microscopy and Imaging Facility, for all of their help with the confocal microscope and ultrastructural analysis. Thank you to Dr. Paul Janssen for all of his help with the physiology studies. Thanks

also to Dr. John Porter for his assistance with microarray analysis and NMJ ultrastructural analysis. Thank you to Dr. JoAnna Wilson and her laboratory for the full-length CASK cDNA.

Thanks to all my family members, especially my Mom and Dad and Grandma and Grandpa Siders. Zach, thanks for the optimism. To all my friends from graduate school, thanks for the fun.

Finally, thanks to my two best friends. To Ellen, thanks for the wake-up calls. To my husband Dan, I simply couldn't have done this without you.

VITA

1999-present……Graduate Student, Molecular, Cellular and Developmental Biology, The Ohio State University, Department of Molecular and Cellular Biochemistry

June, 1999……B.S. Biology, Elmira College, Elmira, NY

September-December, 2000……Teaching Assistant; Biology 101; The Ohio State University

March-June, 2001……Teaching Assistant; Biology 101; The Ohio State University

2000-2002……Secretary/Treasurer, Graduate Student Organization for Molecular, Cellular, Developmental Biology Graduate program

PUBLICATIONS

Research Publications:

1. Sanford, J. L., Mays, T. A., and Rafael-Fortney, J. A. (2004). CASK and Dlg form a PDZ protein complex at the mammalian neuromuscular junction. Muscle Nerve *30*, 164-171.

2. Sanford, J.L., Edwards, J.D., Mays, T.A., Gong, B., Merriam, A.P., and Rafael-Fortney, J.A. (2005). Claudin-5 localizes to the lateral membranes of cardiomyocytes and is altered in utrophin/dystrophin-deficient cardiomyopathic mice. Journal of Molecular and Cellular Cardiology *38*, 323-332.

FIELDS OF STUDY

Major Field: Molecular, Cellular, and Developmental Biology

TABLE OF CONTENTS

LIST OF TABLES

Table Page

LIST OF FIGURES

LIST OF ABBREVIATIONS

AChR, acetylcholine receptor; β-DG, β-dystroglycan; CASK, Ca^{+}, Calmodulin-associated serine/threonine kinase; CNS, central nervous system; DCM, dilated cardiac myopathy; Dko, double knockout; Dlg, Discs Large; GK, guanylate kinase; IP, immunoprecipitation; DMD, Duchenne muscular dystrophy; MAGUK, membrane associated guanylate kinase; MDCK, Madin-Darby canine kidney; *mdx*, muscular dystrophy on the x chromosome; NLS, nuclear localization signal; NMDA, N-methyl-D-aspartate; NMJ, neuromuscular junction; SH3, Src homology 3.

INTRODUCTION

Cell Junctions

Cell junctions can be divided into three basic categories based on their functional characteristics: occluding junctions, anchoring junctions and communicating junctions. Occluding junctions, as their name suggests, are responsible for sealing cells to one another, thereby forming a barrier that regulates diffusion. They are most prevalent in simple and stratified epithelia and endothelial cellular sheets and are typified by the tight junction. Tight junctions are generally found at the basolateral membrane of epithelial cells, regulating intercellular and paracellular transport of molecules between cells and aiding in the establishment of cell polarity (for Reviews see (Lapierre, 2000; Matter and Balda, 2003a; Matter and Balda, 2003c; Tsukita et al., 2001)). Molecularly, tight junctions are composed of claudin protein family members, as well as occludins and various adhesion molecules. The second category of cell junctions are known as anchoring junctions and serve as a mechanical link between the cytoskeleton and adjacent cells and/or the extracellular matrix, allowing the given group of cells to operate as a single entity (Farquhar and Palade, 1963; Perez-Moreno et al., 2003; Wheelock and Johnson, 2003a; Wheelock and Johnson, 2003b). Adherens junctions are the most common type of anchoring junction, consisting of cadherin and catenin protein family

members that provide a link between the actin filaments in the cytoplasm of adjacent cells (Perez-Moreno et al., 2003; Wheelock and Johnson, 2003a; Wheelock and Johnson, 2003b). Desmosomes are a second type of anchoring junction that form discrete points of attachment by indirectly linking intermediate filaments of adjacent cells. Cadherins, plakins and armadillo proteins are the major constituents of desmosomes, providing attachment to the intermediate filaments (Getsios et al., 2004; Wheelock and Johnson, 2003a; Wheelock and Johnson, 2003b). Generally speaking, anchoring junctions are found in any cell type that is subject to intense mechanical stress including both epithelial and non-epithelial cell types (including smooth and striated muscle). The final category of cell junctions, the communicating junction, is perhaps the most diverse of the intercellular junctions. Communicating junctions assist in the transmission of electric or chemical signals across the intercellular space of two adjacent cells. The two primary communicating junctions are gap junctions and chemical synapses. Gap junctions connect the membranes of two cells at discrete points, forming a uniform "gap". This gap is transduced by members of the connexin protein family, forming a pore or channel that joins the intercellular space of the two cells (Farquhar and Palade, 1963; Wei et al., 2004). The regulatory properties of the gap junction can vary between cell types depending on the distinct connexin subunits that comprise a given gap junction (Wei et al., 2004). Chemical synapses are unequivocally the most complex and specialized of all the cell junctions, encompassing both central and peripheral nervous system synapses, including the neuromuscular junction (NMJ).

The work of this dissertation is to examine the *in vivo* biological and physiological role of two cell junction proteins, CASK and claudin-5, in skeletal muscle and cardiac muscle, respectively. CASK is a very diverse molecule that has been thoroughly investigated in epithelial cells and synapses in the central nervous system (Butz et al., 1998; Hata et al., 1996a; Hoskins et al., 1996; Kaech et al., 1998). The bulk of the experimentation on CASK function, including interacting partners, has been elucidated via *in vitro* biochemical experiments. The work of this thesis is to examine CASK protein function at the neuromuscular synaptic junction, a communicating cell junction formed between the motor neuron and the skeletal muscle fiber. Claudin-5, a member of the claudin protein family, is a transmembrane protein that is a major structural component of tight junctions, including those of endothelial cells of the blood brain barrier (Morita et al., 1999b; Nitta et al., 2003). We examine the role of claudin-5 protein in cardiomyocytes, focusing on its expression and localization in normal and cardiomyopathic hearts. Overall, this work marks the first, thorough *in vivo* investigations into both CASK and claudin-5 at the neuromuscular junction and cardiomyocytes, respectively.

The CASK protein domain structure

The mammalian CASK (Ca2+/Calmodulin serine/threonine kinase) gene was first cloned from a yeast two-hybrid screen searching for binding partners of the neuronal cell surface protein, neurexin (Hata et al., 1996b). Neurexins are post-synaptic cell surface adhesion proteins that aid in the formation of the synaptic intercellular junction via their interactions with pre-synaptic neuroligins (Ichtchenko et al., 1996; Ushkaryov et al.,

1992). Concurrently, the CASK protein was also identified and characterized in both *Drosophila* and *Caenorhabditis elegans* (*C. elegans*). The *C. elegans* homologue of CASK, termed Lin-2, was initially discovered in a genetic screen searching for genes involved in vulval development (Ferguson and Horvitz, 1985; Hoskins et al., 1996). CASK/Lin-2 was found to be required for the activation of a RAS signaling pathway that leads to vulval induction. The domain structure of this newly identified protein was found to be similar to that of what is now known as the membrane associated guanylate kinase (MAGUK) protein family. In fact, the *Drosophila* homologue of CASK, CamGuk, was found in a search for fly MAGUKs (Dimitratos et al., 1997). MAGUKS are an extensively studied family of modular adaptor proteins, consisting of one to three amino (N)-terminal PDZ domains, an SH3 domain and a guanylate kinase domain (Anderson, 1996; Caruana and Bernstein, 2001; Fanning and Anderson, 1999; Hata et al., 1996a). Occasionally, these MAGUKs also contain an L27 domain located carboxy (C)-terminal to the PDZ domain and a HOOK (or Hinge) region located between the SH3 and GK domain (Cohen et al., 1998; Doerks et al., 2000; Feng et al., 2004; Lue et al., 1994a; Marfatia et al., 1995; Marfatia et al., 1996). The CASK protein is unique in that it also contains an N-terminal sequence similar to Ca^{2+}/Calmodulin protein kinase, termed the CaMK like domain (Hata et al., 1996b). Hence the protein was named Ca^{2+}/calmodulin associated serine/threonine kinase (CASK) and was the first protein identified to contain this unique combination of domains (Dimitratos et al., 1997; Hack et al., 1998; Hata et al., 1996b). It is the novel combination of domains contained in CASK, and other MAGUK protein family members, which makes them particularly well-suited to function as scaffolding and stabilizing molecules at various types of cell junctions. It allows these

molecules to anchor signaling complexes, which is essential for maintaining cell polarity and facilitating signal transduction. A brief discussion of the molecular properties of each domain, the PDZ domain, the L27 domains, the SH3, HOOK and GK domain, along with the CaMK domain, demonstrates the diversity of the CASK protein, and provides a necessary foundation for understanding its fundamental molecular nature.

The PDZ domain was first discovered as a 90 amino acid repeat in the synaptic junction protein, PSD-95, the *Drosophila* protein Discs Large (Dlg) and the tight junction protein, Zo-1; the PDZ domain was named after these first three proteins found to contain the domain. Initially, PDZ domains were termed DHR domains, for Dlg homologous region, and/or GLGF repeat, due to an Gly-Leu-Gly-Phe amino acid repeat conserved within the PDZ domain (for reviews see (Craven and Bredt, 1998; Fanning and Anderson, 1999; Garner et al., 2000; Hata et al., 1998; Ponting et al., 1997)). The crystal structures for a variety of PDZ domains are solved, elucidating the structure and binding properties that characterize this domain (Daniels et al., 1998; Doyle et al., 1996; Fuh et al., 2000; Morais Cabral et al., 1996; Songyang et al., 1997). Overall, the PDZ domain is composed of two alpha helices and six beta sheets which fold to form a beta sandwich. Ligands for PDZ domains contain a consensus sequence that binds to an area between the second beta sheet and the second alpha helix, known as the "carboxylate binding loop", which contains the GLGF repeat. The C-termini of PDZ domain ligands bind as antiparallel beta strands within this binding loop (Doyle et al., 1996). In fact, classification of PDZ domains into three subtypes is based on the C-terminal consensus motifs of their ligands. Class I PDZ domains bind to C-terminal consensus motifs X-

ser/thr-X-val-COOH, where X represents any amino acid (Doyle et al., 1996). Class II PDZ domains, first identified via the crystal structure of the hCASK protein, bind preferentially to C-terminal motifs ending in X-Phe/Tyr-X-Phe/Val/Ala-COOH, or more simply, X-Φ-X-Φ, where Φ represents any hydrophobic amino acid (Daniels et al., 1998; Im et al., 2003a). Finally, the most recently identified Class III PDZ domains, bind to X-P/E-X-Φ consensus motifs (Maximov et al., 1999). It seems that the -2 amino acid residue is the critical determinant for classification, as the side chain of the -2 amino acid interacts with the beta helix in the PDZ domain; class I PDZ domains prefer a serine or threonine residue at this -2 position, while class II and III prefer a hydrophobic and negatively charged residue at this position, respectively (Maximov et al., 1999). Further specificity of PDZ domains for their ligands also appears to be conferred by residues outside the core consensus motif at residues from the -3 to -8 position. Moreover, there is recent evidence to suggest that PDZ domains can also bind internal sequences if the secondary structure of these internal amino acids resembles that of a free C-terminus (Garner et al., 2000).

PDZ domain-containing proteins that localize to synapses have been most intensively examined in the central nervous system. A vast number of channel and receptor ligands have been discovered primarily via *in vitro* biochemical experiments (for Reviews see (Craven and Bredt, 1998; Fanning and Anderson, 1999; Garner et al., 2000; Hata et al., 1998; Ponting et al., 1997)). The PDZ domain of PSD-95 protein has demonstrated the ability to bind to both the NMDA and kainate receptors, two types of glutamate receptors (Kim et al., 1996; Kim et al., 1995; Kornau et al., 1995; Muller et al., 1996; Nagano et

al., 1998). AMPA-type glutamate receptors have also been shown to bind the PDZ domain of Dlg/SAP97 in CNS synapses (Amalfitano et al., 1997; Cai et al., 2002; Leonard et al., 1998; Rumbaugh et al., 2003; Sans et al., 2001). Perhaps the most significant contribution of the PDZ domain is its ability to cluster these channels and receptors at points of intercellular contact (Kim et al., 1995; Tejedor et al., 1997). This capability is facilitated by the fact that PDZ domains can homo- or heterodimerize to each other, promoting scaffold formation (Im et al., 2003a; Im et al., 2003b; Kim et al., 1996). Furthermore, many PDZ domain-containing proteins, including MAGUKs, often include additional protein-protein interaction domains that help in stabilizing these receptor proteins at discrete membrane locations. Studies of the PDZ domain-containing protein, Dlg, demonstrated a direct role for PDZ domains in clustering channels *in vivo* at the *Drosophila* larval NMJ (Tejedor et al., 1997). Tejador et. al. demonstrated that Shaker-type potassium channels interact with PDZ domains 1 and 2 of Dlg *in vitro*, while co-transfection studies revealed that when these proteins are co-expressed in heterologous cells, it results in a redistribution of both proteins from diffuse intracellular locations to compact clusters at the cell surface. *In vivo*, an allele of a Shaker-type potassium channel containing a mutation in its C-terminal sequence resulted in the channel being localized around the entire membrane, rather than in clusters, while Dlg localization remained normal (Tejedor et al., 1997). In addition, examination of a variety of different Dlg mutants revealed that Dlg participates in the localization of Shaker-type potassium channels to the proper cellular location (Tejedor et al., 1997).

The SH3 (src homology 3) and GK (guanylate kinase) domain are two well characterized protein-protein interaction domains present in tandem in all MAGUK proteins. The SH3 domain was initially described in varying signaling molecules, including Src family members and Crk adaptor proteins (Reviewed in (Buday, 1999; Mayer, 2001; Pawson and Scott, 1997)). This domain is a relatively small domain, 60 amino acids in size, and has not been found to possess any catalytic activity in MAGUKs (Mayer, 2001). Typically, the domain consists of a flat hydrophobic surface for ligand binding (Kay et al., 2000; Mayer, 2001). Proteins that bind to SH3 domains usually have a left handed helix, containing a PXXP consensus motif (Buday, 1999). GK-like domains were named for their sequence similarity to yeast guanylate kinases. However, crystal structures of the GK domain of MAGUKs demonstrate that it lacks guanine and ATP binding residues and therefore does not boast any kinase activity (Kuhlendahl et al., 1998; McGee and Bredt, 1999; Olsen and Bredt, 2003). The guanylate kinase domain of MAGUKs have been shown to bind a variety of different proteins, including the microtubule associated protein 1A (MAP1A) and a guanylate kinase associated kinesin (GAKIN), as well as guanylate kinase associated proteins (GKAPs) (Brenman et al., 1998; Hanada et al., 2000; Kim et al., 1997; Nahirney and Ovalle, 1993; Naisbitt et al., 1997; Wu et al., 2000). However, the most notable interacting partners of the GK and SH3 domains are each other.

Recently, various studies have found that the SH3 and GK domains can interact intramolecularly, as well as intermolecularly (MacLennan and Edwards, 1990; McGee and Bredt, 1999; McGee et al., 2001; Nix et al., 2000; Shin et al., 2000; Tavares et al.,

2001). One particularly pertinent study demonstrated that the SH3 and GK domains of CASK and Dlg could interact in both an intra- and intermolecular fashion (Nix et al., 2000). The finding was especially interesting considering the GK domain does not contain a PXXP motif. Crystal structure determinations of these two domains determined from the PSD-95 protein revealed that these two domains actually form an integrated unit (McGee and Bredt, 1999). Surprisingly, the folds of the SH3 domain are actually divided by the HOOK and GK domains, a feature that is unique to the SH3 domain of MAGUKs. The HOOK domain is present in many MAGUKs and has most notably been shown to bind protein 4.1, providing an important link between MAGUKs and the cytoskeleton (Cohen et al., 1998; Lue et al., 1996; Lue et al., 1994a; Marfatia et al., 1994; Marfatia et al., 1996). The authors of the SH3-GK crystal structure postulate that the SH3 subdomains assemble separately to interact with the GK and HOOK domains, proposing a model in which these subdomains could swap intermolecularly as well as intramolecularly (McGee and Bredt, 1999). Overall, the interaction between the SH3, HOOK and GK domains suggests a possible mechanism by which MAGUK proteins can regulate interactions with potential binding partners. Interestingly, multiple studies have shown that the HOOK domain, also called the hinge region, is involved in this regulation. For example, calmodulin has been shown to bind to the HOOK region of SAP97 (Paarmann et al., 2002). Calmodulin is a versatile molecule that, upon binding calcium, undergoes a conformational change that allows binding to a given substrate; in turn the substrate's conformation is often changed in response to calmodulin binding (Kortvely and Gulya, 2004; Yamniuk and Vogel, 2004). The study suggests that calmodulin binding may regulate the SH3-GK intramolecular interaction (Paarmann et al., 2002;

Yang et al., 1998). It is postulated that the intramolecular SH3-GK interaction within a MAGUK is in a "closed" conformation that essentially prevents interaction of either domain with other molecules; the closed SH3-GK intramolecular interaction has been shown to inhibit binding of the SAP97 GK domain to GKAP (Wu et al., 2000). When a molecule such as calmodulin binds to the HOOK domain, it could "open" the SH3-HOOK-GK conformation, allowing the domains to engage in interactions with various other ligands. Another illustration of this SH3-GK mediated regulation is demonstrated by the fact that mutations in the SH3-GK sequence of the PSD-95 protein result in a disruption of the potassium channel clustering capabilities of the protein, as shown by co-transfection studies in COS cells (Shin et al., 2000).

The most recently identified protein interaction domain of MAGUKs is the L27 domain. The L27 domain was first identified in Lin-2, the *C. elegans* homologue of CASK, and was so named because this domain was the minimal sequence required for an interaction between lin-2 (CASK) and lin-7 (Doerks et al., 2000). The mammalian CASK protein also contains two L27 domains, that are located in tandem between the CaMK and PDZ domains. These domains are relatively unstructured, but can heterodimerize and form a helical structure upon interaction, interacting in a 1:1 stoichiometry overall. Recent NMR studies have also shown the heteromeric L27 domain containing proteins can form tetramers (Harris et al., 2002). One such L27 heterodimerization, aside from the interaction between CASK and Lin-7, is an interaction between the L27 domain of CASK/Lin-2 and the L27 domain of Dlg/SAP97, whose

NMR structure revealed that these proteins can form tetrameric structures via the N-terminal L27 domain of CASK and the L27 domain of SAP97 (Feng et al., 2004; Lee et al., 2002).

The final domain of CASK to be discussed is the CaMK (Ca^{2+}/calmodulin dependent kinase) domain. The CaMK like domain is completely unique to the CASK protein and hence its characterization was concomitant with the initial description of the protein as a whole (Hata et al., 1996b). The most detailed analysis of the domain was conducted by Hata et al, who first isolated the mammalian CASK gene. The sequence of the CaMK like domain was found to exhibit a high sequence similarity to all members of the CaMK family, but is most similar to the CaMKII (50% sequence similarity) (Hata et al., 1996b). Members of the CaMK family are responsible for mediating the effects of Ca^{2+} influx in the cell by phosphorylating their given substrate(s) (Braun and Schulman, 1995; Lisman et al., 2002). In these initial studies, the possibility that the CaMK domain confers kinase activity to the CASK protein was examined. The recombinant CASK protein did not exhibit any kinase activity. However, CASK was found to bind calmodulin in Ca^{2+} dependent manner *in vitro*; this binding has not been demonstrated *in vivo* (Hata et al., 1996a). The ability of CASK to bind calmodulin, is due to the conserved sequence similarity between the calmodulin binding region of CaMK and CASK.

The CASK/Mint/Veli tripartite complex

Arguably, the most extensively studied interaction of the CASK protein is its participation in a tripartite complex with the proteins Lin-10/Mint and Lin-7/Veli. This

tripartite complex provides insight into the *in vivo* role that CASK and its binding partners may be playing at cell junctions, including receptor localization, cell adhesion and vesicle exocytosis (Borg et al., 1998; Butz et al., 1998; Hoskins et al., 1996; Kaech et al., 1998; Maximov et al., 1999; Schuh et al., 2003). Therefore, a thorough discussion and understanding of this complex is essential. The tripartite complex was first identified in *C. elegans* by means of genetic screens searching for genes required in vulval development and was subsequently found to be present at the post-synaptic membrane at synapses in the mammalian central nervous system (Butz et al., 1998; Hoskins et al., 1996). The Lin-2 gene was first isolated in screens of *C. elegans* that resulted in a vulvaless phenotype (Ferguson and Horvitz, 1985; Horvitz and Sulston, 1980). Lin-2 was subsequently found to be the *C. elegans* homologue of the mammalian CASK gene, with a 52% sequence similarity and containing all the same protein-protein interaction domains (Hoskins et al., 1996). Two other genes, Lin-7 and Lin-10, were also found in the same genetic screen as the CASK/Lin-2 gene (Ferguson and Horvitz, 1985; Horvitz and Sulston, 1980). Lin-7 and Lin-10 were thought to closely associate with Lin-2/CASK, as mutations in all three genes results in mislocalization of the LET-23 receptor. Structurally, Lin-7 contains a single PDZ domain, while Lin-10 contains two PDZ domains and a phosphotyrosine binding (PTB) domain (Ide et al., 1998; Kim and Horvitz, 1990; Okamoto and Sudhof, 1997; Rongo et al., 1998; Simske et al., 1996). *In vitro* biochemical studies confirmed that the PDZ domain of Lin-7 bound to the C-terminus of the *C. elegans* Let-23 receptor tyrosine kinase (RTK). The mechanism by which these PDZ domain-containing proteins resulted in a vulvaless phenotype was revealed in studies conducted by Kaech et. al. (Kaech et al., 1998). Yeast two-hybrid

studies combined with immunoprecipitations (IPs) from cell culture showed that Lin-2 was able to interact in a tripartite complex with Lin-7 and Lin-10, but that Lin-7 and Lin-10 do not interact with each other (Kaech et al., 1998). Therefore, if any of the components are mutated such that it interferes with binding of the tripartite members, the complex cannot anchor the LET-23 receptor at the correct location. At the same time that the *C. elegans* Lin-2/Lin-7/Lin-10 complex was identified, their mammalian counterparts, CASK, Veli and Mint (Munc-18 interacting protein), respectively, were also shown to form a complex *in vivo* at mammalian central nervous system synapses (Borg et al., 1998; Butz et al., 1998). These studies found that Mint and Veli bind to the CaMK and L27 domains of CASK, respectively. Similar to the experiments conducted in *C. elegans*, CASK was shown as the link in binding between Mint and Veli. Interestingly, none of the interactions between these three proteins were found to involve the PDZ domain, leaving the PDZ domains free to form interactions with other channels and receptors.

The CASK-containing tripartite complexes identified in *C. elegans* vulval epithelial cells and brain, suggest many potential roles for the CASK protein. In vulval epithelia Lin-2/CASK provides a link that helps to localize LET-23 receptor tyrosine kinase to the basal lamina, thereby aiding in the establishment of cell polarity. As indicated by the Lin-2/CASK mutants, this anchoring of the RTK Let-23 also ensures the proper vulval development in this organism (Ferguson and Horvitz, 1985; Kaech et al., 1998). Further data demonstrates that the tripartite complex is also involved in the localization/binding of channels in central nervous system synapses. It was found that the long splice variant of N-type calcium channels can bind to a PDZ domain of Mint *in vivo* in rat brain

(Maximov et al., 1999). Furthermore, this study showed that these N-type calcium channels contain a proline rich region that is able to interact with the SH3 domain of CASK *in vitro*, although this interaction was not confirmed *in vivo* (Maximov et al., 1999).

Notably, the tripartite protein complex has also been coupled to vesicle exocytosis, via the Mint protein, which was isolated and named based on its interaction with Munc-18. In turn, Munc-18 was identified through its association with syntaxin, a synaptic vesicle fusion protein (Kim and Horvitz, 1990; Okamoto and Sudhof, 1997). The association in brain between CASK and Mint with calcium channels and the interaction of Mint with proteins involved in vesicle exocytosis suggests a possible role for the tripartite complex in regulating neurotransmission (For reviews see (Burgoyne and Clague, 2003; Gerber and Sudhof, 2002; Lin and Scheller, 2000)). Calcium is a key component in regulating the release of neurotransmitters via vesicle exocytosis. It is therefore fortuitous that these calcium channels and synaptic vesicle proteins are docked in close proximity via their interactions with CASK and Mint. Interestingly, CASK has also been shown to interact with another protein associated with vesicle exocytosis, rabphilin3a, a membrane associated effector protein of the Rab3a GTPase (Shirataki et al., 1993; Takai et al., 1993). Yeast two-hybrid analysis performed from human brain first predicted the association between CASK and rabphilin3a, but the interaction has not been shown *in vivo* (Zhang et al., 2001).

In addition to calcium channels, the CASK/Mint/Veli complex has also been shown to be associated with the localization of potassium channels in both renal epithelial cells and

in brain (Leonoudakis et al., 2004; Olsen et al., 2002). Proper localization and sorting of potassium channels is required to ensure that potassium is secreted efficiently based on the needs of the cell. In studies conducted in the Madin-Darby canine kidney (MDCK) renal epithelial cell line, CASK was found to interact with the human orthologue of Lin-7/Veli, named Lin7b (Olsen et al., 2002). These experiments revealed that the CASK/Lin7b complex is also conserved in mammalian epithelial cells and that the complex acts to retain the Kir 2.3 inward rectifying potassium channel in the basolateral membrane. This study helped to elucidate one aspect as to how potassium channels may be sorted to correct subdomains in the cell, a process that is poorly understood. More recently, it has been shown that the potassium channel Kir 2.2 can also interact with the tripartite complex in brain (Leonoudakis et al., 2004). These studies authenticated the dynamic nature of the complex, demonstrating that there are multiple ways in which the complex can be formed, i.e. there are at least two distinct macromolecular complexes that can be formed. *In vitro* binding studies suggest that Kir 2.2 can interact with hDlg/SAP97, which then recruits CASK, Veli and Mint (Leonoudakis et al., 2004). Alternatively, there is evidence for a separate complex in which Kir 2.2 interacts with Veli and recruits hDlg/SAP97 and CASK, but not Mint. Finally, in brain, a novel CASK binding partner known as Caskin 1 (CASK interacting protein 1), competes with Mint for binding, forming alternative complexes and further demonstrating the dynamic nature of the tripartite complex (Tabuchi et al., 2002).

CASK's interaction with cell surface adhesion molecules and the cytoskeleton

Complementary to its participation in the tripartite complex, CASK has also been shown to bind adhesion molecules and the actin cytoskeleton. The interaction of CASK with adhesion molecules and the cytoskeleton allows CASK to engage in stabilizing its associated complex, helping to maintain cell polarity. As discussed previously, the mammalian homologue of CASK was originally cloned and characterized based on its interactions with neurexin, a neuronal specific cell surface adhesion molecule (Butz et al., 1998; Hata et al., 1996a; Ichtchenko et al., 1996; Ushkaryov et al., 1992). CASK helps to support the neurexin-neuroligin complex via its interaction with protein 4.1, which functions to stabilize F-actin-spectrin interactions in the cytoskeleton (Biederer and Sudhof, 2001; Hata et al., 1996a; Hoover and Bryant, 2000). The interaction of protein 4.1 with CASK occurs through a conserved 4.1 binding site present in the HOOK region of CASK (Biederer and Sudhof, 2001; Cohen et al., 1998).

In addition to its interaction with neurexins, CASK is capable of participating in interactions with the cell surface junctional adhesion molecule (JAM) (Cohen et al., 1998; Hsueh et al., 1998; Martinez-Estrada et al., 2001). JAM is an immunoglobin-like cell adhesion molecule and is localized to the intercellular contacts in epithelial and endothelial cells (Martin-Padura et al., 1998). *In vitro* overexpression experiments demonstrate that the C-terminus of JAM interacts with the PDZ domain of CASK and that the two proteins co-localize at intercellular junctions of CACO-2 cells (Martinez-Estrada et al., 2001). The potential association of CASK with JAM further suggests that

CASK may have a general role in cell adhesion at cell contacts. It is important to note that *in vivo* verification of the CASK-JAM complex, has yet to be firmly established.

The last class of cell surface adhesion molecules that interacts with CASK are the syndecan family members; CASK interacts with syndecans in both neuronal synapses and epithelial cells. Syndecans are transmembrane heparan sulfate proteoglycans located on cell surfaces at sites of cell adhesion. The four members of the syndecan family, Syndecans 1-4, participate in a variety of functions, including binding to growth factors and acting as co-receptors for growth factors with receptor tyrosine kinases, such as fibroblast growth factor receptor (FGFR) (Bass and Humphries, 2002; Bernfield et al., 1993; Bernfield et al., 1992; Rapraeger, 2000). Syndecans also provide a means of cell adhesion by binding to components of the ECM such as laminin and collagen. Two studies, conducted concurrently, utilized yeast two-hybrid and various other *in vitro* studies to demonstrate that the PDZ domain of CASK interacts with the C-terminus of syndecan-2 in neuronal cell lines, and syndecans-1 and -2 in epithelial cells (Cohen et al., 1998; Hsueh et al., 1998). These studies did not determine whether CASK could bind syndecans -3 and/or – 4; however, all four syndecans contain an identical C-terminal EFYA PDZ domain binding consensus motif (Bernfield et al., 1993; Bernfield et al., 1992; Carey, 1997). Although *in vivo* co-immunoprecipitations were unable to be achieved, both studies showed *in vivo* co-localization to distinct subcellular domains in both brain and epithelial cells. Furthermore, mutating the C-terminal consensus motif results in mislocalization of the syndecans (Cohen et al., 1998; Hsueh et al., 1998). Overall, these studies suggest that CASK provides a link between the ECM and the actin

cytoskeletal network via its interaction with syndecans and protein 4.1. The CASK-syndecan interaction may also provide a function analogous to the role that CASK plays in *C. elegans* epithelial cells, as the interaction between CASK and syndecan provides a possible role for CASK in stabilizing the FGFR in mammalian cells. Interestingly, syndecans are present in skeletal muscle satellite cells and are implicated in skeletal muscle regeneration and differentiation (Cornelison et al., 2001).

CASK as a transcription factor

Perhaps one of the most intriguing discoveries regarding possible CASK functions was its identification as a co-activator of transcription (Hsueh et al., 2000). Studies conducted by Hsueh et. al., using a yeast two-hybrid screen, demonstrated that the GK domain of CASK interacts specifically with TBR-1, a brain enriched T-Box transcription factor essential for development of the cerebral cortex (Bulfone et al., 1995; Hsueh et al., 2000). The T-box family of transcription factors was first characterized by studies of the Brachyury gene (For reviews see (Kispert and Hermann, 1993; Kispert et al., 1995; Minguillon and Logan, 2003; Muller and Herrmann, 1997; Papaioannou, 2001; Papaioannou and Silver, 1998; Tada and Smith, 2001). Crystal structures of the Brachyury protein have revealed that T-box proteins can form dimers that associate with both the major and minor grooves of DNA. The T-box proteins, including TBR-1, all contain a DNA binding domain approximately 180 amino acids in length, which binds to a palindromic DNA sequence known as the T-element. The interaction of CASK with TBR-1 was further confirmed by *in vivo* co-immunoprecipitation data from rat brain (Hsueh et al., 2000). Co-transfection studies revealed that when CASK is co-expressed

with TBR-1 in COS cells or cultured hippocampal neurons, CASK protein is redistributed from the cytoplasm to the nucleus. Moreover, gel shift assays confirmed that CASK and TBR-1 form a complex which binds to the T-element. Luciferase assays revealed that CASK binding to TBR-1 enhanced transcription in a manner that is dependent on the presence of the guanylate kinase domain of CASK (Hsueh et al., 2000). These experiments also provided evidence that CASK could enhance transcription alone, although not to the same degree as when complexed with TBR-1. The authors of this study also examined the effect of the CASK-TBR-1 complex on the reelin gene (Hsueh et al., 2000). Reelin seemed a likely target for the CASK-TBR-1 complex as it contained a T-element sequence, and mice with a knock-out of either the reelin or TBR-1 gene display similar phenotypes (Bulfone et al., 1998; Hevner et al., 2001; Hsueh et al., 2000). Co-expression of CASK and TBR-1 in neurons containing a luciferase gene under the control of the reelin T-element enhanced transcription 28 fold, as compared to 2-fold and 16-fold when CASK and TBR-1 were expressed individually (Hsueh et al., 2000). An analysis of other possible targets of the TBR-1/CASK complex was recently undertaken. These studies showed that the TBR-1/CASK complex could enhance the transcription of the non-palindromic T-element sequence containing genes NR2B, glycine transporter, and IL-7R in cultured hippocampal neurons, and OX2 and FGF4 in COS cells (Wang et al., 2004b). An *in vivo* role for this complex was supported by studies in TBR-1 knock-out mice in which the expression of NR1 and NR2B was significantly decreased as compared to heterozygous mice (Hevner et al., 2001).

Recently, another binding partner for CASK has been identified, and has provided further insight into the molecular mechanisms behind CASK transcriptional properties. Once again, a yeast two-hybrid approach was employed to identify binding partners for the GK domain of CASK. This screen identified a novel protein found to possess a nucleosome assembly protein domain and was so named, CINAP, for CASK Interacting Nucleosome Assembly Protein (Wang et al., 2004a). The CINAP protein was confirmed to interact with CASK *in vivo* in rat brain and to act as nucleosome assembly protein via demonstration of interactions with histones and its ability to form a nucleosome in a DNA super-coiling assay (Wang et al., 2004a). Although CINAP and TBR-1 both bind to the GK domain of CASK they do not appear to compete for binding, but rather form a ternary complex. The purpose of this ternary complex was elucidated in a series of elegant *in vitro* biochemical studies that demonstrated that the CASK/TBR-1/CINAP complex can regulate transcription of Reelin, and NR2B, an NMDA receptor subunit recently found to contain a TBR-1 binding site (Wang et al., 2004a). The most fascinating aspect of these studies is the fact that CINAP was found to downregulate transcription of NR2B in a neuroblastoma cell line, yet upregulated transcription in cultured hippocampal neurons. Moreover, it appears that transcriptional activation of this complex may be controlled in part by synaptic activity. Synaptic activity was found to activate a proteolytic pathway through NMDA receptors that results in degradation of the CINAP protein, which would in turn enhance or inhibit transcription of genes under the control of the CASK/TBR1/CINAP complex (Wang et al., 2004a). Finally, although TBR-1 is present almost exclusively in brain, both CASK and CINAP are expressed

ubiquitously, suggesting that there may be other transcription factor partners in other tissues still to be identified (Cohen et al., 1998; Hata et al., 1996a; Wang et al., 2004a).

CASK's interaction with Dlg

As mentioned previously, the CASK protein interacts with another MAGUK, Dlg, which has a domain structure very similar to CASK. Dlg, Discs Large, was initially identified via mutations in the *Drosophila* Dlg that result in overgrowth of imaginal discs, thereby identifying Dlg as a tumor suppressor gene (Woods and Bryant, 1991a). Subsequently, Dlg was found to be a member of a MAGUK family of proteins and an isoform of the PSD-95 protein (Cho et al., 1992; Koonin et al., 1992; Muller et al., 1995; Woods and Bryant, 1991a). Homologues of Dlg have been identified and cloned in *C. elegans*, mouse, rat and human (Bossinger et al., 2001; Cho et al., 1992; Firestein and Rongo, 2001; Kistner et al., 1993; Lin et al., 1997; Lue et al., 1994b). The domain structure of Dlg is typical of the MAGUK family, containing three N-terminal PDZ domains, an SH3 domain, a HOOK domain, a GK domain (Lue et al., 1996; Lue et al., 1994a; Woods and Bryant, 1991b). It is also worth noting that the human and rat Dlg homologues, hDlg and SAP97, also contain an L27 domain N-terminal to the PDZ domains (In background studies conducted in mammalian cells or animals that are described in this introductory chapter, Dlg will be referred to as hDlg/SAP97, while in invertebrate studies the protein is simply referred to as Dlg. For this chapter and remaining chapters, the mouse homologue will be referred to as Dlg) (Feng et al., 2004; Marfatia et al., 2000; Nakagawa et al., 2004). Dlg plays a role in stabilizing molecules at virtually all types of cell junctions. In *Drosophila*, Dlg has been shown to be critical in

the maintenance of the septate junction in epithelial cells, a structure analogous to the vertebrate tight junction (Woods and Bryant, 1991a). Loss of Dlg function in imaginal disc cells in *Drosophila* results in complete loss of apicobasal polarity as well as septate junctions; adherens junctions and gap junctions are not affected (Woods et al., 1996). In *Drosophila* salivary epithelial cells, mutations in Dlg result in septate junctions that are reduced in length by ~90%, mislocalization of adherens junctions and perturbation of the basolateral membrane. Redistribution of cytoskeletal proteins, including Coracle, the *Drosophila* homologue of protein 4.1, and two proteins involved in cellular adhesion, Fascilin III and neuroligin, has also been shown to be an affect of loss of Dlg protein function (Woods and Bryant, 1991a; Woods et al., 1996). Furthermore, studies of flies mutant for Dlg have also implicated the protein in recruitment of plasma membrane associated proteins and formation of the plasma membrane (Lee et al., 2003). Overall, these genetic analyses suggested that loss of distinct domains of Dlg results in varying phenotypes depending on the cell type. Dlg is also required for the normal epithelial cell development and apical junction formation, as well as organization of the actin cytoskeleton in *C. elegans* (Bossinger et al., 2001; Firestein and Rongo, 2001; McMahon et al., 2001). Interestingly, these functions are also conserved in the vertebrate Caco-2 intestinal epithelial cell line, where hDlg/SAP97 has been shown to interact with E-Cadherin. Additionally, knockdown of Dlg in this cell line by RNAi leads to mislocalization of both E-cadherin and F-actin, resulting in reduced adherens junction stability (Laprise et al., 2004).

Data suggests that hDlg/SAP97 also plays a variety of different roles at chemical synaptic junctions in the central nervous system. Various *in vitro* studies have shown that hDlg/SAP97 are involved in the clustering and localization of AMPA, NMDA and potassium channels at synaptic junctions (Cai et al., 2002; Chetkovich et al., 2002; Kim et al., 1996; Kim et al., 1995; Kornau et al., 1995; Leonard et al., 1998; Leonoudakis et al., 2004; Leonoudakis et al., 2001; Rumbaugh et al., 2003; Sans et al., 2001; Tiffany et al., 2000). The hDlg/SAP97 homologue, PSD-95, interacts with the NMDA receptor subunit, NR2A at the postsynaptic density of synapses (Kornau et al., 1995). *In vivo*, evidence for this interaction is supported by the fact that the PSD-95 mutant mice have impaired spatial learning (Migaud et al., 1998). Additionally, PSD-95 and NMDA are co-localized with each other at sites of cell adhesion in glumeruli (Petralia et al., 2002). The PSD-95 protein may also be involved in cell adhesion through its interaction with neuroligin (see previous discussion). In contrast to PSD-95, hDlg/SAP97 is localized both at the postsynaptic densities and axons, and is associated with AMPA receptors, NMDA receptors, ErbB receptors and potassium channels (potassium channel interactions are discussed below) (Bassand et al., 1999; Cai et al., 2002; Garcia et al., 2000; Gardoni et al., 2003; Leonoudakis et al., 2004; Leonoudakis et al., 2001; Rumbaugh et al., 2003; Sans et al., 2001; Tiffany et al., 2000). hDlg/SAP97 interacts via its PDZ domain with GluR1 AMPA receptor subunits and has been implicated in the trafficking , targeting and regulation of these receptors through its interactions with A kinase anchoring proteins, protein 4.1, and the motor proteins, myosin VI and KIF1Bα (Colledge et al., 2000; Mok et al., 2002; Osterweil et al., 2005; Tavalin et al., 2002).

As discussed earlier, Dlg has also been shown to be critical in the development of the *Drosophila* NMJ, where it is responsible for the clustering of inward rectifying potassium channels. The experiments conducted at the glutamatergic *Drosophila* NMJ demonstrate that Dlg is involved in the formation of the NMJ and promotes adhesion of this cell junction through its interaction with fascilin II (Tejedor et al., 1997). Further *in vivo* experiments in *Drosophila* show that targeting of Dlg to the larval NMJ required the presence of PDZ domains 1 and 2 of the protein, the HOOK domain, and the GUK domain (Tejedor et al., 1997; Thomas et al., 2000). Interestingly, a mutant of Dlg which lacks the C-terminal region 3' to the PDZ domains was mislocalized to the nuclei. Finally, studies conducted in our lab have demonstrated that hDlg/SAP97 is also present at the cholinergic mammalian NMJ (Rafael et al., 1998a).

The interaction between CASK and Dlg has been observed in *Drosophila*, as well as a number of different epithelial cell lines, and the A-172 human neuroblastoma cell line (Feng et al., 2004; Lee et al., 2002; Nix et al., 2000). However, in the studies conducted in epithelial cells, there are conflicting reports as to what domains are responsible for the interactions between the two proteins. Experiments conducted by Nix et. al. showed that CASK and hDlg/SAP97 co-immunoprecipitate from the intestinal Caco-2 cell line and a yeast two-hybrid screen revealed that this interaction occurred between the GK domain of CASK and the SH3 domain of hDlg/SAP97 (Nix et al., 2000). These studies also demonstrated that the SH3 and GK domains not only participated in intermolecular interactions, but also intramolecular interactions. In contrast to these findings, Lee et. al. reported that the N-terminus of hDlg/SAP97 interacts with the N-terminal L27 domain of

CASK (Lee et al., 2002). This interaction was elucidated through a series of domain deletions, pulldown assays, and immunoprecipitations from the MDCK and HEK293 epithelial cell line and was shown to be stronger than the interaction between the GK and SH3 domains of CASK and hDlg/SAP97 (Lee et al., 2002). The hDlg/SAP97 protein was also able to associate in a complex with the entire CASK/Mint/Veli tripartite complex in these cell lines. A dominant negative form of the CASK protein lacking the C-terminal half of the protein resulted in mislocalization of the CASK protein in the MDCK cell line, and subsequently improper localization of the hDlg/SAP97 protein. CASK constructs deleted for the L27 domains did not affect hDlg/SAP97 localization, suggesting that hDlg/SAP97 localization is dependent on association with CASK (Lee et al., 2002).

As briefly mentioned above, hDlg/SAP97, is also able to associate with CASK as a component of the CASK/Mint/Veli tripartite complex. Furthermore, there are different versions of this complex that can exist, containing different Veli isoforms (Leonoudakis et al., 2004). The studies demonstrate a direct *in vivo* binding of hDlg/SAP97 to multiple inward rectifying potassium channels, Kir 2.1, 2.2 and 2.3. Interestingly, expression of a dominant negative form of CASK in MDCK cells resulted in mislocalization of Kir 2.2 from the basolateral membrane to intracellular locations (Leonoudakis et al., 2004).

Perhaps the most intriguing aspect of the CASK-Dlg interaction is the fact that *in vivo* knock-outs of CASK and Dlg protein function in mice result in strikingly similar developmental phenotypes (Caruana and Bernstein, 2001; Laverty and Wilson, 1998). A transgenic insertion into the CaMK domain of CASK gene results in cleft palate (Laverty

and Wilson, 1998). The protein product that results from this insertion has not been extensively characterized. As CASK is an X-linked gene, male mice died within 24 hours of birth; viability of female mice seemed to be dependent on strain background. Phenotypically, both sexes exhibited smaller head size compared with wild-type littermates, and defects in mandible and maxilla development were clear, including pointed snouts and shortened lower jaws; the phenotypic abnormalities observed in the females can most likely be attributed to X-activation which occurs during embryonic development. Females that survived also exhibited spinal kinks and significantly lower body weight (Laverty and Wilson, 1998).

The Dlg mutant mouse model was produced by isolation of a gene trap LacZ insertion into the Dlg gene in ES cells (Caruana and Bernstein, 2001). The resulting fusion protein contains the N-terminal portion of the protein and lacks the SH3, HOOK and GK domains. Mice that were heterozygous did not possess any phenotypic abnormalities, unlike the CASK knock-out heterozygous females. However, homozygous expression of the mutated Dlg results in a phenotype very similar to the CASK mice, including craniofacial morphogenesis and cleft palate; all homozygous pups died within 24 hours of birth (Caruana and Bernstein, 2001; Laverty and Wilson, 1998). Given the similarity of the CASK and Dlg knock-out phenotypes and the interaction between the two proteins, it has been suggested that the two proteins function in the same developmental pathway and that the similar phenotypes are a result of the inability of the two proteins to interact in

the respective mouse models. Moreover, it is postulated that the disruption of the CASK-Dlg interaction may cause abberant cell junction adhesion and signaling defects (Caruana, 2002).

The Neuromuscular Junction

The NMJ is a specialized form of a communicating cell junction whose function is to reliably transmit signals from the motor neuron end plate to the skeletal muscle fiber. Morphologically, the NMJ is composed of three distinct cell types that act in concert as a cohesive unit to relay information in the form of electrical or chemical stimulation. The three primary components of the NMJ are the motor neuron, the Schwann cell, and the muscle fiber. The NMJ has been historically used as a model system for understanding the molecular and physiological tenants that govern synaptic transmission across all types of chemical synapses, including those of the central nervous system (CNS). This situation is due in part to the fact that the NMJ, especially when compared to CNS synapses, lends itself more readily to experimentation because of its size and accessibility. The size of an NMJ synapse allows for easy visualization, and more importantly, a single NMJ can be easily isolated, given that a single muscle fiber is innervated by a single axon from a motor neuron. Overall, this has led to a wealth of knowledge regarding the structure and physiology of the NMJ (For reviews see (Meier and Wallace, 1998; Sanes and Lichtman, 1999).

Acetylcholine is the primary neurotransmitter released from the motor nerve terminal and the NMJ is hence known as a cholinergic synapse, as opposed to CNS synapses,

whose primary neurotransmitters are glutamatergic (Sanes and Lichtman, 1999). The acetylcholine is released from vesicle pools that are positioned at points known as active zones, near the motor neuron membrane that is closest to the muscle fiber. This localization allows the acetylcholine to be released in large quantities following vesicular fusion to the motor neuron membrane. The acetylcholine travels across the synaptic cleft where the muscle fiber is structurally and molecularly specialized to receive the signal with rapidity and high fidelity. The area directly opposed to the motor neuron on the muscle fiber is referred to as the postsynaptic membrane and structurally consists of a series of folds. The molecular composition of the postsynaptic folds is fairly polarized, with molecules such as the acetylcholine receptors (AChR) being positioned at distinct areas of the folds (Banks et al., 2003; Luo et al., 2003; Patton, 2003). The AChRs are found in extremely high concentrations at the tops of the folds, thereby positioning the AChRs at a prime location for receiving the acetylcholine molecule (Fertuck and Salpeter, 1976; Madhavan and Peng, 2003). Moreover, other molecules, including cytoskeletal elements and ion channels are also found at discrete locales within the postsynaptic membrane. For example, dystrophin and sodium channels are found at the bottom depths of the folds, while utrophin and α-dystrobrevin are found at the crests of the folds (Sanes and Lichtman, 1999; Trinidad et al., 2000).

One area of intense investigation regarding the neuromuscular junction has been the trophic and signaling factors that result in the accumulation of the AChRs. Although skeletal muscle fibers can form small clusters of acetylcholine receptors at structures that somewhat resemble the postsynaptic membrane in the absence of neuronal input, it is the

molecule agrin that is primarily responsible for generating a fully functional postsynaptic apparatus (For reviews see (Meier and Wallace, 1998; Ruegg and Bixby, 1998; Sanes and Lichtman, 1999)). Agrin is a heparan sulfate proteoglycan that was first isolated from basal laminal extracts of the synaptic cleft of the NMJ from Torpedo electric organ (Godfrey et al., 1984; Nitkin et al., 1987; Smith et al., 1987). The agrin receptor is a muscle specific serine kinase, known as MuSK. MuSK became the leading putative agrin receptor when it was discovered that MuSK knock-out mice are unable to form NMJs (DeChiara et al., 1996; Sanes and Lichtman, 1999). Interestingly, MuSK has not been shown to interact directly with agrin *in vivo*. This finding has led investigators to postulate that there is another unidentified receptor that associates with MuSK, acting as a co-receptor for agrin (Glass et al., 1996). Upon activation by agrin, MuSK and yet unidentified binding partners, initiate a signal cascade that results in gene transcription at synaptic nuclei and formation of the entire postsynaptic apparatus; this includes clustering of AChRs and the cytoskeletal components of the postsynaptic folds (Glass and Yancopoulos, 1997; Sanes and Lichtman, 1999). The acetylcholine receptors are transcribed in vast quantities from synaptic nuclei, ensuring a large pool of acetylcholine receptors is available, and in close proximity, to be inserted into the membrane of the postsynaptic apparatus. Transcription of the genes encoding the AChR subunits is thought to be transduced in part by agrin stimulation, and another trophic factor, known as neuregulin (For reviews see (Buonanno and Fischbach, 2001; Falls, 2003a; Falls, 2003b; Loeb, 2003; Si et al., 1998). Here, it is worth mentioning, that the Erb family of proteins are the receptors for neuregulin; one such Erb family member, ErbB1 is homologous to the LET-23 receptor of *C. elegans* (Garcia et al., 2000).

Following transcription and translation of AChR subunits, and clustering of complete AChRs, they are anchored to cytoskeletal elements of the postsynaptic apparatus by rapsyn. Finally, transcription of AChRs is ceased after the formation of a fully functional postsynaptic apparatus is completed. The transcription appears to be halted by synaptic transmission; in other words, once acetylcholine binds the AChRs, gene expression is repressed.

Although the AChR complex has been thoroughly investigated, few studies on the role of MAGUKs at this cholinergic synapse have been carried out. This thesis describes an investigation into the *in vivo* role of the MAGUK family member, CASK, in skeletal muscle at the neuromuscular junction.

Claudin-5

In epithelial and endothelial cells, the tight junction is responsible for acting as the major barrier between cells to regulate paracellular transport (For reviews see (Bushby et al., 1991; Lapierre, 2000; MacLennan and Edwards, 1990; Matter and Balda, 2003a; Matter and Balda, 2003c; Sawada et al., 2003; Tsukita et al., 2001)). Therefore, much work has centered around determining the molecular components of this cell junction. Cytoplasmic tight junction accessory proteins such as ZO-1, ZO-2 and ZO-3, and Cingulin, were among the first components identified. However, these proteins are considered peripheral and are involved in adhesion and scaffolding of protein complexes at the tight junction, but are not involved in its formation or structural integrity. It was not until the discovery of occludin that our knowledge of the molecular architecture of

the tight junction began to take shape. Occludin, a four transmembrane protein, was the first tight junction specific integral membrane protein to be identified (Furuse et al., 1993; McCarthy et al., 1996; Tsukita et al., 1997). Subsequent examination of the occludin protein demonstrated that it was involved in cell adhesion, and contributes to the barrier function of tight junctions (Furuse et al., 1996; Furuse et al., 1993; McCarthy et al., 1996; Tsukita et al., 1997). Yet, experiments conducted in occludin knock-out ES cells were still able to form a structurally intact network of tight junctions (Balda et al., 1996; Saitou et al., 1998). This suggested that there was still another major integral membrane component of tight junctions yet to be determined. Ultimately, this led to the discovery of the claudin protein family as the major contributors to tight junction molecular architecture.

The first claudins were identified based on their ability to co-partition with occludin in fractionation studies, and were designated claudin-1 and claudin-2 (Furuse et al., 1998a). Claudin-1 and claudin-2 were found to have a molecular mass of ~22 kDa and consist of four transmembrane domains, similar to occludin; however, they are not similar in sequence to occludin. Further analysis revealed that claudins are the major structural components of tight junctions based on transfection of these proteins into fibroblast cell lines which lack tight junctions (Furuse et al., 1998b). When FLAG-tagged claudin-1 and/or claudin-2 were transfected into fibroblasts, which lack tight junctions, it resulted in the formation of *de novo* tight junctions at sites of cell contact. When occludin was transfected into these fibroblasts, it resulted in only a small number of short tight junction strands. Interestingly, when occludin was co-transfected with claudin-1, occludin

distribution was changed and became localized along the entire strand of the claudin-1 based tight junctions (Furuse et al., 1998b). Together, these results affirmed that claudins are the integral membrane proteins essential for the establishment of tight junction architecture.

Since the initial characterization of claudins-1 and -2, the claudin protein family has expanded to include over 24 members. These claudins all exhibit distinct patterns of tissue specific expression and distribution. Claudin protein family members have all been shown to localize to tight junctions in transfection studies, and further experimentation has revealed that the majority of tight junctions consist of a heterogenous mixture of at least two different claudin proteins. In fact, the distinct claudin species present within a given tight junction are thought to be responsible for the unique biochemical properties of tight junctions in varying epithelial and endothelial cell types. Claudin protein composition directs tight junction barrier function by determining such properties as size selectivity of molecules that pass through the tight junction via paracellular diffusion (For review see(Matter and Balda, 2003b; Morita et al., 1999a; Tsukita and Furuse, 2000a; Tsukita and Furuse, 2000b)).

Aside from their role in regulating tight junction adhesion and barrier function, the claudin and occludin proteins are also involved in anchoring macromolecular complexes to the tight junction through their interactions with cell junction scaffolding molecules. *In vitro* experiments have revealed that occludin and a variety of different claudin proteins interact with the MAGUKs, ZO-1-3, via their cytoplasmic domain and carboxy terminus, respectively (Ibraghimov-Beskrovnaya et al., 1992; Itoh et al., 1999a; Itoh et

al., 1999b; Tracey et al., 1995). The ZO proteins are the major constituent of what is known as the tight junction 'plaque', a macromolecular complex of proteins that is directly associated with the integral membrane proteins and links them to the actin cytoskeleton. *In vitro* evidence has even suggested that when the C-terminus of claudin-1 is mutated to interfere with ZO-1 binding, the result is abberant tight junction strands (Kobayashi et al., 2002). This result seems to suggest that the association of claudins and occludin with the MAGUK scaffolding proteins is responsible for maintaining and perhaps targeting of these proteins to the tight junction.

The claudin-5 gene, also known as trasmembrane protein deleted in velo-cardio-facial syndrome (TMVCF), is one of the most distinct members of the claudin protein family. The identification and characterization of the TMVCF gene was conducted before the discovery of the claudin protein family and has subsequently been designated claudin-5/TMVCF (Morita et al., 1999b). Chromosomal deletions in chromosome 22q11, encompassing the claudin-5/TMVCF gene, result in velo-cardio-facial syndrome (VCFS) and DiGeorge syndrome (Sirotkin et al., 1997). Both syndromes exhibit severe, yet highly variable phenotypes, and are among the most common types of congenital birth defects, with an overall incidence of 1/4000. In general, patients with VCFS display craniofacial abnormalities, including cleft palate, learning disabilities, and defects in the conotruncal region of the heart. Patients with DGS are known to exhibit many of the phenotypes associated with VCFS, as well as additional phenotypes that include hypocalcemia and immune disorders resulting from parathyroidism or thymus defects (Sirotkin et al., 1997). The fact that both of these syndromes result in phenotypes that

encompass multiple organ systems has led to the belief that the claudin-5/TMVCF gene results in a developmental field defect (Goldmuntz and Emanuel, 1997).

Claudin-5 is different from most members of the claudin protein family in that it has been shown to be expressed ubiquitously in all tissues tested, including spleen, kidney, lung, skeletal muscle and heart (Morita et al., 1999b) . Its expression in heart is of particular interest given the heart defects associated with the VCFS and DGS, yet characterization of claudin-5 in heart has not been carried out. Immunofluorescence analysis of varying epithelial and endothelial cell types has demonstrated that claudin-5 is localized to all blood vessel segments in fetal and adult brain, as well as in the lung. However, claudin-5 expression in kidney seemed to be localized solely to the arteries, while in other tissues claudin-5 was only found in a subset of blood vessel segments. These experiments were unable to detect any claudin-5 expression in epithelial cell types (Morita et al., 1999b). Therefore, unlike most members of the claudin protein family, claudin-5 expression at tight junction strands seems to be restricted to endothelial cell types, although not all endothelial cells, and is absent from epithelial cells (Morita et al., 1999b).

The presence of claudin-5 at tight junctions of endothelial cells has been most extensively examined at the blood-brain barrier (BBB). The BBB is responsible for providing a protective barrier between blood vessels and the brain by maintaining homeostasis and preventing influx of potentially harmful molecules into the CNS; tight junctions in endothelial cells of blood vessels in the brain are key regulators of these functions at the BBB. Claudin-5 knock-out mice were therefore generated to examine the

role of claudin-5 at the BBB (Nitta et al., 2003). Claudin-5 homozygous knock-outs were born at the expected Mendelian ratios, but died within 10 hours of birth. Examination of blood vessels in these mice revealed normal morphology, and tight junctions within the endothelial cells seemed unaffected (Nitta et al., 2003). Since tight junctions of endothelial cells in brain blood vessels are composed of claudin-5 and claudin-12, it is likely that these tight junctions in claudin-5 knock-out mice are composed solely of claudin-12. Alternatively, another member of the claudin protein family could be upregulated to compensate for the loss of claudin-5, although this is a less likely alternative given the endothelial cell location. Experiments conducted analyzing uptake of tracer molecules into the CNS of claudin-5 knock-out mice demonstrated that the BBB was significantly affected. The tight junctions in the endothelial cells of the blood vessels became more permeable to small molecules of less than 800 daltons, while unaffected for larger molecules (Nitta et al., 2003). Overall, these results suggest that claudin-5 is a major determinant of brain endothelial cell permeability. This thesis decribes an investigation of claudin-5 in the heart and in two cardiomyopathic mouse models.

Work Described in this Dissertation

The short-term goals of the research presented in this dissertation are to acquire new insights into the physiological function of two cell junction proteins, CASK and claudin-5, in striated muscle. The long-term goals of this project are to contribute to the advancement in understanding and treatment of neuromuscular disorders, many of which are characterized by cardiomyopathy, in addition to their skeletal muscle pathology.

Therefore, it is critical that the role of cell junction proteins in both skeletal muscle and cardiac muscle be delineated. Accordingly, we focus on determining the *in vivo* roles these proteins at regions in which they had not previously been characterized, the neuromuscular junction of skeletal muscle and cardiomyocytes of heart muscle. This thesis is thereby composed of two separate research projects, which undertake an investigation of the CASK and claudin-5 cell junction proteins in skeletal muscle and the cardiac muscle, respectively.

Chapter 1 reports the initial characterization of the CASK protein, *in vivo*, in skeletal muscle. The CASK protein is expressed in skeletal muscle and is specifically localized to the NMJ. Confocal microscopy analysis reveals that this CASK protein is localized predominantly to the postsynaptic membrane, with a small amount of presynaptic staining. Furthermore, this chapter identifies hDlg/SAP97 as *in vivo* binding partner of CASK in skeletal muscle at the NMJ.

Chapter 2 details the expression and localization of CASK in the C2C12 mouse myogenic cell line. At the myoblast stage, CASK is localized almost exclusively to the nucleus in C2C12 cells. However, as myoblasts mature and fuse into multinucleated myotubes, the CASK protein moves from the nucleus to the cytoplasm, and is almost completely excluded from the nucleus by day 7 post-differentiation. Western analysis reveals that the change in CASK localization in these cells is not associated with a change in CASK isoform expression. This chapter also investigates the possible mechanisms that might underly recruitment of CASK and Dlg, to the NMJ. Interestingly, immunofluoresecence experiments reveal that neither CASK, nor Dlg, is recruited to AChR complexes in response to agrin or laminin treatment.

Chapter 3 describes the generation and characterization of two lines of CASK transgenic mice in order to begin to dissect the functions of the CASK protein *in vivo*. CASK F.L. mice overexpress a full-length version of the CASK protein in skeletal muscle, while CASKΔ mice overexpress a truncated version of the protein in skeletal muscle. Histological and functional analysis reveals that overexpression of either CASK protein does not affect the morphology or functional properties of the muscle. Moreover, while overexpression of the CASK F.L. or CASKΔ protein in skeletal muscle does not appear to affect the size or gross morphology of the NMJ, it does appear to affect the presynaptic localization of CASK at the NMJ. Immunofluorescence analysis of the CASK interactor, Dlg, also demonstrates that overexpression of CASK F.L. or CASKΔ protein does not influence Dlg's localization, as had been suggested by previous *in vitro* experiments.

Chapter 4 is an examination of the tight junction protein, claudin-5, in cardiac muscle. We demonstrate for the first time that claudin-5 protein is expressed in cardiac muscle and is localized to the lateral membranes of cardiomyocytes. As cell junction proteins have recently been implicated in dilated cardiomyopathy, we investigated the expression and localization of the claudin-5 protein in two models of muscular dystrophy, the *mdx* and dko mouse; both the *mdx* mouse and the dko mouse exhibit cardiomyopathic features in addition to their skeletal muscle pathology. These studies demonstrate that claudin-5 is specifically downregulated in cardiac muscle of dko mice, while the expression and localization of other cell junction proteins of cardiomyocytes are unaltered.

CHAPTER 1

CASK and Dlg form a PDZ protein complex at the mammalian neuromuscular junction

Introduction

PDZ domain-containing proteins are found at synapses in the central nervous system and in specialized regions of the plasma membrane such as cell-cell junctions. The approximately 90 amino-acid PDZ domain, named for the first three proteins found to contain the motif (PSD-95, Dlg, Zo-1), is a protein interaction domain composed of two α-helices and six β-sheets (Doyle et al., 1996; Morais Cabral et al., 1996). PDZ domains interact with consensus T/S-x-V amino acid motifs found in the carboxy-terminus of many ion channels and receptors and function to cluster these classes of proteins (Anderson, 1996; Garner et al., 2000; Hata et al., 1998). PDZ domains are often found in tandem and can interact with PDZ domains from other proteins, allowing scaffolds containing these molecules with channels and receptors (Brenman et al., 1996; Lumeng et al., 1999). Over 50 PDZ domain proteins have been identified to date and the majority of mammalian studies have focused on the central nervous system (reviewed elsewhere (Garner et al., 2000)).

Chapter 1 published with permission of *Muscle and Nerve*

The membrane-associated guanylate kinases (MAGUK) are modular adapter proteins that contain one to three amino-terminal PDZ domains followed by a Src homology 3 (SH3) domain and a guanylate kinase (GK) domain (Anderson, 1996). Neither the SH3 nor the GK domain has been shown to possess any kinase activity, but both domains bind a diverse array of proteins such as adhesion molecules and cell signaling proteins (Fanning and Anderson, 1999; Hata et al., 1998). Recently, *in vitro* studies have also shown that the SH3 and GK domains of MAGUKs can interact both intermolecularly and intramolecularly, adding another dimension to the scaffolding properties of these proteins (Nix et al., 2000). The combination of domains in MAGUKs makes them particularly well suited for organizing receptors and channels and for stabilizing signaling pathway components at synapses and cell-cell junctions.

Calcium, calmodulin-associated serine/threonine kinase (CASK) is a MAGUK that has been well characterized by *in vitro* biochemical studies and in the central nervous system (Butz et al., 1998; Hata et al., 1996a; Hoskins et al., 1996). CASK is distinct from other MAGUKs in that it contains a CaMKII kinase-like domain N-terminal to its PDZ domain. Additionally, CASK contains two L27 domains and a HOOK region that contains a binding site for protein 4.1 (Cohen et al., 1998; Lee et al., 2002). CASK was first identified in a yeast two-hybrid screen using the highly polymorphic neuronal cell-surface proteins, the neurexins, as bait (Hata et al., 1996a). The interaction of CASK with neurexins helps to stabilize the pre- and postsynaptic intercellular junction by the interaction of neurexin with neuroligins (Biederer and Sudhof, 2001; Fanning and Anderson, 1999; Hata et al., 1996a; Ichtchenko et al., 1996).

The first *in vivo* evidence for the clustering capability of PDZ domains came from studies of Lin-2, the *C. elegans* homologue of mammalian CASK (Craven and Bredt, 1998; Simske et al., 1996). In *C. elegans*, Lin-2, along with Lin-10 and Lin-7, is required for localization of the Let-23 receptor, which is similar to the mammalian EGF receptor (Hoskins et al., 1996; Kaech et al., 1998). This complex is also present at central nervous synapses where CASK interacts with the mammalian Lin-10 and Lin-7 homologues, Mint and Veli, to form a tripartite complex. *In vitro* biochemical experiments suggest that this complex associates with neuronal-specific presynaptic voltage-gated calcium channels (Butz et al., 1998; Maximov et al., 1999). CASK has also been shown to interact with the heparan sulfate proteoglycans syndecans, junctional adhesion molecule and Rabphilin3a; the latter two interactions suggest that CASK is also involved in stabilizing vesicle exocytosis (Hauser et al., 1997; Hsueh and Sheng, 1999a; Hsueh et al., 1998; Martinez-Estrada et al., 2001; Zhang et al., 2001).

One of the mammalian homologues of the *Drosophila* tumor suppressor gene Discs Large is hDlg/SAP97 (hereafter referred to as Dlg), which is another member of the MAGUK family. Dlg contains 3 PDZ domains and has been well characterized at synapses in the central nervous system. One of the most prominent examples of clustering activity of PDZ domains has been shown at the *Drosophila* larva glutamatergic neuromuscular junction (NMJ). In wild-type flies, Shaker-type K^+ channels are clustered at the NMJ. In these studies, various Dlg mutations caused Shaker-type K^+ channels to be mislocalized to the extrajunctional regions and muscle membrane, rather than clustered at the NMJ (Tejedor et al., 1997). Mammalian Dlg homologues, including PSD-95, have also been shown to interact with the NMDA-type glutamate receptors via

their PDZ domains (Kim et al., 1996; Kornau et al., 1995; Muller et al., 1996). Recently, several studies have demonstrated an interaction between Dlg and CASK. One study conducted in the Caco-2 intestinal epithelial cell-line demonstrated an interaction between the GK domain of CASK and the SH3 domain of Dlg. More recently, two other studies have shown that an interaction also occurs between the L27 domain of CASK and the N-terminus of Dlg; this interaction is stronger than the interaction between the GK and SH3 domains (Chetkovich et al., 2002; Lee et al., 2002; Nix et al., 2000).

Both CASK and Dlg also play a critical biological role in mammals. Laverty et. al. showed that disruption of the murine CASK locus by transgenic insertion resulted in cleft palate and death within 24 hours of birth. Similarly, Dlg lacking the SH3 and GK domains results in cranial dysmorphogenesis, as well as cleft palate and perinatal death in mice (Caruana and Bernstein, 2001; Laverty and Wilson, 1998).

Studies at glutamatergic synapses in both the mammalian central nervous system and in *Drosophila* suggest a role for CASK and Dlg as important scaffolding molecules. However, it is unknown whether PDZ proteins play a similar role at the cholinergic mammalian NMJ. We therefore investigated whether CASK and Dlg might play a role at this cholinergic synapse. We have previously demonstrated that Dlg is present in skeletal muscle and localizes to the NMJ (Rafael et al., 1998a). We now show that CASK is also expressed in mature skeletal muscle and localizes to the NMJ. Furthermore, confocal analysis of CASK and Dlg immunolocalization demonstrates that these proteins are enriched postsynaptically at the NMJ. Immunoprecipitation data demonstrates that CASK and Dlg associate in skeletal muscle, providing evidence for a MAGUK complex at the mammalian NMJ.

Materials and Methods

Immunohistochemistry and Confocal Microscopy

Immunohistochemistry for CASK detection was performed on unfixed 8-µm cryosections of quadriceps muscles. Quadriceps muscles were dissected from either 10-week-old C57BL/10 mice or adult rats and frozen in OCT (VWR, West Chester, PA) in isopentane cooled by liquid nitrogen. Sections were blocked in 1% gelatin in Hartman's phosphate-buffered saline (KPBS) for 15 minutes. Following blocking, sections were washed and incubated for two hours with either an affinity-purified rabbit polyclonal antibody raised against CASK (Zymed, San Francisco, CA) for mouse sections, or a mouse monoclonal CASK antibody (Chemicon, Temecula, CA) for rat sections. Sections were then washed and incubated for 1 hour in Cy3-conjugated goat anti-rabbit or anti-mouse (Jackson Immunoresearch, West Grove, PA). All antibodies were diluted in KPBS and 0.5% gelatin (KPBSG) + 1% normal goat serum (NGS). Dilutions were as follows: CASK 1:30, Cy3 anti-rabbit 1:200 and Cy3 anti-mouse 1:400. Alexa 488 α-bungarotoxin (Molecular Probes, Eugene, OR) was diluted 1:1000 in the secondary antibody dilution for the detection of acetylcholine receptors (AChR). The DNA dye DAPI was diluted 500 ng/ml in Vectashield (Vector Labs, Burlingame, CA) mounting media to stain for nuclei. Images were obtained using a Nikon Eclipse E800 microscope (Nikon Corporation, Tokyo, Japan), a SPOT-RT slider digital camera and SPOT software (Diagnostic Instruments, Inc., Sterling Heights, MI).

Immunohistochemistry experiments for confocal microscopy were conducted on fixed, transverse 8-µm cryosections of C57BL/10 mouse quadriceps muscle. Mouse

quadriceps were fixed in 1% formaldehyde in KPBS for 1 hour then placed in a 20% sucrose in KPBS solution overnight. Quadriceps were then placed in OCT on cork and frozen in liquid phase, liquid nitrogen-cooled isopentane. For immunohistochemistry, slides were equilibrated in KPBS, washed in 0.1M glycine in KPBS for 1-2 hours and then extracted for 5-15 minutes on ice with 0.5% Triton X-100 in KPBS. Following the triton extraction, slides were washed in KPBS and blocked for 1 hour with 1% gelatin in KPBS. Sections were then incubated overnight in primary antibody dilutions containing either an affinity purified polyclonal synaptophysin antibody (Novacastra, Newcastle upon Tyne, UK), a polyclonal CASK antibody, or a polyclonal Dlg antibody (gift from A. Chishti). Primary antibodies were prepared as described above with the following dilutions: synaptophysin 1:100, CASK 1:25, and Dlg 1:10,000. Following primary antibody incubation, slides were washed three times for 15 minutes in KPBSG plus 0.1% Tween-20 and then incubated with secondary antibody for 3 hours. Secondary antibody dilutions were prepared as described above. Cy3 anti-rabbit was used at a 1:1500 dilution and Alexa 488 α-bungarotoxin was diluted 1:200. Slides were again washed three times for 15 minutes in KPBSG plus 0.1% Tween-20 following secondary antibody incubation. Confocal analysis was conducted using a Zeiss 510 Meta Laser Scanning Microscope. All images were taken using the 63x objective and 3x zoom, the pinhole was kept constant for all images, and gain was adjusted for each image.

Mice were treated in accordance with the Institutional Laboratory Animal Care and Use Committee.

Immunoblots

Mouse quadriceps muscle and cardiac muscle from C57BL/10 mice were homogenized in Newcastle buffer and protein concentrations were determined using the Dc Protein Assay (Bio-Rad, Richmond, CA). Protein (100-µg) was then run out on 8% or 10% Sodium Dodecyl Sulfate- polyacrylamide gel electrophoresis (SDS-PAGE) gels at 80 V. We used KCl-washed membrane microsome preparations to enrich for membrane proteins as previously described (Ohlendieck et al., 1991). Triton-extracted microsomes were extracted with 1% Triton X-100. Proteins were transferred from SDS-PAGE gels to nitrocellulose (Schleicher and Schuell Bioscience, Keene, NH) at 80 V for 75 minutes on a wet-transfer apparatus. Western blots were first blocked in 5% nonfat milk in Tris-buffered saline plus 0.1% Tween-20 (TBST) and 1% NGS for 1 hour. Blots were then incubated in primary antibody diluted in TBST plus 1% NGS for 2 hours at the following dilutions: CASK polyclonal 1:250, CASK monoclonal 1:1000 and monoclonal Dlg 1:500 (Transduction Labs, Lexington, KY). Blots were then washed three times for 15 minutes in TBST and incubated with either HRP-conjugated goat anti-rabbit and HRP-conjugated goat anti-mouse secondary antibody (Jackson Immunoresearch, West Grove, PA) for 1 hour. Both secondary antibodies were diluted 1:10,000 in TBST plus 1% NGS. Enhanced chemiluminescence (ECL kit- Amersham Biosciences, Little Chalfont, UK) was used for detection of bound primary antibody.

For western analysis of the C2C12 mouse myogenic cell line, cells were grown in 100 mm plates (Nalge Nunc, Rochester, NY) in complete growth media (Dulbeccos' modified eagle media, 10% fetal bovine serum, 4 mM L-glutamine and 1%

penicillin/streptomycin); (Sigma, St. Louis, MO). After 4 hours, or 50 % confluency, the complete growth media was removed and replaced with differentiation media (Dulbecco's modified eagle media, 10% horse serum, 4 mM L-glutamine, and 1% penicillin/streptomycin). Cells were allowed to differentiate for 7 days post-media switch. Western analysis was conducted on myoblasts (pre-differentiation media) and Day 7 post-differentiation myotubes; cells were trypsinized, scraped from plates, and prepared as described above.

Immunoprecipitations

Immunoprecipitations were performed using Triton X-100 solubilized microsome preparations from 4-6 month old C57BL/10 mice in 0.3 M sucrose, 20 mM Tris maleate, pH 7.0, 10 mM NaHPO4, 5 mM EDTA, and 150 mM NaCl. Solubilized microsomes (30 µl) were preadsorbed with protein G sepharose (Amersham Biosciences, Little Chalfont, UK) for 1 hour, the supernatant was then incubated with 13 µl (3-13 µg) of antibodies against either a monoclonal CASK antibody (Chemicon, Temecula, CA), monoclonal Dlg, a monoclonal β-dystroglycan (Novacastra, Newcastle-upon-Tyne, UK), or a monoclonal dystrophin antibody (Novacastra) for ≥ 3 hours. The mixture was next incubated with protein G sepharose for 3 hours to overnight. Dystrophin and β-dystroglycan antibodies were used as the control immunoprecipitations for the CASK and Dlg immunoblots, respectively. The protein-bead suspension was then spun down and the supernatant kept as unbound. Beads were washed three times and boiled in 30 µl of Laemmli dye to release bound material, which was then run on an 8% or 10 % SDS-PAGE gel and immunoblotted as described above.

Results

CASK localizes to the neuromuscular junction

CASK is present at the presynaptic side of central synapses, as well as in lung, liver, and kidney, and interacts with Dlg (Hata et al., 1996a; Lee et al., 2002; Nix et al., 2000). In order to determine whether CASK protein is present in skeletal muscle, western analysis was performed on quadriceps muscle from C57 BL/10 mice. A band of the predicted 110 kDa size was detected in total skeletal muscle preparations by both a polyclonal CASK antibody (Fig. 1.1A) and a monoclonal CASK antibody (Fig. 1.2B). Analysis of CASK protein expression in membrane protein-enriched skeletal muscle microsome preparations showed that CASK is present at the skeletal muscle membrane, and is detergent-soluble with Triton X-100 (Fig. 1.1A and 1.1B). The presence of CASK protein in skeletal muscle was further confirmed by western analysis conducted on protein extracts from the C2C12 myogenic cell line; a band of the predicted 110 kDa size was detected in both myoblasts and to a greater extent in Day 7 post-differentiation myotubes (Fig. 1.1C). CASK was also found in membrane and nuclear-enriched fractions of mouse heart, which is the other type of striated muscle (Fig. 1.1A and 1.1B and data not shown).

To determine where CASK protein is localized in skeletal muscle, we performed immunohistochemical analysis on cryosections of mouse quadriceps muscle. Immunofluorescence showed that CASK co-localized with acetylcholine receptors at the NMJ, and is also present at lower levels in a subset of nuclei (Fig. 1.2A). Additional immunohistochemical analysis was conducted in the tibialis anterior, soleus, extensor

digitorum longus and diaphragm muscles, and on rat quadriceps muscle sections with a CASK monoclonal antibody; these experiments confirmed CASK localization at the NMJ in concordance with what was observed in mouse quadriceps muscle (data not shown and Fig. 1.2 B).

CASK and Dlg are enriched postsynaptically in vivo at the NMJ

The vertebrate NMJ is composed of the muscle fiber, motor neuron axon terminal, and Schwann cell (Sanes and Lichtman, 1999). Western analysis and immunolocalization demonstrate that CASK and Dlg are present in skeletal muscle and enriched at the NMJ *in vivo*; however these data did not definitively identify whether CASK and Dlg are localized to the pre or postsynaptic membrane of the NMJ *in vivo*. We therefore utilized confocal microscopy to compare the localization of CASK and Dlg to synaptophysin, a presynaptic axon terminal marker, and acetylcholine receptors (AChR), a postsynaptic marker.

Confocal immunohistochemical analysis was conducted on fixed transverse sections of mouse quadriceps muscle. As a point of reference, all sections were stained with Alexa 488 α-bungarotoxin to label AChRs, which are found post-synaptically in the primary folds of the muscle fiber at the NMJ. In analyzing the confocal immunohistochemical data, staining on the muscle side of the α-bungarotoxin staining or co-localized with α-bungarotoxin is postsynaptic. Conversely, staining on the axon terminal side of the α-bungarotoxin staining at the NMJ is presynaptic. We analyzed the localization of each protein at 10-15 NMJs; representative images are shown in Figure 1.3. All NMJ images are shown in side view so that pre and postsynaptic sides of the NMJ are easily distinguished.

We first conducted confocal immunohistochemical analysis with a control antibody against synaptophysin. Synaptophysin is a presynaptic vesicle protein that is present in the axon terminal and serves as a presynaptic marker (Buckley and Kelly, 1985; Trinidad et al., 2000). As predicted, synaptophysin is localized to the presynaptic side of the AChRs in all NMJs analyzed (Fig. 1.3A). We then carried out the same experiment with antibodies against CASK and Dlg. CASK protein localized both pre- and postsynaptically. CASK localization was observed on the postsynaptic side of every NMJ analyzed, especially in the primary gutter region, co-localized with α-bungarotoxin. CASK localization presynaptically varied in terms of expression levels in different NMJs. At some NMJs, CASK showed almost equal distribution pre- and postsynaptically (Fig. 1.3B), whereas in other instances most CASK staining was postsynaptic. Figures 1.3B-D demonstrate this variability. In contrast to CASK localization, Dlg localization at all NMJs was predominantly postsynaptic. The majority of Dlg staining is seen directly beneath the primary gutter region in the secondary folds (Fig. 1.3E). However, small amounts of Dlg were also observed on the presynaptic side of every NMJ analyzed (arrow).

CASK and Dlg form a PDZ domain protein complex at the NMJ

Since CASK and Dlg interact *in vitro*, we investigated whether these proteins interact with each other at the NMJ. We performed immunoprecipitations with CASK and Dlg antibodies on Triton X-100 solubilized membrane protein-enriched microsome preparations from mouse skeletal muscle. A monoclonal CASK antibody is able to co-immunoprecipitate Dlg (Fig. 1.4B), and conversely, a monoclonal antibody against Dlg is able to co-precipitate CASK (Fig. 1.4A). The control immunoprecipitations performed

with unrelated antibodies did not co-precipitate CASK or Dlg (Fig. 1.4A,B, control IP lane), and reciprocal immunoprecipitations with CASK and Dlg antibodies did not co-precipitate β-dystroglycan (data not shown). As a positive control, the β-dystroglycan antibody that is unable to precipitate Dlg is able to precipitate itself (Fig. 1.4C). These data suggest that CASK and Dlg form a complex at the NMJ.

Discussion

We have shown two PDZ domain-containing MAGUKs, CASK and Dlg, to be present in skeletal muscle and localize to the NMJ. The presence of CASK in skeletal muscle was confirmed by western analysis in the myogenic C2C12 cell line; CASK expression was observed to be greatly increased in differentiated myotubes compared with myoblasts. Confocal microscopy data demonstrated that both CASK and Dlg are enriched at the postsynaptic membrane of the NMJ, but that both CASK and Dlg are also present in small amounts presynaptically, suggesting these proteins are also present in the axon terminal. CASK and Dlg can be co-precipitated from mouse skeletal muscle samples, showing that they form a complex at the NMJ. However, it is unclear whether this complex is forming presynaptically or under the primary gutter where the two proteins co-localize. Since both pre- and postsynaptic membrane components are present in membrane preparations of total skeletal muscle, immunoprecipitated complexes from both locations are possible.

At the mammalian neuromuscular junction AChRs interact with rapsyn and MUSK, as well as the utrophin-associated complex, to form a scaffold at the NMJ (reviewed elsewhere (Sanes and Lichtman, 1999)). *In vitro*, members of the AChR and

utrophin complex can be clustered by an isoform of the molecule agrin, forming an aneural pseudo-NMJ (Burden, 1998; Meier et al., 1996). However, experiments conducted in the mouse myogenic C2C12 cell line have demonstrated that neither CASK nor Dlg is clustered in response to agrin (J.L.S. and J.A.F., data not shown). These data suggest that this newly identified PDZ domain protein complex is independent of the AChR and utrophin-associated complexes. Furthermore, since CASK and Dlg are MAGUKs that have multiple protein-protein interaction domains, and previous work has shown the PDZ domains are not involved in their interaction, it is likely there are still other members of this complex yet to be identified (Nix et al., 2000). This newly identified NMJ PDZ domain protein complex may serve to anchor channels and receptors at the NMJ, and may be involved in multiple signal transduction pathways, similar to the roles of these proteins in other systems. Channels and receptors that may be organized by this complex include K+ and calcium channels, which have been shown to bind to Dlg and CASK, respectively (Maximov et al., 1999; Tejedor et al., 1997). Another receptor candidate are glutamatergic NMDA receptors, which bind Dlg at central synapses (Dong et al., 1997; Kornau et al., 1995; Wyszynski et al., 1998). These receptors have not been extensively studied at the NMJ, as the NMJ is considered a classic cholinergic synapse; but they are present there and have an uncertain role (Grozdanovic and Gossrau, 1998) (J.L.S. and J.A.F., unpublished data). It is possible that the CASK-Dlg complex is involved in the clustering of these receptors and channels at the NMJ, similar to the roles of these proteins in the brain.

Overall, these studies suggest a role for CASK and Dlg in both developing and adult skeletal muscle. The discovery of a PDZ domain complex provides new insight

into the basic structure and biology of the mammalian NMJ and alterations in these proteins could cause abnormalities of muscle function by disruption of the channels and receptors they bind.

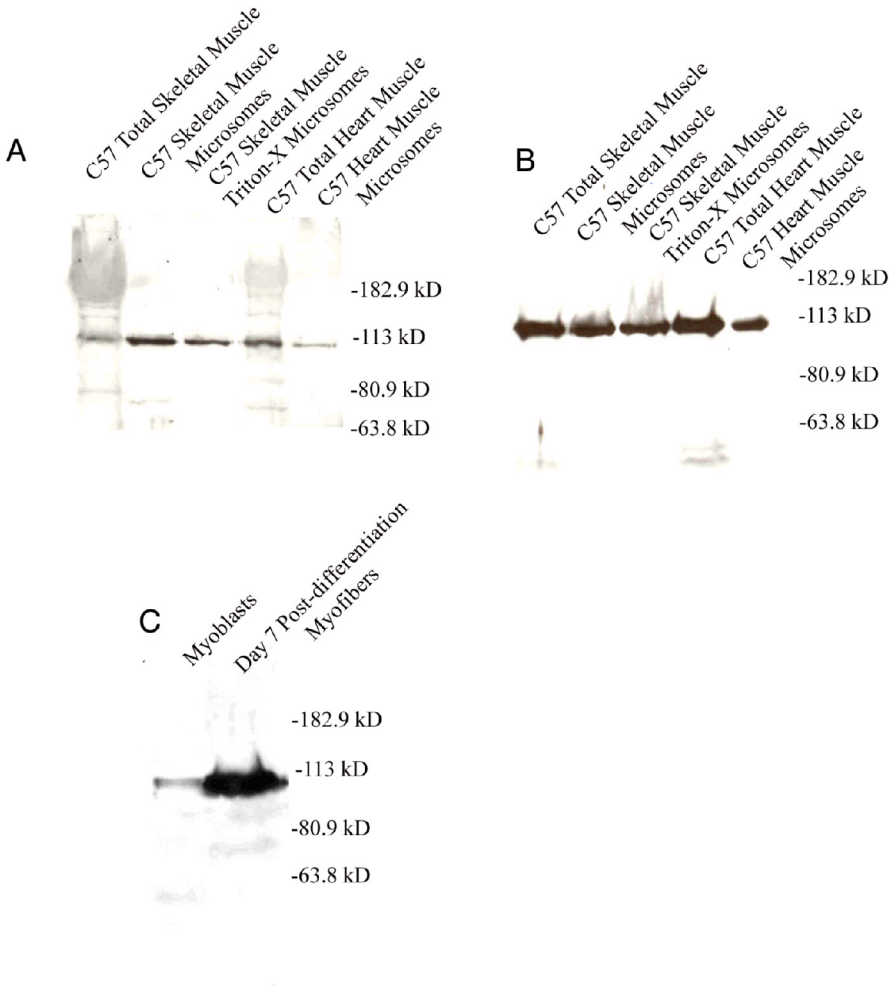

Figure 1.1: Western analysis of CASK in skeletal and cardiac muscle

(A) An affinity-purified polyclonal antibody raised against CASK and (B) CASK monoclonal antibody detect a 110 kD band on a western blot containing total protein from skeletal muscle, corresponding to the reported size for CASK in rat brain. CASK is present in membrane protein microscome preparations and can be solubilized with the non-ionic detergent, Triton X-100. CASK is also present in protein extracts from cardiac muscle and is enriched in cardiac muscle membrane preparations. (C) A 110 kDa band corresponding to CASK is also present in C2C12 cell protein extracts and shows an increase of protein expression in Day 7 post-differentiation myotubes compared with myoblasts.

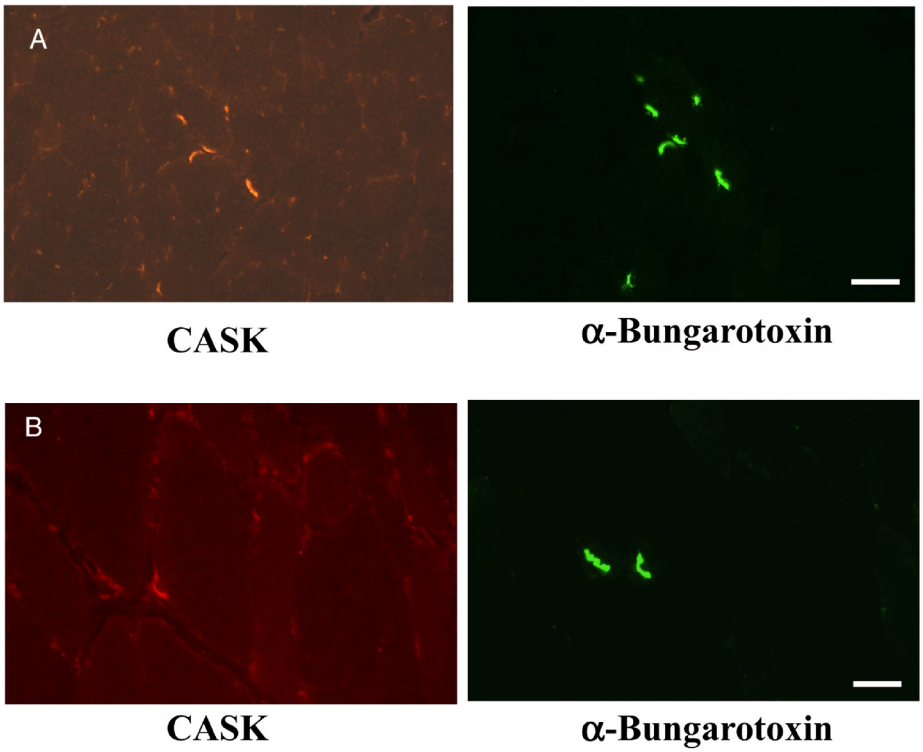

Figure 1.2

Figure 1.2: Immunolocalization of CASK in C57 mouse quadriceps muscle

(A) Immunostaining of cross-sections from wild-type mouse quadriceps muscle demonstrates that CASK (red) co-localizes specifically to the neuromuscular junction with Alexa-488 α -Bungarotoxin-labeled acetylcholine receptors (green). CASK is also present at lower amounts in a subset of nuclei. (B) Immunostaining of rat quadriceps muscle with a CASK monoclonal antibody confirms co-localization of CASK with acetylcholine receptors at the NMJ in skeletal muscle. Bar, 44 μm

Figure 1.3 A-E. CASK and Dlg are enriched postsynaptically at the NMJ

Immunostaining of fixed wild-type mouse quadriceps muscles followed by confocal microscopy shows the localization of synaptophysin, CASK and Dlg (red) relative to Alexa 488 α-bungarotoxin-labeled acetylcholine receptors (green). The α-bungarotoxin (α-BT) and Cy3 columns are single channel images taken under the excitement of 488 nm and 543 nm wavelength lasers, respectively. The third column is a merged image of the α-BT and Cy3 channels. The presynaptic and postsynaptic sides of the NMJ are designated "Pre" and "Post" in the merged images. The last column shows schematics of the observed green and red staining for each set of images in the context of the axon terminal, primary gutter, and secondary folds. Relative protein levels are depicted by the thickness of the red lines. (A) Synaptophysin staining is found exclusively presynaptically at the axon terminal. AChRs are present in the primary gutter of the postsynaptic membrane. (B-D) CASK staining is enriched postsynaptically in the primary gutter region, coincident with α -bungarotoxin staining (co-localization appears as lime-green to yellow in the merged image). The presynaptic localization and expression of CASK is variable. In panels B and C, CASK expression appears equal pre- and postsynaptically, whereas in panel D CASK localization is almost entirely postsynaptic. (E) Dlg localization is almost entirely postsynaptic and is enriched in the secondary folds of the NMJ. However, low levels of Dlg are present presynaptically (arrow). Bar, 25 nm

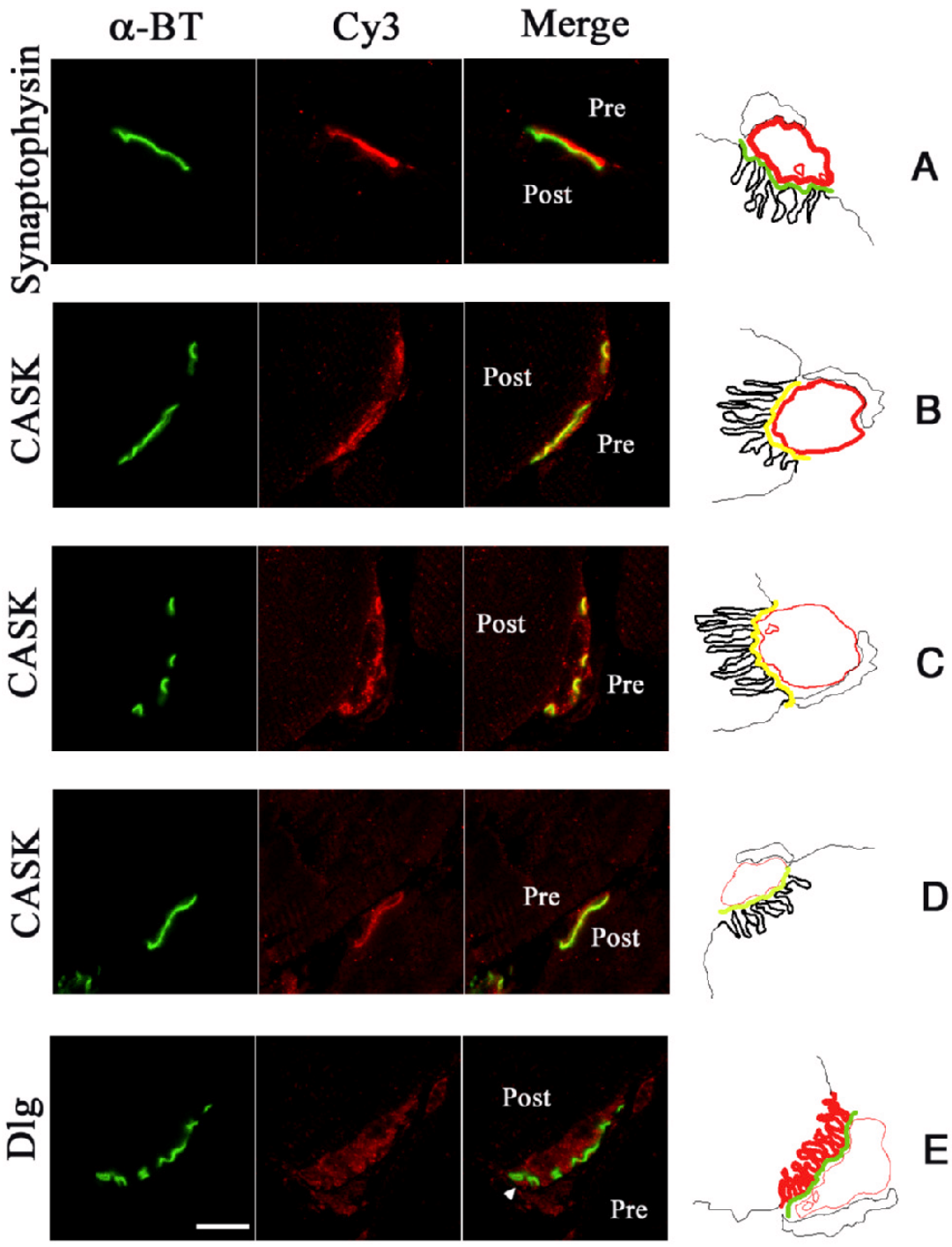
α-BT
Cy3
Merge
Synaptophysin
CASK
CASK
CASK
Dlg
Pre
Post
Post
Pre
Post
Pre
Pre
Post
Post
Pre
A
B
C
D
E

Figure 1.3 A-E

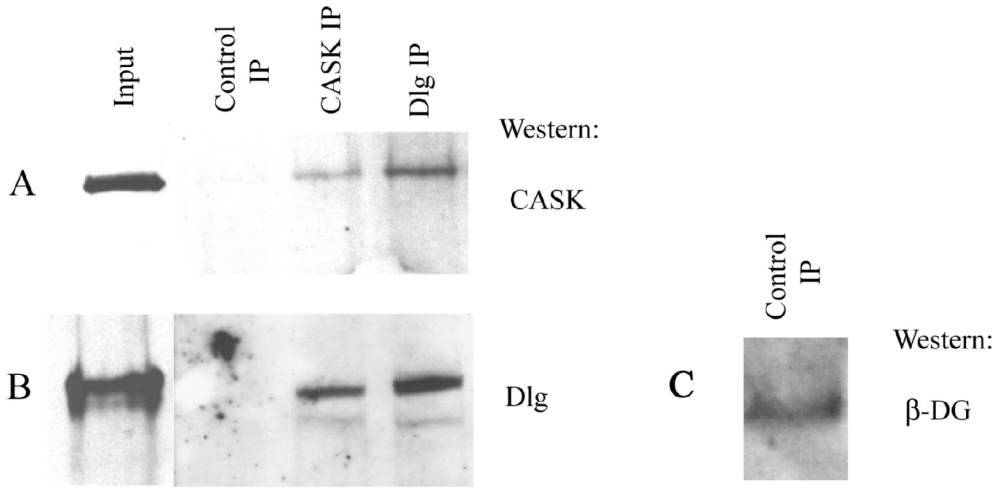

Figure 1.4 A-C CASK and Dlg co-immunoprecipitate from mouse quadriceps muscle

Immunoprecipitations were performed with CASK, Dlg or a unrelated control antibody; bound material from each precipitation was run side by side on SDS-polyacrylamide gels. Proteins were then transferred to nitrocellulose and probed with antibodies to either CASK or Dlg (western - labelled on right). (A) CASK can be co-precipitated by CASK and Dlg, but not an unrelated antibody (control IP). (B) CASK and Dlg antibodies both co-precipitate Dlg, but Dlg is not precipitated by the control antibody (control IP). (C) A control experiment shows that an antibody against β-dystroglycan that is unable to precipitate Dlg in panel B, is able to precipitate itself.

CHAPTER 2

Characterization of CASK and Dlg in the skeletal muscle C2C12 cell line

Introduction

CASK, Ca+/Calmodulin associated serine kinase, is a membrane associated guanylate kinase that is present at points of cell contact in epithelial cells and at synapses in the central nervous system. Recently, in addition to its role at cell junctions, CASK was unexpectedly shown to be involved in transcription by binding to TBR-1, a T-box transcription factor. In co-transfection assays, CASK protein is redistributed from the cytoplasm to the nucleus when co-expressed with TBR-1 in COS cells and cultured hippocampal neurons (Hsueh et al., 2000). In the nucleus, the CASK/TBR-1 complex binds to its target DNA sequence, the T-element, to promote transcription of T-element containing genes. The CASK-TBR-1 complex has also been shown to interact with a novel nucleosome assembly protein, CINAP. Together, this CASK-TBR1-CINAP ternary complex is able to promote transcription of the reelin gene and NR2B, an NMDA receptor subunit (Hsueh et al., 2000; Wagner et al., 1993; Wang et al., 2004a; Wang et al., 2004b). Experiments conducted by Schuh et. al. have also suggested that T-element dependent transcription can be altered by expression of the CASK Ca+ channel interactor, PMCA4b (Schuh et al., 2003).

In addition to being present at epithelial cells and synapses in the CNS, we have recently shown that CASK is also present in skeletal muscle and is specifically localized to the postsynaptic membrane of the neuromuscular synaptic junction, as well as a subset of nuclei, as described in Chapter 1 (Sanford et al., 2004). The NMJ has been used as a model for understanding synaptic transmission at both peripheral and central nervous system synapses (for review see (Meier and Wallace, 1998; Sanes and Lichtman, 1999)). Compared to central nervous synapses, the NMJ is easily accessible and has hence been the subject of intense investigation. The focus of these studies has been to elucidate the molecular mechanisms of synapse formation, synaptic transmission and resultant signal transduction pathways. The NMJ constitutes a functional motor unit capable of reliable excitatory synaptic transmission which occurs via the release of acetylcholine from the presynaptic motor neuron. Postsynaptically, the muscle fiber is highly structured at the point of nerve contact, consisting of deep invaginations, or folds. Interactions between the basal lamina, adhesion molecules and members of the cytoskeleton, such as utrophin and dystroglycans provide structural integrity to these postsynaptic folds (Banks et al., 2003; Luo et al., 2003; Meier and Wallace, 1998; Patton, 2003; Sanes and Lichtman, 1999). Embedded in distinct subcellular domains of this postsynaptic apparatus are various signaling molecules, including sodium channels and acetylcholine receptors. Acetylcholine receptors are optimally positioned at the crests of these folds, a region known as the primary gutter, which ensures fast and efficient synaptic transmission. Postsynaptic differentiation and clustering of postsynaptic components is initiated primarily through the release of agrin from the motor neuron (Ruegg and Bixby, 1998; Sanes and Lichtman, 1999). Agrin is a heparan sulfate proteoglycan whose receptor,

MuSK initiates a cascade of signaling events and transcriptional activity that results in accumulation of AChR and utrophin associated complexes at the site of nerve muscle contact, *in vivo* (Burden, 1998; Nawrotzki et al., 1998; Ruegg and Bixby, 1998). *In vitro*, a motor neuron agrin isoform, when included in cell culture media, can cluster all the members of these complexes, forming an aneural pseudo-neuromuscular junction in C2C12 myotubes (Burden, 1998).

In our previous analysis of CASK in skeletal muscle we employed confocal microscopy to determine the subcellular distribution of CASK at the neuromuscular junction. CASK protein was found to be present both presynaptically and postsynaptically. Postsynaptically, CASK is co-localized with AChRs at the crests of folds in the primary gutter. Our initial analysis of CASK in skeletal muscle also revealed that CASK interacts *in vivo* with Dlg at the NMJ (Sanford et al., 2004). Interestingly, Dlg localizes subcellularly to the secondary folds of the NMJ, with a slight amount of presynaptic localization (Sanford et al., 2004) .

In order to further characterize the CASK protein, and its interactor, Dlg, at the pre- and postsynaptic components of the NMJ we have currently undertaken an investigation into the expression and localization of these proteins in the C2C12 mouse myogenic cell line. We demonstrate that CASK is expressed in a developmentally specific manner in the C2C12 cell line. CASK protein localization moves from the nucleus to the cytoplasm as C2C12 myoblasts fuse into mature myotubes. In mature myotubes, CASK is completely excluded from the nucleus. Western analysis confirmed that there is not a switch in CASK isoforms as differentiation of C2C12 myoblasts into myotubes

progresses. Unlike CASK, Dlg is localized only in the cytoplasm of C2C12 cells throughout their development. Finally, our *in vitro* C2C12 data also demonstrated that neither CASK, nor Dlg, is clustered to AChR complexes in response to agrin or laminin treatment.

Materials and Methods

Cell culture and Immunocytochemistry

The mouse myogenic cell line C2C12 was grown in plastic 2-chambered tissue-culture slides (NalgeNunc, Rochester, NY) in complete growth media (Dulbecco's Modified Eagle Media, 10% Fetal Bovine Serum, 4mM L-glutamine and 1% Pennicillin/Streptomyocin) (Sigma, St. Louis, MO). After 4 hours, or 50% confluency, the complete growth media was removed and replaced with differentiation media (Dulbecco's Modified Eagle Media, 10% horse serum, 4mM L-glutamine and 1% Pennicillin/Streptomyocin). Immunocytochemistry on C2C12 cells was conducted pre-differentiation and every 24 hours post-differentiation for 7 days. For immunocytochemistry, cells were fixed with 3.7% formaldehyde, rinsed and extracted with 0.5% Triton-X 100. Cells were then blocked with 1% NGS in KPBS for 30 minutes. Following blocking, cells were washed again and incubated overnight with primary polyclonal CASK antibody (1/50) (Zymed, San Francisco, CA), a monoclonal Dlg antibody (1/50) (Transduction Labs, Lexington, KY) or a monoclonal β-DG antibody (1/50) (Novacastra, Newcastle upon Tyne, England) diluted in KPBSG + 1% NGS + 0.1% Tween-20. Images of the cells were obtained using a Nikon Eclipse E800 microscope (Nikon Corporation, Tokyo, Japan), a SPOT-RT slider digital camera and

SPOT software (Diagnostic Instruments, Inc., Sterling Heights, Michigan). Exposure times for the images were cut in half after days 3 and 5 post-differentiation. For agrin treatment, cells were treated with the motor neuron secreted form of agrin (R&D Systems, Minneapolis, MN) at 6 days post-differentiation for 20 hours. For laminin treatment, cells were treated at 5 days post-differentiation for 24 hours with 100 nM laminin (BD BioSciences, Bedford, MA). After agrin or laminin treatment, cells were fixed and stained as described above with the exception of the addition of Alexa 488 α-bungarotoxin (Molecular Probes, Eugene, OR) to the secondary antibody dilution for the detection of AChR. The DNA dye DAPI was diluted to 500 ng/ml in Vectashield (Vector Labs, Burlingame, CA) mounting media to stain for nuclei.

Immunoblots

For western blot analysis of the C2C12 mouse myogenic cell line cells were grown in 100-mm plates, (Nalge Nunc, Rochester, New York) in complete growth media and then induced to differentiate as described above. Protein was harvested from C2C12 cells at the myoblast stage and every day post-differentiation through day 7 for western analysis. Protein was collected from both cell lines by trypsinizing plates, pelleting the cells at 1000 RPM for 10 minutes, and resuspending the cells in Newcastle buffer (1M Tris, pH 6.8, 20% SDS, 8M urea). Total protein concentration was determined using the Dc Protein Assay Kit (Bio-Rad, Richmond, CA). 50 μg of protein was then run out at 80V on an 8% sodium dodecyl sulfate-polyacrylamide gel. Protein was then transferred to a nitrocellulose membrane, using a wet transfer apparatus, at 80V for 70-90 minutes. Western blots were then blocked for 2 hours in 5% nonfat milk in tris-buffered saline

plus 0.1% tween (TBST) and 1% normal goat serum (NGS). Membranes were incubated in primary antibody diluted in TBST plus 1% NGS for 2 hours at the following dilutions: monoclonal CASK 1:500 (Chemicon, Temecula, CA) and polyclonal Dlg 1:500 (kind gift from A. Chishti). Blots were then washed 3 X 15 minutes in TBST and incubated with either HRP conjugated goat α mouse or α rabbit secondary antibodies (Jackson Immunoresearch, West Grove, PA) at a 1:10,000 dilution in TBST plus 1% NGS. ECL chemiluminescence (ECL kit; Amersham Biosciences, Little Chalfont, United Kingdom) was used for the detection of bound primary antibody.

Results

CASK localization is developmentally regulated in the C2C12 skeletal muscle cell line

We assessed the developmental expression and localization of CASK as replicating myoblasts matured into multi-nucleated terminally differentiated myotubes. Myoblasts were induced to form mature myotubes by changing from complete growth media to differentiation media. Cells were then subjected to immunocytochemical analysis every 24 hours post-differentiation media for 7 days. We observed that at the myoblast stage CASK is found almost exclusively in the nucleus of C2C12 cells (Fig. 2.1A). As myoblasts fuse and mature into multi-nucleated myotubes, CASK begins to slowly move out of the nucleus and into the cytoplasm by day 3 post-differentiation (Fig. 2.1A). By day 5/6 post-differentiation, CASK is seen almost exclusively in the cytoplasm and appears excluded from the nucleus (Fig. 2.1A). Lastly, confocal images for the C2C12 cells at day 6 post-differentiation confirmed that the CASK localization in mature myofibers was cytoplasmic (Fig. 2.1B). Furthermore, immunoblots of purified nuclear

and cytoplasmic fractions of C2C12 cells, probed with a monoclonal CASK antibody, confirms the nuclear expression of the CASK protein at the myoblast stage and the cytoplasmic localization of CASK in mature myotubes (data not shown). We also analyzed the expression of Dlg in C2C12 cells from the myoblast stage through Day 7 post-differentiation. Unlike CASK, Dlg localization was cytoplasmic throughout development of C2C12 cells (data not shown).

Western analysis of the CASK protein in C2C12 cells and MN-1 cells

We next conducted western analysis to determine if CASK's movement from the nucleus to the cytoplasm is accompanied by a switch in CASK protein isoform and to ascertain whether CASK is upregulated during C2C12 differentiation. The major CASK isoform is 110 kDa, but there are also two reports of a smaller CASK isoform, of ~75 kDa in size (Cohen et al., 1998; Laverty and Wilson, 1998). Western analysis (conducted by Katherine Gardner) was conducted with both monoclonal (Fig. 2.2A) and polyclonal (Fig. 2.2B) CASK antibodies on C2C12 protein homogenates from myoblasts to Day 7 post-differentiation. The protein levels of the major 110 kDa CASK isoform were found at a constant level from myoblast through Day 7 post-differentiation (Fig. 2.2A and 2.2B). A second smaller CASK isoform of ~50 kDa is also present throughout differentiation; levels of this isoform appear to be reduced at Day 5-7 post-differentiation. This isoform may correspond to an alternatively spliced version of the CASK mRNA, but further experimentation will be needed to determine the exact nature of this smaller 50 kDa isoform. Overall, this western analysis reveals that the change in CASK localization in C2C12 cells is not accompanied by a change in CASK isoform expression.

CASK and Dlg are not co-clustered with acetylcholine receptor complexes upon agrin or laminin treatment

In an effort to further define the role of CASK at the NMJ, we wanted to determine if CASK is a component of the AChR complex. We treated six day post-differentiation myofibers with agrin to determine if CASK would co-cluster with AChR. β-dystroglycan is a member of the utrophin-associated complex at the NMJ and was included as a positive control since it is known to co-cluster with AChR complexes in response to agrin treatment (Nawrotzki et al., 1998). Immunofluorescence of agrin treated myotubes showed that, as expected, β-DG co-clustered with AChR (Fig. 2.3A). Our results showed that CASK is not co-clustered with AChR in response to agrin. To determine whether this result was specific for CASK or would apply to other NMJ-concentrated PDZ proteins, we also decided to analyze Dlg in this context. Like CASK, Dlg was not co-clustered with AChR complexes by agrin (Fig. 2.3A).

Laminins are proteoglycans that are a major structural component of basal lamina, including that of adult skeletal muscle. Several isoforms of laminin exist, each of which are expressed in a developmentally specific manner. Two such isoforms, laminin-1 and laminin 2/4 (merosin), are expressed in early in skeletal muscle development and have been shown to cluster AChRs via a signaling pathway that overlaps that of agrin in many ways, yet is distinct in that it is not dependent on MuSK (Marangi et al., 2002; Montanaro et al., 1998; Sugiyama et al., 1997). We therefore treated C2C12 cells at Day 5 post-differentiation with laminin to further examine possible mechanisms for CASK and Dlg clustering to AChR. The results of these experiments reveal that neither CASK,

nor Dlg, are clustered in response to laminin (Fig. 2.3B, data by KG). These experiments suggest that the CASK-Dlg protein complex is separate and independent of AChR and utrophin-associated complexes, respresenting a novel protein complex at the postsynaptic membrane of the NMJ.

Discussion

The findings of this chapter demonstrate that the CASK protein is developmentally regulated in the C2C12 skeletal muscle cell line. In myoblasts of C2C12 cells CASK is localized almost exclusively to the nucleus, however as myoblasts mature into myotubes, CASK protein moves from the nucleus to the cytoplasm. Western analysis reveals that this redistribution of CASK from the nucleus to the cytoplasm is not accompanied by a switch in CASK isoforms. Dlg expression in this mouse myogenic cell line is not developmentally regulated as it is localized in the cytoplasm from the myoblast to myotube stage. Notably, further studies conducted on C2C12 myotubes revealed that neither CASK, nor Dlg, are co-clustered with AChR in response to agrin or laminin treatment.

The morphology and formation of the postsynaptic apparatus of the NMJ is critical to gaining a more advanced understanding of synaptic transmission, both at the NMJ as well as CNS synapses. Moreover, alterations in NMJ molecular structure and neurotransmission are associated with a variety of neuromuscular disorders, including congenital myasthenic syndromes, myasthenia gravis, and various channelopathies (Boonyapisit et al., 1999; McConville and Vincent, 2002; Ptacek, 1997). It is well

established, that while skeletal muscle is to some extent pre-patterned to form NMJs, it is the release of agrin from the motor neuron, along with expression of the agrin receptor, MuSK, which is indispensable for generating a fully structured and functional postsynaptic apparatus (Luo et al., 2003; Madhavan and Peng, 2003; Zhou et al., 1999). *In vitro*, agrin recapitulates its *in vivo* effects, and triggers the clustering AChRs, along with the other major structural components of the postsynaptic apparatus, including the utrophin-associated complex (Ruegg and Bixby, 1998; Sanes and Lichtman, 1999). Therefore, it was intriguing to discover that neither CASK, nor Dlg, are clustered in C2C12 myotubes in response to agrin. These proteins are among only a handful of NMJ-specfic proteins that are not clustered in response to agrin. Furthermore, these proteins were also unresponsive to treatment with laminin. These data suggests that neither of these MAGUKs are involved in the initial formation of postsynaptic membrane architecture and are most likely recruited to the postsynaptic membrane by yet unidentified motor neuron signals. One possibility is that there is another trophic factor, similar to agrin or laminin, that induces these proteins to cluster at the postsynaptic membrane. Another possibility is that CASK and Dlg are clustered by signal transduction pathways initiated by synaptic transmission itself.

Interestingly, another MAGUK protein, Magi-1, is also present at the postsynaptic membrane of the NMJ in mature skeletal muscle and interacts with MuSK *in vivo* (Dobrosotskaya et al., 1997b; Strochlic et al., 2001). Similar to CASK and Dlg, Magi-1 is not clustered with AChRs in response to agrin treatment, suggesting that perhaps MAGUKs in general are recruited to the postsynaptic membrane by agrin-independent

mechanisms. Furthermore, despite the fact that MAGI-1 is not recruited in the initial postsynaptic assembly, it most likely still plays a significant role in NMJ biology as it interacts with MuSK and has been postulated to play a role in organizing and/or stabilizing subdomains of the postsynaptic apparatus (Strochlic et al., 2001). It is therefore possible that CASK and Dlg may also function in this same manner, stabilizing the postsynaptic apparatus and binding channels and receptors at the NMJ, analogous to their function at cell junctions and CNS synapses.

These studies also suggest a role for CASK in nuclei in skeletal muscle. *In vitro*, in C2C12 myoblasts CASK was found to localize almost exclusively to the nucleus, while *in vivo*, CASK is observed in a subset of nuclei in mature skeletal muscle (Sanford et al., 2004). Furthermore, work conducted in our laboratory has also examined the expression and localization of CASK and Dlg in the MN-1 motor neuron cell line in order to further understand the presynaptic localization of these proteins observed in the confocal analysis, described in Chapter 1. Immunofluorescence analysis conducted on day 3 post-differentiation MN-1 cells demonstrate that CASK is localized exclusively to the nucleus in some cells, while in other cells, CASK protein is observed in both the nucleus and the cytoplasm. Dlg is localized exclusively to the nucleus in this MN-1 cell line (Work done by KG).

Nuclear localization of MAGUK proteins is not unprecedented. Zonula occludens proteins (ZO-1, ZO-2 and ZO-3), one of the founding members of the MAGUK protein family, are well documented to translocate to the nucleus, containing both nuclear localization and export signals (Benmerah et al., 2003; Gonzalez-Mariscal et al., 1999;

Traweger et al., 2003). Furthermore, the Magi-1 protein also contains bipartite nuclear localization signals and has the ability to shuttle between the nucleus and the plasma membrane (Dobrosotskaya et al., 1997b; Strochlic et al., 2001). Alternatively spliced insertions of the hDlg protein, termed I2 and I3, and located in the HOOK region of the protein between the SH3 and GK domains, have been shown to contain putative nuclear localization amino acid signals (NLS) (Kohu et al., 2002; McLaughlin et al., 2002). Dlg isoforms containing these I2 and I3 insertions localize to distinct nuclear regions in both MCF10F and COS cells (Gonzalez-Mariscal et al., 1999; Kohu et al., 2002; McLaughlin et al., 2002). All tissues examined to date express the NLS containing alternatively spliced isoforms of Dlg including skeletal muscle; to our knowledge, peripheral motor neurons have not been examined in this context. It is perplexing that despite the fact that the NLS-containing Dlg isoforms are present in skeletal muscle, we have not observed any *in vivo* nuclear localization of Dlg in mature wild-type skeletal muscle (unpublished observations) and in C2C12 cells Dlg localization is cytoplasmic at all developmental stages. However, Dlg localization has been shown to localize to the nucleus of regenerating muscle fibers in the *mdx* mouse model of muscular dystrophy (Rafael et al., 1998a). In contrast to Dlg, the CASK protein has been observed *in vivo* in a subset of nuclei, but has not yet been shown to possess a nuclear localization or export signal sequence (Sanford et al., 2004). Strikingly, we have currently demonstrated that in the C2C12 mouse myogenic cell line, CASK is only present in the nucleus at the myoblast stage, while excluded from the nucleus in myotubes. At first glance, these results seem to conflict with our *in vivo* observations, however it is noteworthy that the C2C12 immunohistochemical analysis was conducted in aneural *in vitro* environment.

Therefore, it is conceivable that there are signals from the nerve that could cause nuclear localization *in vivo*, which are absent from the system used in these experiments. More generally, the C2C12 cultures are not likely to wholly mimick the biological and physiological environment of skeletal muscle *in vivo*. These issues may also account to some extent for our observations of the Dlg protein.

The nuclear localization observed for CASK is particularly interesting given that CASK has been shown to bind TBR-1, a T-box transcription factor. When CASK is co-expressed with TBR-1 in Cos-7 cells it translocates from the cytoplasm to the nucleus and binds to TBR-1 to act as a co-activator of transcription of T-element containing genes (Hsueh et al., 2000). However, when CASK is co-expressed with syndecan-3, CASK localizes with syndecan-3 in the cytoplasm (Hsueh et al., 2000). These studies show that the localization of CASK can be shifted between the nucleus and the cytoplasm by altering the balance of CASK binding partners. As previously discussed, the MAGUK proteins ZO 1-3 and Magi-1, are also able to move between the membrane and the nucleus (Dobrosotskaya et al., 1997a; Strochlic et al., 2001). Therefore, it has been proposed that perhaps some MAGUK proteins are in a unique position to transmit information from the membrane and/or cell junctions, such as tight junctions or chemical synapses, to the nucleus. CASK, a MAGUK and a co-activator of transcription, seems particularly well-suited to be involved in the transport of information from the NMJ to the nucleus. Further *in vivo* investigation into CASK and Dlg, including animal models, will be required to discover the exact structural and physiological roles these proteins

might be playing at both the pre- and postsynaptic components of the NMJ, and perhaps the nucleus, in skeletal muscle.

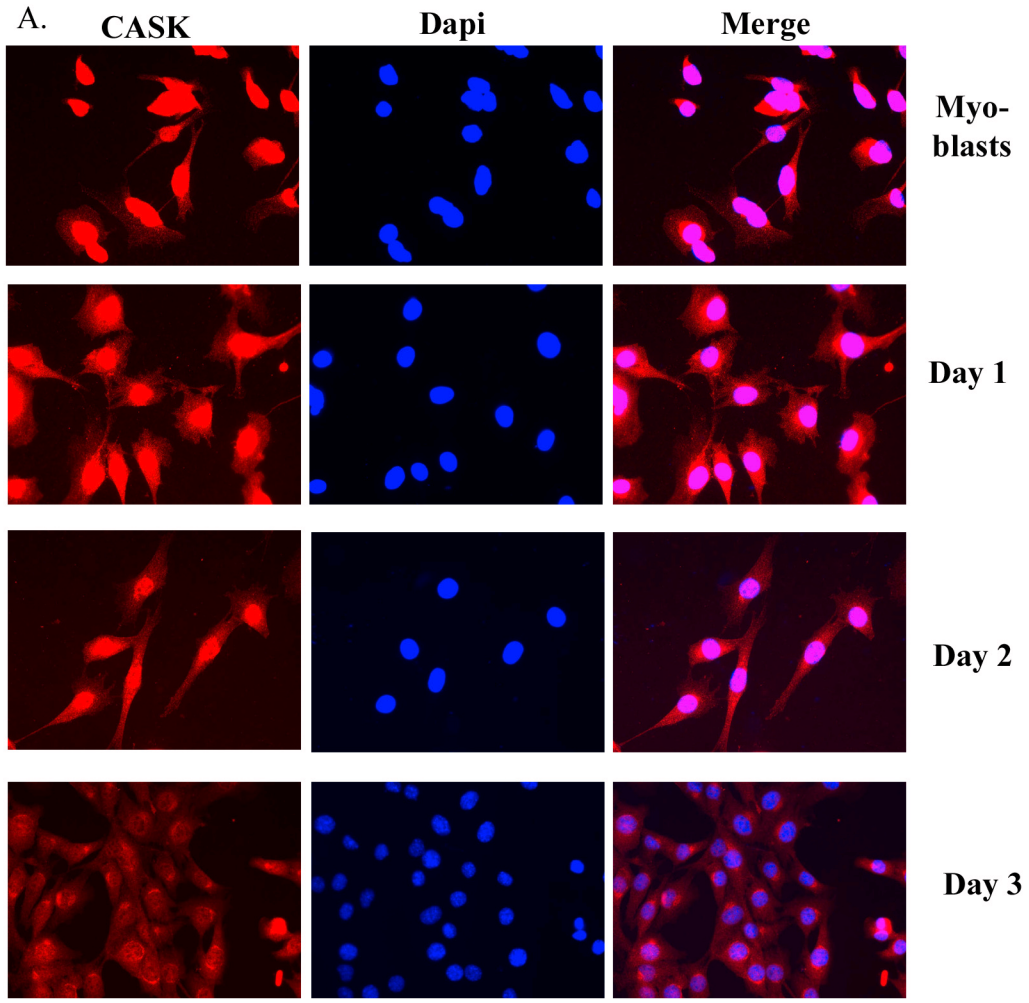

Continued

Figure 2.1 A-B: CASK localization in differentiating C2C12 myogenic cultures

(A.) CASK (red) localizes to the nucleus in cultured myoblasts. CASK translocates from the nucleus into the cytoplasm from Days 1-3 post-differentiation. By Day 4 post-differentiation, as myoblasts fuse into multinucleated myofibers, CASK no longer localizes to the nucleus. As the myofibers continue to mature through Day 7, CASK appears excluded from nuclei. Nuclei were labeled using the DNA stain DAPI (blue). Localization of CASK in the nucleus is shown in pink in the merged images (merge). Bar = 44 µm. (B.) Confocal microscopy analysis of Day 7 myotubes demonstrates that CASK (red) protein is excluded from the nucleus.

Figure 2.1 A-B continued

A.

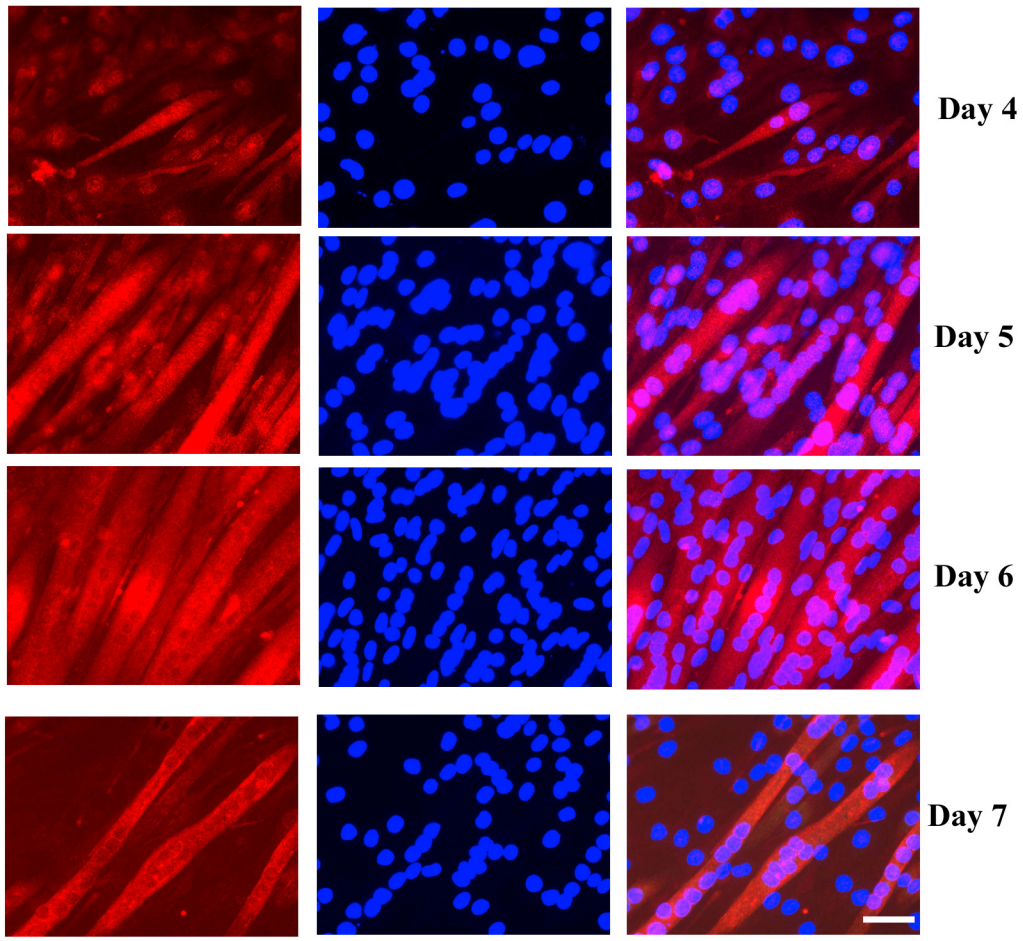

B.

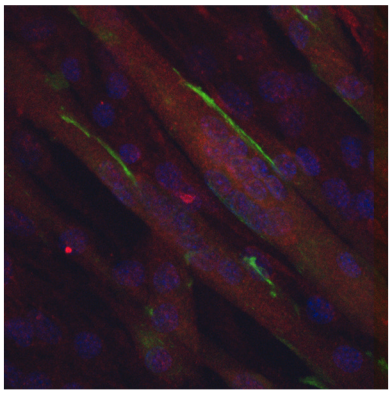

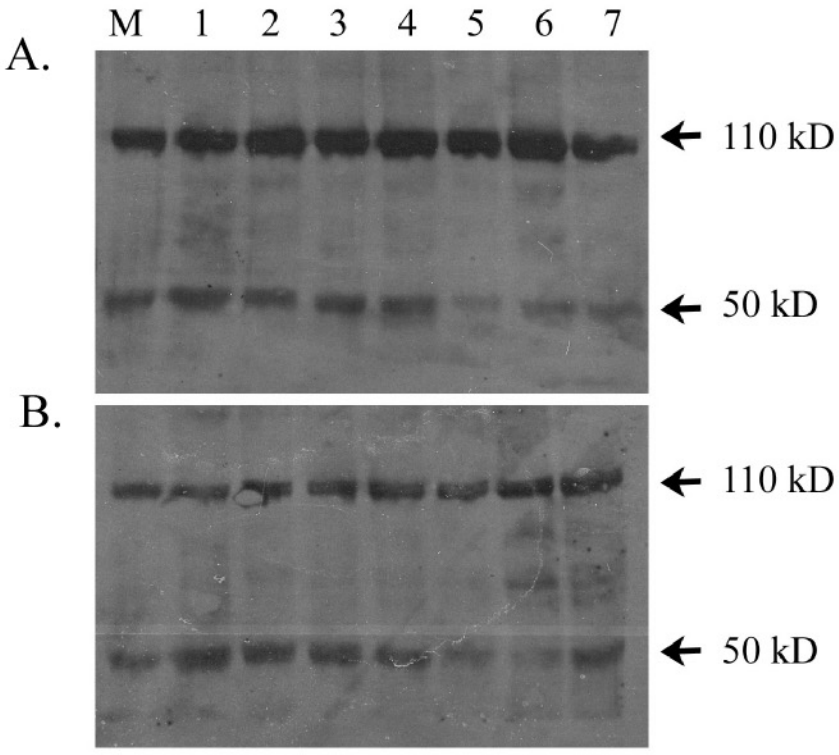

Figure 2.2 A-B: Western analysis of CASK in C2C12 cells, myoblasts through Day 7 post-differentiation

An affinity purified polyclonal antibody raised against CASK (A.) and a CASK monoclonal antibody detect a major 110 kDa isoform of CASK at all points at equivalent levels. A minor CASK isoform, ~ 50 kDa, was also detected at all time points by both CASK antibodies, with an apparent reduction in amount at Day 5 post-differentiation.

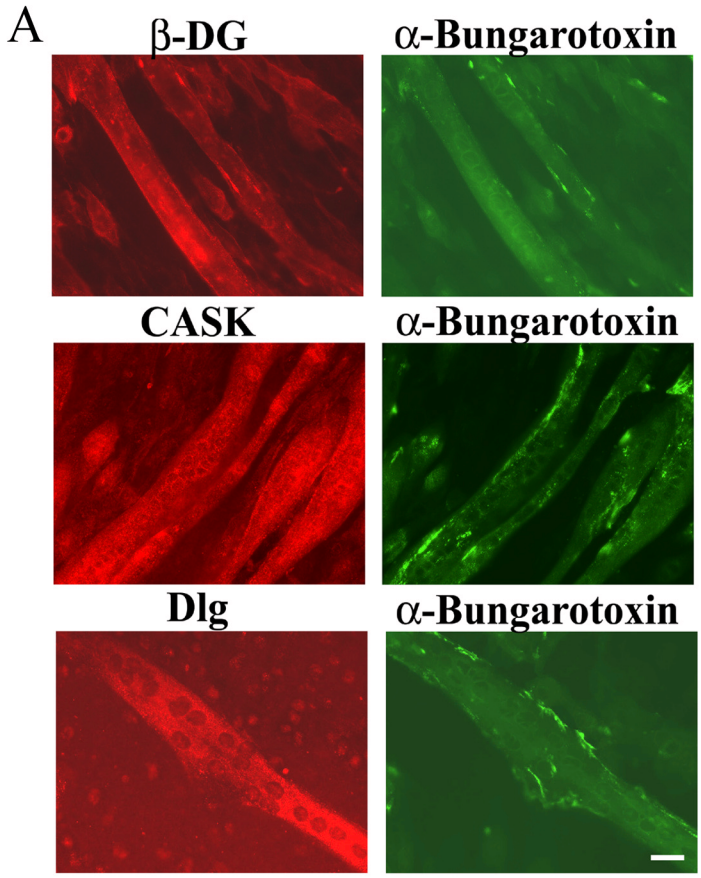

Continued

Figure 2.3 A-B: CASK and Dlg localization in agrin and laminin treated Day 6 C2C12 myotubes

Immunolocalization of CASK and Dlg (red) in C2C12 multi-nucleated myotubes were treated with the motor neuron secreted form of agrin (A) at 6 days post-differentiation, as well as laminin (B). The results demonstrate that these proteins are not co-clustered with α-Bungarotoxin labeled AChRs (green). β -DG was used as the positive control and did co-cluster with AChR (green) in response to agrin treatment. Bar = 60 μm

Figure 2.3 A-B continued

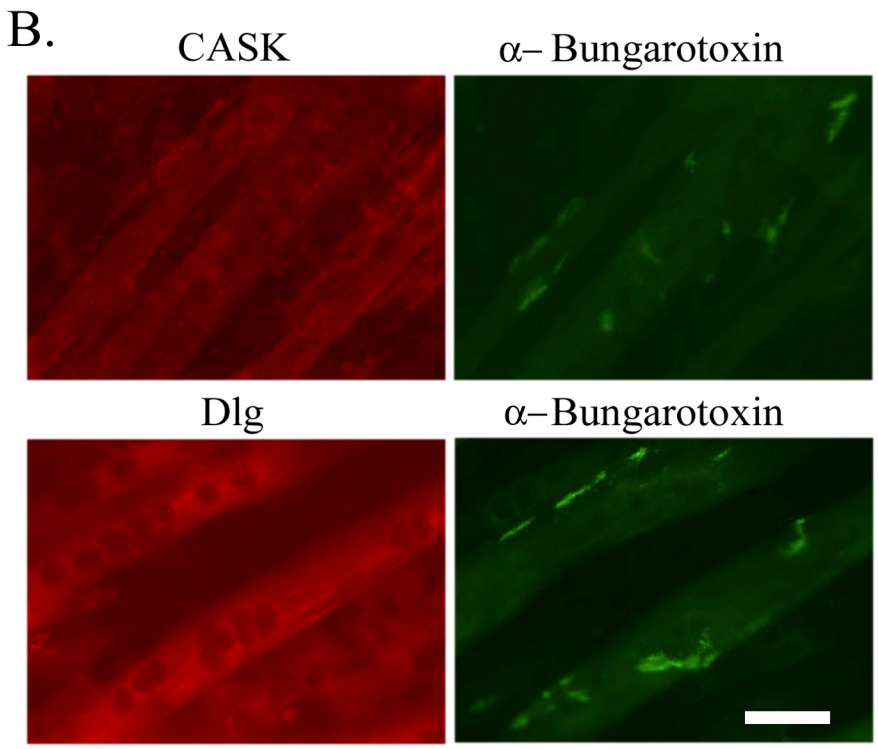

CHAPTER 3

TRANSGENIC OVEREXPRESSION OF A FULL-LENGTH CASK PROTEIN AND A TRUNCATED VERSION OF CASK PROTEIN IN SKELETAL MUSCLE

Introduction

The CASK protein is a member of the membrane associated guanylate kinase (MAGUK) family of proteins, whose protein structure consists of all the hallmark MAGUK domains: a PDZ domain, a Src homology 3 (SH3) domain and a guanylate kinase domain (GK) (Anderson, 1996; Fanning and Anderson, 1999). In CASK, the standard domains are accompanied by four additional domains: the CaMK domain, the HOOK domain and two L27 domains (Cohen et al., 1998; Doerks et al., 2000; Feng et al., 2004). CASK is the only known protein to possess this distinct combination of domains. Therefore, a knowledge of these domains is a prerequisite for understanding the protein as a whole.

The PDZ domain was originally identified in the PSD-95 protein, and was named for the first three proteins found to contain the domain: PSD-95, Discs Large (Dlg), and Zo-1 (for review see(Craven and Bredt, 1998; Fanning and Anderson, 1999; Garner et al., 2000; Kim and Sheng, 2004; Ponting et al., 1997)). The domain is among the most abundant in the mammalian genome. Despite the fact that it was first identified only ~10

years ago, the PDZ domain-containing proteins have rapidly become the focus of widespread investigation due to their ability to form large macromolecular complexes and to cluster channels and receptors. There are two chief factors that contribute to the scaffolding properties of PDZ domain-containing proteins. First, PDZ domains have shown the capacity to form homo- and/or heterodimers with themselves (Hsueh and Sheng, 1999b; Im et al., 2003a; Im et al., 2003b; Kim et al., 1996). Secondly, PDZ domains are often found in conjunction with other protein-protein interaction domains, as is the case for MAGUK protein family members (Fanning and Anderson, 1999; Garner et al., 2000). The PDZ domains cluster channels and receptors at sites of cell contact and synapses via consensus motifs located within the C-terminus of PDZ domain ligands (Fanning and Anderson, 1999; Garner et al., 2000; Kim et al., 1995; Kornau et al., 1997; Tejedor et al., 1997). Channels and receptors shown to interact with PDZ domains are numerous and include sodium channels, potassium channels, calcium channels, and ErbB receptors, as well as NMDA and AMPA receptors (Bassand et al., 1999; Cai et al., 2002; Gardoni et al., 2003; Kim et al., 1995; Kornau et al., 1995; Leonard et al., 1998; Leonoudakis et al., 2004; Leonoudakis et al., 2001; Muller et al., 1996; Nagano et al., 1998; Rumbaugh et al., 2003; Sans et al., 2001).

The SH3 and GK domains are found in tandem at the C-terminus of all MAGUKs, and recent crystal structure evidence suggests that these domains can form a single integrated unit. Neither the SH3, nor the GK domain, have been shown to possess any catalytic activity, suggesting they act solely as protein-protein interaction domains (McGee et al., 2001). In the case of the CASK protein, and other MAGUKs family members, such as hDlg/SAP97, there is a HOOK domain located in between the SH3 and

GK domain. The HOOK domain is responsible in many instances for providing a connection between MAGUKs and the cytoskeleton through binding to protein 4.1 (Cohen et al., 1998; Lue et al., 1996; Lue et al., 1994a; Marfatia et al., 1994; Marfatia et al., 1996). Interestingly, it has been shown that the SH3 and GK domains can interact with each other, both intermoleculary and intramolecularly, with the HOOK domain acting as a 'hinge' between the two domains (McGee et al., 2001). In fact, the GK domain of the CASK protein has been shown to interact with the SH3 domain of the hDlg/SAP97, as well as intramolecularly with its own SH3 domain (Nix et al., 2000). The intramolecular interaction between the SH3 and GK domains is unique to MAGUKs and is thought to confer a mechanism by which MAGUKs may self-regulate interactions with potential binding partners (McGee et al., 2001; Paarmann et al., 2002; Wu et al., 2000). For example, the closed intramolecular interaction between the SH3 and GK domain of hDlg/SAP97 is thought to inhibit its binding to GKAP (guanylate kinase interacting protein) (Wu et al., 2000).

The final two domains of the CASK protein to be discussed are the CaMK domain and the L27 domains. The CaMK domain is unique to the CASK protein and shares a high sequence similarity to the CaMK family of proteins. Examination of the CASK CaMK domain has found that this domain does not exhibit any kinase activity, but is able to bind calmodulin in a calcium dependent manner (Hata et al., 1996a). The L27 domain was initially identified in the *C. elegans* homologue of CASK, Lin-2, and was so named because it consists of the minimal sequence necessary for Lin-2 to bind Lin-7 (Doerks et al., 2000; Harris et al., 2002). Overall, the domain is not highly structured, but is able to heterodimerize, resulting in a helical structure (Feng et al., 2004; Harris et al., 2002).

Notably, the CASK protein contains two L27 domains, thereby conferring yet another means of protein-protein interaction (Doerks et al., 2000; Feng et al., 2004; Harris et al., 2002).

The distinct multidomain structure of the CASK protein serves to couple the protein to a diverse array of cellular activities. This is exemplified by CASK's participation in an evolutionarily conserved tripartite complex, present in both *C. elegans* and mammalian central nervous system synapses (Borg et al., 1998; Butz et al., 1998; Hoskins et al., 1996; Kaech et al., 1998; Maximov et al., 1999; Schuh et al., 2003). The tripartite complex was first characterized in *C. elegans*, and consists of Lin-2, the *C. elegans* homologue of CASK, along with Lin-7 and Lin-10 (Hoskins et al., 1996; Kaech et al., 1998). All three of the tripartite protein members were identified in genetic screens searching for mutations that perturbed normal vulval development in *C. elegans* (Ferguson and Horvitz, 1985; Horvitz and Sulston, 1980). Subsequently, it was found that this tripartite complex functions to localize the LET-23 receptor. Molecular experiments revealed that the LET-23 receptor binds to the PDZ domain of Lin-7, while CASK/Lin-2 serves as the link between Lin-7 and Lin-10; mutations that result in ablation of binding between any of the components of the tripartite complex result in a mislocalization of the LET-23 receptor (Hoskins et al., 1996; Kaech et al., 1998).

Concurrently with the molecular characterization of this tripartite complex in *C. elegans*, it was discovered their mammalian homologues form the same complex at synapses in the central nervous system. In brain, the complex is composed of Veli/Lin-7 and Mint/Lin-10, which bind to the L27 and CaMK domain of CASK/Lin-2, respectively (Borg et al., 1998; Butz et al., 1998). The CASK/Mint/Veli complex is thought to

participate in the localization and stabilization of both potassium and calcium channels (Leonoudakis et al., 2004; Maximov et al., 1999; Schuh et al., 2003). Interestingly, the tripartite complex has been shown to exhibit an intrinsic dynamic nature via formation of alternative complexes (Leonoudakis et al., 2004; Tabuchi et al., 2002). For example, the potassium channel, Kir 2.2, can interact with hDlg/SAP97, which then recruits the tripartite complex. However, an alternative complex can also be formed, in which Kir 2.2 binds Veli, and recruits hDlg/SAP97 and CASK, excluding Mint (Leonoudakis et al., 2004).

In addition to its role as a member of the tripartite complex, CASK is also involved in cell adhesion through its interactions with neurexins and syndecans (Cohen et al., 1998; Hata et al., 1996a; Hsueh et al., 1998). The mammalian homologue of CASK was first found in a yeast two-hybrid screen searching for binding partners of neurexins, a cell surface protein found at synapses (Cohen et al., 1998; Hata et al., 1996a; Hsueh et al., 1998). The CASK-neurexin complex, found at the postsynaptic side of neuronal synapses, contributes to adhesion through binding neuroligin, a presynaptic cell surface protein. CASK has also been shown to interact with syndecan family members in both epithelial and neuronal cell types (Cohen et al., 1998; Hsueh et al., 1998). Syndecans are cell surface heparan sulfate proteoglycans that aid in cell adhesion (Bernfield et al., 1993; Bernfield et al., 1992; Carey, 1997). Furthermore, syndecans are implicated in developmental processes, such as skeletal muscle differentiation, through their association with growth factors and growth factor receptors (Rapraeger, 2000). Finally, it

is worth noting that CASK is thought to further promote and stabilize cell adhesion by anchoring complexes to the cytoskeletal apparatus through binding protein 4.1 via its HOOK domain (Cohen et al., 1998).

hDlg/SAP97 is another well examined binding partner of CASK. Like CASK, Dlg has a role in stabilizing molecules at cell junctions, and contributes to cell polarity through binding adhesion molecules and protein 4.1 (Bossinger et al., 2001; Firestein and Rongo, 2001; Lue et al., 1994a; Thomas et al., 1997; Woods and Bryant, 1991a; Woods et al., 1996). At chemical synaptic junctions, Dlg is involved in binding and localizing a variety of channels and receptors, including NMDA and AMPA receptors, and as mentioned earlier, postassium channels (Bassand et al., 1999; Cai et al., 2002; Gardoni et al., 2003; Leonoudakis et al., 2004; Leonoudakis et al., 2001; Rumbaugh et al., 2003; Sans et al., 2001). Interestingly, some of the first *in vivo* evidence of the clustering capabilities of PDZ domains came from studies of *Drosophila* Dlg, where it was shown to be responsible for clustering inward rectifying potassium channels at the *Drosophila* larval NMJ (Tejedor et al., 1997).

CASK and hDlg/SAP97 have been shown to interact in a variety of different epithelial cell types. In addition to the interaction between the GK and SH3 domains of CASK and Dlg mentioned previously, a stronger interaction has been demonstrated to occur between L27 domain of CASK and the N-terminus of Dlg in the MDCK and HEK293 cell lines (Feng et al., 2004; Lee et al., 2002). In fact, a dominant negative form of the CASK protein has been shown to result in mislocalization of the hDlg/SAP97 protein *in vitro* in MDCK cells (Lee et al., 2002). Given this close association, it is not surprising that mutant mouse models of the CASK or Dlg protein result in very similar phenotypes

(Caruana and Bernstein, 2001; Laverty and Wilson, 1998). A transgenic insertion into the CASK gene and a LacZ gene trap insertion into the Dlg gene both result in mice which exhibit craniofacial abnormalities, including cleft palate; mice from both mutant models die within 24 hours of birth (Caruana and Bernstein, 2001; Laverty and Wilson, 1998).

Interestingly, in addition to its role at cell junctions, the CASK protein has also been implicated as co-activator of transcription (Hsueh et al., 2000). The GK domain of CASK is able to form a ternary complex with TBR-1, a T-box transcription factor that promotes transcription of T-element containing genes, and CINAP (CASK interacting nucleosome assembly protein), a novel CASK interacting protein that functions as a putative nucleosome assembly protein (Wang et al., 2004a; Wang et al., 2004b). Together these proteins have been shown to regulate transcriptional activity of a variety of T-element containing genes, including reelin, glycine transporter, FGF4 and NR2B (Wang et al., 2004a; Wang et al., 2004b). Additionally, luciferase assays utilizing the promoter of the reelin gene suggest that CASK can act alone as a transcription factor, but with less efficiency then when complexed with TBR-1 (Hsueh et al., 2000; Wang et al., 2004a).

Recently, our lab has demonstrated that the CASK protein is present in skeletal muscle and is concentrated at the neuromuscular junction (NMJ). Furthermore, we have found that CASK forms a complex *in vivo* in skeletal muscle with Dlg; Dlg has been previously shown by our lab to be present in skeletal muscle and to localize to the NMJ (Rafael et al., 1998; Sanford et al., 2004). However, any role for MAGUKs at the mammalian NMJ has not yet been thoroughly investigated. Most examination into the

physiological functions and binding partners of CASK and other MAGUKs has relied heavily on *in vitro* biochemical studies. Although mice null for CASK protein have been generated, skeletal muscle was never examined in these mice, and the mice died within 24 hours of birth, making a thorough examination into the physiological effect of CASK in various cell types, difficult to achieve (Laverty and Wilson, 1998). To begin to test the hypotheses regarding CASK protein interactions generated by *in vitro* studies, we sought to modify CASK protein interactions in a mammalian *in vivo* model, which are similar to experiments done in simpler epithelial cell culture and invertebrate models. We have therefore generated two transgenic mouse models, named CASK F.L. and CASKΔ, which overexpress a full-length and truncated version of the CASK protein, respectively, in mature skeletal muscle.

Materials and Methods

Generation of CASK Full Length and CASK delta constructs

The full-length CASK cDNA was a kind gift from the laboratory of Dr. Joanna B. Wilson. The CASK sequence provided was a fusion of mouse and human sequence. The sequence is mouse from the N-terminus to the PflmI restriction site located within the PDZ domain sequence, and is human from this PflmI site to the C-terminus. The CASK sequence was provided in the pcDNA3.1/Myc-HisB vector and was cloned into the EcoR1 and Xho1 sites within the multiple cloning site of the vector. Linear CASK cDNA was excised from the pcDNA3.1 vector by restriction digest at the HINDIII and XbaI sites in the multiple cloning site of the vector. The DNA was then purified using the Qiaex II DNA purification kit (Qiagen, Valencia, CA). The CASK cDNA fragment

was then blunt ended with T4 polymerase (New England BioLabs, Beverly, MA), followed by ligation of NOTI linkers to the ends of the CASK sequence (O/N at 16° C), and then digestion with NOTI enzyme (4hrs at 37°C). This was followed by DNA clean-up with the Promega DNA clean-up kit to eliminate the NOTI linkers. The resultant CASK cDNA was then cloned into the NOTI site into an HSA-Bsx expression vector, which contains human skeletal actin promoter, an enhancer VP1 intron and a polyA signal contained within a bluescript plasmid (Stratagene, Cedar Creek, TX) (A kind gift from K. Davies and J. Chamberlain). The CASK cDNA was then screened for proper orientation with the HSA-Bsx vector (with primers HSA 5047 and CASK 1001, see below). The HSA-CASK F.L. transgene was excised from the vector backbone by digestion with ClaI and PvuI enzymes (New England BioLabs). The CASKΔ transgene was generated by recombinant PCR methods as previously described. The two primers adjacent to the PDZ domain were as follows: primer 1, 5' TGGCACAA TCTTGAA/AACTCTGGTCACATT 3' and primer 2, 5' AATGTGACCAGAG TT/TTCAAGATTGTGCCA 3'. The outside primer sequences were as follows: CASK 1003, 5' CAGTGGAGCCATATCTCTGAAAGTG 3' and CASK 1004, 5' GATCGAAGTAGTGTGCATATGTTCTC 3'. Briefly, Primer 1 and CASK 1003 primer were used to generate a PCR product 5' to the PDZ domain, while Primer 2 and CASK 1004 were used to generate a PCR product 3' to the PDZ domain. These two PCR products were then combined in a PCR reaction using the two outside primers, CASK 1003 and CASK1004. The resultant PCR product, which was deleted for the PDZ domain DNA sequence, was digested with AflII and BspEI enzymes and cloned into these restriction sites in the pcDNA3.1-CASK vector, resulting in a pcDNA3.1-CASKΔ

sequence. The pcDNA3.1-CASKΔ sequence was then cut with BamHI and AgeI and cloned into the Bsx-HSA-CASK Full- Length vector, the resulting HSA-CASKΔ transgene was once again cut out of the bluecript vector by digestion with ClaI and PvuI enzymes. The entire HSA-CASKΔ sequence was sent to the Ohio State University Center for Molecular Neurobiology Sequencing Core for sequencing to ensure the deleted transgene had no sequence errors and was in frame. The HSA-CASK Full-Length and HSA-CASKΔ constructs were sent to The Ohio State University Center for Molecular Neurobiology Transgenic Core for generation of F0 mice. Briefly, transgenes were injected into fertilized eggs from superovulated FVB females. Injected eggs were then transferred to the oviduct of pseudopregnant females. This ultimately resulted in nine CASK Full-Length and ten CASKΔ founder lines. F0 mice were screened by Southern analysis and CASK PCR primers (see genotyping primers below). Subsequent generations of transgenic mice generated by mating transgenic positive mice to C57/BL10 mice, and the resulting progeny were used for all analyses shown in this paper.

All mice were treated in accordance with the Institutional Laboratory Animal Care and Use Committee.

Genotyping

All mice were genotyped from genomic DNA prepared from tail biopsies. F0 mice and all subsequent progeny were genotyped with two sets of primers. Primers HSA 5047 (complementary to sequence in the HSA promoter) and primer CASK 1001 (complementary to CASK sequence) generate a 485 bp PCR product and were used to screen for presence of the transgene. Primers CASK 1006 and CASK 1008,

complementary to sequence adjacent to the PDZ domain, were used to screen for deletion of the PDZ domain. Primers HSA 5047 and CASK 1001 result in a PCR product of 485 kb in both transgenic lines. Primers CASK 1006 and CASK 1008 result in a PCR product of 649 bp in CASK Full-Length mice and a smaller PCR product of 421 bp in CASKΔ mice due to absence of the PDZ domain sequence. The genotyping primers were as follows: HSA 5047, 5' TCACAGG GAGCTTGAAAGAAGAACCC 3'; CASK 1001, 5' GTACACATCCTCGAACAGCACGTC 3'; CASK 1006, 5' CTGTTTGGTCTTCTCCATGGCAA 3'; CASK 1008, 5' TGATGAAGCATTAAGG GTCACACCT 3'. Annealing temperatures for the PCR reactions are as follows: 64° for primers HSA 5047 and CASK 1001 and 52° for primers CASK 1006 and CASK 1008.

Western Analysis

Mouse quadriceps muscle from Tg- (all "Tg-" designations refer to transgenic negative littermates of CASK F.L. or CASKΔ transgenic positive mice), CASK Full-Length and CASKΔ mice were homogenized in Newcastle buffer, and protein concentrations were determined using the Dc Protein Assay (Bio-Rad, Richmond, CA). 100 μg of protein was then run out on 8% sodium dodecyl sulfate-polyacrylamide gel electrophoresis (SDS-PAGE) gels at 80 V for 2-3 hrs on a Mini-Protean 3 apparatus (Bio-Rad). Proteins were then transferred from SDS-PAGE gels to nitrocellulose (Schleicher and Schuell Bioscience, Keene, NH) at 80V, for 30-80 min on a wet-transfer apparatus. Following transfer, blots were blocked in 5% nonfat milk in Tris-buffered saline plus 0.1% Tween-20 (TBST) and 1% NGS for 1 hr. Blots were then incubated in primary antibody diluted in TBST plus 1% NGS for 2 hr at the following dilutions: CASK

polyclonal (which recognizes amino acids 315-416 of the CASK protein) (Zymed, San Francisco, CA), 1:250; CASK monoclonal (which recognizes amino acids 318-415) (Chemicon, Temecula, CA), 1:1000. Blots were then washed 3 x 15 min in TBST and incubated with either horseradish peroxidase (HRP)-conjugated goat anti-rabbit or HRP-conjugated goat anti-mouse secondary antibody (Jackson Immunoresearch,city,PA) for 1 hr. Secondary antibodies were diluted 1:10,000 in TBST plus 1 % NGS. Enhanced chemiluminescence (ECL Kit; Amersham Biosciences, Little Chalfont, UK) was used for detection of bound primary antibody.

Cell Culture

The COS-7 cell line was grown in 100 mm plastic tissue culture plates (Nalge Nunc, Rochester, NY) in complete growth media (DMEM, 10% FBS, 4mM L-glutamine, and 1% P/S). Cells were transfected when they reached ~80% confluency. For transfection, the cells were transfected with 2 μg of either pcDNA-CASK F.L or pcDNA-CASKΔ, using the Fugene 6 transfection reagent (Roche Diagnostics Corporation, Indianapolis, IN). Transfection efficiency was ~80%, as determined by a reporter gene assay in which COS cells were transfected with pCMV-β-Gal. 48 hours after transfection, cells were trypsinized, scraped off the plate, and pelleted by centrifugation at 1000 x g for 10 minutes. COS-7 cells were then resuspended in Newcastle Buffer and protein concentrations were determined using the Dc Protein Assay Kit (Bio-Rad, Richmond, CA). 100 μg of protein was then subjected to western analysis and probed with the CASK monoclonal antibody, as described above.

Histological Analysis

Diaphragm, quadriceps, extensor digitorum longum (EDL), soleus (SOL), and tibialis anterior (TA) muscles were dissected from Tg-, CASK Full-Length and CASKΔ mice at 4 wks, 8 wks, 12 wks, 6 months and 1 year for histological analysis by hematoxylin and eosin staining. After dissection, muscles were immediately placed in OCT mounting medium (VWR, West Chester, PA) and frozen in liquid-nitrogen-cooled isopentane. Unfixed frozen tissue blocks were then cut into 8 μm cryosections. For hematoxylin and eosin staining slides were post-fixed in 100% ethanol for 30 sec, washed in tap water, stained in hematoxylin for 30 sec, washed, stained in eosin for 20 sec, washed, and rinsed successively in 70%, 90%, and 100% ethanol. Lastly, slides were then washed 2X in histoclear (Sigma) and mounted in Permount.

Ultrastructural analysis

Quadriceps were dissected from 6 month old Tg-, CASK F.L., and CASKΔ mice. A thin longitudinal section was then removed and immediately placed in fix (4% paraformaldehyde, 3% glutaraldehyde in 0.1 M sodium phosphate buffer, pH 7.4) at RT for 1 hour. The samples were then transferred to a 3% glutaraldehyde in 0.1 M sodium phosphate buffer, pH 7.4, overnight at 4° C. Quadriceps muscle was then washed 2x15 min in 0.1 M sodium phosphate buffer. For subsequent identification of NMJ-containing sections, samples were then subjected to acetylcholinesterase staining, as outlined below. Following the washes in sodium phosphate buffer, the quadriceps were placed in fresh 0.1 sodium phosphate buffer overnight at 4° (all subsequent steps in the acetylcholinesterase staining were also conducted at 4°). Quadriceps muscles were then

washed 3 x 20 min in acetylcholinesterase rinse solution (0.2 M sodium cacodylate, 0.2 M cacodylic acid, 0.2 M calcium acetate and 0.1 M sodium sulfate) and incubated for 2 hrs in acetylcholinesterase incubation solution at pH 5.3 (acetylcholine iodide, copper sulfate, glycine, 0.1 M sodium sulfate, iso-OMPA, 0.5 M succinic acid). Samples were then washed 2 x 30 min in solution A (0.5 succinic acid, 0.2 calcium acetate, 0.1 M sodium sulfate, adjusted to pH 5.3 with NaOH), 2 x 30 min solution B (0.5 M succinic acid, 0.2 M calcium acetate, 0.1 sodium sulfate, adjusted to pH 5.3 with 4% sodium sulfide), and 2 x 15 min in Solution A. Finally, samples were washed 2 x 15 min in 0.1 M sodium phosphate buffer and sent for EM processing. Samples were then prepared for analysis as previously described (Sanford et al., 2004)and viewed using a Phillips CM12 transmission electron microscope. Ultrastructrual analysis was conducted on quadriceps samples from at least three mice of each genotype.

Immunofluorescence Analysis

Immunohistochemistry for epifluorescent and confocal analysis of the CASK candidate interactors was performed on unfixed or fixed 8µm cryosections of quadriceps muscle. Quadriceps muscle were dissected from 6 month old Tg-, CASK F.L. or CASKΔ mice, embedded either fixed or unfixed in OCT (VWR) and frozen in liquid nitrogen-cooled isopentane. Fixed samples were first immersed in 1 % paraformaldehyde for 1 hr, then in 20 % sucrose solution in KPBS at 4°, O/N. Sections were blocked in 1 % gelatin in potassium buffered saline (KPBS) for 15 minutes. Following blocking, sections were washed and incubated for 2 hours with affinity-purified rabbit polyclonal antibodies. All antibodies were diluted in KPBS and 0.5 % gelatin (KPBSG) plus 1 %

NGS. The primary antibody dilutions were as follows: CASK 1:25 (Zymed), Dlg 1:10,000 (kind gift of A. Chishti), Kir 2.2 1:200 (Chemicon, Temecula, CA), Kir 2.3 1:200 (Chemicon), Girk2 1:100 (Chemicon), NR2A 1:50 (Upstate,Waltham, MA), NR2B 1:50 (Upstate), syndecan-3 1:250 (Zymed). Following primary antibody incubations, slides were washed 3 x 5 minutes in KPBS and then incubated for 1 hr with CY3 anti-rabbit secondary antibody, diluted 1:200 in KPBSG plus 1% NGS. Alexa 488 α Bungarotoxin (Molecular Probes, Eugene, OR) was also diluted 1:1000 with secondary antibody for detection of AChRs at the NMJ. After incubation in secondary antibody, slides were washed for 3 x 5 minutes in KPBSG. Slides were then mounted in Vectashield (Vector Labs, Burlingame, CA) and coverslipped. The DNA dye DAPI was diluted to 500 ng/mL in Vectashield for nuclei detection. Images were obtained using a NIKON Eclipse E800 microscope (Nikon Corporation, Tokyo, Japan), a SPOT-RT slider digital camera and SPOT software (Diagnostic Instruments, Inc., Sterling Heights, MI). Confocal images were obtained using a Zeiss 510 Meta laser scanning microscope (Carl Zeiss, Thornwood, NY). All confocal images were captured using the 63 x objective and 3x zoom, the pinhole was kept constant for all images and gain was adjusted for each image.

For NMJ measurements and confocal analysis, quadriceps muscle was dissected at 4 weeks and 8 weeks from 10 Tg-/Tg+ pairs from CASK F.L. and CASKΔ litters. Transverse sections were then cut from quadriceps and immediately placed in fix (1 % paraformaldehyde in KPBS). Tissue was then placed in 20 % sucrose in KPBS O/N and frozen on cork in OCT in liquid-phase cooled liquid-nitrogen. 30 μm sections were then cut and subjected to immunohistochemical analysis. Slides were first equilibrated in

KPBS for 5 minutes, then washed for 1 hour in 0.1 M glycine in KPBSG. Sections were then extracted with 0.5% Triton X-100 in KPBS on ice for 5 minutes. Following triton extraction, slides were washed in KPBS and blocked in 1 % gelatin in KPBS for 1 hour. For confocal staining, sections were then incubated at RT in polyclonal CASK primary antibody at 1/25 dilution O/N and washed for 3 x 15 minutes in KPBSG plus 0.1% Tween-20. Sections were then incubated for 3 hours with Alexa-488 α bungarotoxin at a 1:200 dilution in KPBSG plus 1 % NGS. Finally, slides were washed 3 X 15 minutes in KPBSG plus 0.1 % Tween-20, mounted in Vectashield, and coverslipped. For NMJ staining, slides were simply incubated in Alexa-488 α bungarotoxin immediately after triton extraction, as described above. NMJ's were measured *en face*, by tracing the circumference of the NMJ, using the SPOT software (Diagnostic Instruments). At least 20 NMJs were measured from each mouse, and values were normalized to mouse weight.

Functional Analysis

For Grip strength analysis, forelimb strength was measured using a grip strength meter. Mice were allowed to grasp a horizontal, flat platform, and then pulled away until the mouse released its grip from the platform. Forelimb strength, or resistance, was then measured by the grip meter force transducer in Newtons. Mice were subjected to ten successive grip strength measurements, without pause between trials. For data calculation, the top and bottom two values were dropped from the ten trials and the remaining six trials were averaged and divided by body weight.

For physiological analysis, EDL muscles were dissected, tendon to tendon, from mice of all three genotypes. Muscles were then attached horizontally via their tendons to a

force transducer and an electromagnetic length adaptor, in Krebs Solution at 20° C. Optimum length of the EDL was then ascertained by subjecting the muscle to successive twitches and determining the length at which maximum isometric force is achieved. Maximum tetanic contraction measurements were obtained by subjecting the muscle to 5 tetanic stimulations of 350 ms at 2 minute intervals, and using a stimulation frequency of 125 Hz. The measurements are expressed per unit cross-sectional area (mN/mm2), which is determined by dividing the fiber length by the wet weight of the muscle.

Proteomic analysis

300 µg of homogenized total skeletal muscle protein (quadriceps and hindlimbs) from each genotype was passively rehydrated onto 11 cm, pH 4-7, IEF strips (BioRad) and then subjected to first dimension isoelectric focusing using a PROTEAN IEF machine (BioRad). The isoelectric focusing conditions were as follows: start voltage was 0 V, end voltage was 8000 V, and the IEF was run for 20- 35,000 V-hr. Protein on the strips then was run in the second dimension on a 8-16 % gradient gel (BioRad) for 65 minutes at 200 V. Gels then were either silver stained or Coomassie stained for detection of proteins. For silver staining, the Bio-Rad Silver Stain Plus Kit (Bio-Rad) was used. Gels were fixed in fixative enhancer solution (50% methanol, 10% acetic acid, 10 fixative enhancer concentrate, and 30 % dH2O) for 20 minutes. Following fixation, gels were rinsed 2 x 20 minutes in dH2O, and submerged in staining solution (7.7 % silver complex solution, 7.7 % reduction moderator solution, 7.7 % image development reagen, and 76.9 % development accelerator solution) for 15-30 minutes. Staining was stopped with 5 % acetic acid and were stored in 5 % acetic acid. For Coomassie staining, gels were fixed

O/N in fixing solution (50% ethanol, 10% acetic acid, 40% dH2O). Following the O/N fixation, gels were washed 2 x 30 minutes in washing solution (50% methanol, 5% acetic acid, and 45% dH2O) and stained 3hr-O/N with Bio-Rad Bio Safe Coomassie stain. Gels were then destained (50% methanol, 5% acetic acid, 45% dH2O) and stored in 5% acetic acid in water. Spot differences observed between the three genotypes on four sets of gels were excised and sent to The Ohio State University Mass Spectrometry Facility for mass spectrometry analysis and protein spot identification.

Results

Generation and characterization of CASK Full-length and CASKΔ overexpressing transgenic mice

In order to begin to understand the functions of the CASK protein *in vivo* in skeletal muscle, we constructed two transgenes for the generation of two transgenic mouse models. The first transgene consisted of the full-length CASK cDNA under the control of the Human Skeletal muscle Actin promoter (HSA), a promoter which drives gene expression in skeletal muscle, and to a lesser extent, cardiac muscle. Using recombinant PCR methods we also generated a transgene that is deleted for the sequence containing the PDZ domain (Fig. 3.1). The concept behind generating the PDZ-deleted version of the transgene was to produce a CASKΔ protein that would perhaps act in a dominant-negative fashion, displacing and/or redistributing endogenous CASK and its binding partners. This approach has been used successfully in the examination of the PDZ domain of α-syntrophin, a member of the dystrophin-associated protein complex localized to the sarcolemma of skeletal muscle (Adams et al., 2001). Both CASK transgenes were

injected into eggs from FVB mice and then transferred to pseudopregnant females. PCR analysis combined with Southern analysis (data not shown) confirmed the generation of nine F0 lines of mice containing the CASK Full-Length transgene (hereafter referred to as CASK F.L.) and ten F0 lines containing the CASKΔ transgene. All lines from each genotype were examined via western analysis and immunofluorescence for protein expression and localization. Transgenic lines that exhibited high protein expression, combined with the most membrane localization across all muscles examined (which included quadriceps, soleus, extensor digitorum longus (EDL), tibialis anterior (TA), diaphragm and heart) and demonstrating the least mosaicism when analyzed by immunohistochemistry, were studied further. Three lines of CASK F.L. and two lines of CASKΔ mice were further analyzed and found not have any gross phenotypic differences. Therefore, the data presented in this chapter is from one line of mice generated from each transgenic construct.

We next performed western analysis with a CASK monoclonal antibody on pooled samples of total skeletal muscle protein homogenates from the CASK F.L. and CASKΔ mice to analyze expression levels of these proteins. A 110 kDa protein, corresponding to the size of the CASK F.L. protein, was observed at significantly higher levels in transgenic positive mice than their transgenic negative littermates (Fig. 3.2A); a 1:10 dilution of the CASK F.L. total protein homogenate produces a stronger signal than undiluted protein from a transgenic negative littermate (data not shown). Unexpectedly, we were unable to detect a CASK protein of the predicted size in the CASKΔ mice. The CASK PDZ domain is 76 amino acids, therefore the predicted size of the CASK protein should have yielded a protein of approximately 100 kDa. However, an abundant protein

of approximately 65 kDa was detected by the CASK antibody in mouse quadriceps muscle containing the CASKΔ transgene (Fig. 3.2A). This protein band is also present in small amounts in Tg- mice, and is barely detectable in CASK F.L. mice (Fig. 3.2A). We also confirmed the presence of this 65 kDa band in a panel of quadriceps muscle from individual CASKΔ mice, diluted 1:10 as compared to Tg- quadriceps muscle (Fig. 3.2B). Furthermore, transfection of COS cells with each of the transgenes, contained in a His/Myc tagged pcDNA3.1 vector, also resulted in the predicted 110 kDa band in CASK F.L. transfectants and an approximately 65 kDa band that was present only in CASKΔ transfectants; it is also worth mentioning that there appears to be an additional CASK protein isoform, of ~75 kDa, that is present in COS cells (Fig. 3.2C). Repeated DNA sequencing of the CASKΔ transgene confirmed the in-frame deletion of sequence encoding the PDZ domain and genomic PCR of the 3'-end of the transgene confirmed the presence of the entire transgene in transgenic positive animals. We next expressed large quantities of a GST fusion with the putative CASKΔ protein to confirm the protein expression of CASK sequences. Protein sequences amino-terminal to the CASK PDZ domain were identified by mass spectrometry analysis, however, no peptides were obtained from beyond the PDZ domain deletion (data not shown). The CASKΔ transgene therefore appears to generate a version of the CASK protein that is truncated just amino-terminal to the PDZ domain in the transgenic mice and is therefore likely overexpressing only the CaMK domain and the two L27 domains of the CASK protein.

To determine the distribution and localization of CASK F.L. and CASKΔ protein we also conducted immunolocalization, using an antibody raised to an area just carboxy-terminal to the CaMK domain, on quadriceps, soleus, EDL, and TA muscles. Both the

CASK F.L. and CASKΔ proteins are expressed at the membrane and the cytoplasm of all muscles examined (Fig. 3.3). CASK F.L. and CASKΔ protein localization to the membrane was confirmed by western analysis of membrane protein enriched preparations (Fig. 3.2D).

Histological analysis

Given that overexpression of CASK F.L. or CASKΔ protein could cause a redistribution of ion channels and/or receptors, combined with the fact that CASK has been shown capable of acting as a co-activator of transcription, it is possible that overexpression of either CASK protein could result in changes in the muscle morphology. Therefore, basic histological analysis was conducted on skeletal muscle from both lines of transgenic mice to determine if overexpression of CASK F.L. or CASKΔ protein resulted in any morphologic abnormalities. Hematoxylin and eosin (H&E) staining was conducted on quadriceps muscle from Tg-, CASK F.L. and CASKΔ mice at 4 weeks, 8 weeks, 12 weeks, 6 months and 12 months, to examine overall muscle morphology. H&E staining at all ages revealed no obvious morphological abnormalities in either line of transgenic mice as compared to Tg- muscle (Fig. 3.4). The percentages of central nuclei were determined in quadriceps muscle sections at 6 months and 1 year and these results indicated that there are no significant differences in regeneration between CASK F.L., CASKΔ, and Tg- controls (data not shown). To confirm that skeletal muscle fiber degeneration was not occurring without any regeneration, the presence of fibrous tissue that can replace degenerated muscle was analyzed by Verhoeff Van –Giesson (VVG) staining. VVG staining revealed that the skeletal muscle from

CASK F.L. and CASKΔ mice do not exhibit any increase in fibrous tissued as compared with their Tg- littermates (data not shown). In order to ascertain whether expression of CASK F.L. or CASKΔ protein has an effect on skeletal muscle fiber type biochemistry, transgenic positive and negative quadriceps muscles were stained for the mitochondrial enzyme, NADH-TR, which is present in high levels in slow oxidative but not fast glycolytic fibers (data not shown). NADH staining revealed that fiber-type composition is not affected by overexpression of either the CASK F.L. or CASKΔ protein.

NMJ analysis

In normal skeletal muscle the CASK protein is localized specifically to the primary gutter of the postsynaptic membrane of the NMJ, where it is colocalized with AChRs. Notably, CASK protein also exhibits a variable amount of presynaptic staining at the motor unit (Sanford et. al. 2004). We therefore utilized confocal microscopy to investigate whether the subcellular localization of CASK at the NMJ is affected in either line of transgenic mice. Immunofluorescence followed by confocal microscopy revealed that CASK localization at the NMJ is still localized to the primary gutter in both CASK F.L. and CASKΔ skeletal muscle. Interestingly, this indicates that the C-terminal portion of CASK, encompassing the PDZ, SH3, HOOK, and GK domains, may not be necessary for targeting the CASK protein to the membrane *in vivo*. Unexpectedly, presynaptic CASK staining was not observed in any of the NMJs analyzed in either CASK F.L. or CASKΔ transgenic mice. Therefore, it appears that overexpression of the CASK protein in skeletal muscle may affect the presynaptic subcellular localization of endogenous CASK protein at the NMJ (Figure 3.5).

We next wanted to investigate whether overexpression of either CASK F.L. or CASKΔ protein affects the morphology and/or size of the NMJs in either line of transgenic mice. Transverse sections of quadriceps muscle were fixed and stained with α-bungarotoxin, which labels AChRs. This procedure allows the visualization of NMJs that are *en face* in orientation, thereby allowing a measurement of the area of the NMJ. We measured the area and examined the morphology from ten Tg-/Tg+ pairs of age-matched, sex-matched, littermates at 4 and 8 weeks of age from both CASK F.L. and CASKΔ transgenic lines. These analyses revealed that there are no marked changes in morphology of the NMJ caused by overexpression of either CASK protein (Fig. 3.6A). Furthermore, sizes of the NMJs, which were normalized to mouse mass, were not affected in either line of transgenic mice (Fig.3.6B).

Since there were no differences in size or gross morphology of the NMJs as determined by immunofluorescence analysis we next examined the ultrastructure of the NMJs by electron microscopy. Acetylcholinesterase staining was used to label NMJs for EM analysis. EM micrographs were analyzed by Dr. John Porter and it was determined that overexpression of CASKΔ protein does not affect NMJ ultrastructure (Fig. 3.6C).

Functional analysis

To determine whether overexpression of CASK F.L. or CASKΔ affected the functional properties of skeletal muscle, we conducted grip strength measurements and physiological analysis. Grip strength analysis was conducted on 3 age-matched pairs of CASK F.L. and CASKΔ mice at 2-3 months and 6 months. We measured grip strength of forelimbs using a grip strength meter and averaging 10 consecutive trials; the force

measurements were then normalized to body weight (Fig. 3.7A). Forelimb grip strength was not different between positive and negative transgenic mice as determined by an unpaired t-test; therefore, overexpression of either CASK protein is not detrimental to this functional parameter.

We also examined maximum tetanic contraction of EDL muscles from Tg-, CASK F.L. and CASKΔ mice, under constant Ca2+ concentrations and constant temperature. EDL muscles were choosen for experimentation because they are conducive to physiological analysis and were expressing both the CASK F.L. and CASKΔ proteins at high levels (Fig. 3.3). This physiological analysis revealed that maximum tetanic force production is not altered in either transgenic line, as compared to transgenic negative mice (Fig. 3.7B).

Western and immunofluorescence localization analysis of CASK protein candidate interactors

Western and immunofluorescent localization analysis were conducted on quadriceps muscle from both lines of transgenic mice to determine if distribution of CASK candidate interactors was affected by overexpression of CASK F.L. and CASKΔ protein. Analysis of CASK using dominant negative mutants in cell culture has demonstrated the re-localization of its interactors, including Dlg and the Kir 2.2 potassium channel (Lee et al., 2002; Leonoudakis et al., 2004).

We began this analysis by determining the distribution of Dlg, a known *in vivo* interactor of CASK in skeletal muscle (Sanford et al., 2004). Immunofluorescence analysis confirmed that Dlg remains concentrated at the postsynaptic membranes in

quadriceps from CASK F.L. and CASKΔ transgenic mice (Fig. 3.8). Dlg was not observed to be redistributed around the sarcolemma or in the cytoplasm of myofibers overexpressing either CASK F.L. or CASKΔ proteins.

As mentioned previously, CASK has also been shown to interact with potassium channels. We therefore analyzed the localization of Girk2, Kir 2.2 and Kir 2.3, three inward rectifying potassium channels, which have previously been shown to localize to the NMJ in wild-type skeletal muscle, making them good candidates to be affected by transgenic CASK proteins. Immunofluorescence analysis revealed that the distribution of the Kir 2.2 and Kir 2.3 potassium channels were unaffected in both lines of transgenic mice (Fig. 3.8). Girk2 expression appears as though it upregulated in the cytoplasm of CASK F.L. and CASKΔ transgenic positive quadriceps muscle (Fig. 3.8); more work will be needed to determine whether Girk2 expression is affected by CASK F.L. or CASKΔ protein.

We also evaluated the localization of the ErbB4 receptor in these transgenic mice. ErbB4 is localized to the post-synaptic membrane at the NMJ and is related to the LET-23 receptor, whose localization is dependent on the CASK tripartite complex in *C. elegans* (Trinidad et al., 2000). ErbB4 distribution was not influenced by the overexpression of either CASK protein (Fig. 3.8).

Next, we investigated the localization of two NMDA glutamate receptor subunits, NR2A and NR2B. NMDA glutamate receptors, until recently, were not thought to be present at the cholinergic NMJ. However, recent work has shown that NMDA receptor subunit 1 is present at the NMJ and work in our laboratory has shown that NR2A and NR2B are also enriched at the NMJ (Grozdanovic and Gossrau, 1998; Luck et al., 2000)

(JLS and JAR, unpublished results). NMDA receptor subunits have been shown to interact with Dlg homologues, while NR2B has been shown to be transcriptionally regulated by CASK in the central nervous system (Kim et al., 1996; Kornau et al., 1995; Niethammer et al., 1996; Wang et al., 2004a; Wang et al., 2004b). Immunofluorescence analysis demonstrated that the NR2A NMDA receptor subunit localization was unaltered in CASK F.L. and CASKΔ overexpressing mice (Fig. 3.8). However, the NR2B receptor subunit appeared to be upregulated in both lines of transgenic mice, exhibiting increased localization to the membrane and increased cytoplasmic localization (Fig. 3.8).

Finally, we also determined whether CASK F.L. or CASKΔ overexpression would affect the distribution of syndecan-3, a member of the syndecan protein family member that is present in the satellite cells of adult skeletal muscle (Cohen et al., 1998; Hsueh et al., 1998; Rapraeger, 2000). Syndecan-3 did not appear to exhibit any changes in protein distribution, as compared to Tg-quadriceps, in either CASK F.L. or CASKΔ mice (Fig. 3.8).

It is also worth mentioning that we were unable, as of yet, to examine whether the localization of the Veli protein, a member of the CASK tripartite complex, is altered in CASK F.L. or CASKΔ mice. RT-PCR and western analysis has demonstrated that Veli is present in skeletal muscle, but Mint does not appear to be expressed in skeletal muscle (JLS and JRF, unpublished data).

Proteomic analysis of skeletal muscle from CASK F.L. and CASKΔ overexpressing transgenic mice

We next turned to a more global approach in determining CASK's function *in vivo* in

skeletal muscle, utilizing our transgenic mouse models. The protein expression profiles of normal, CASK F.L. and CASKΔ total skeletal muscle, were examined using 2-D gel analysis. Pooled protein samples of total leg muscle from multiple mice from each of the three genotypes were subjected to isoelectric focusing, run out on gradient gels and silver-stained. These silver-stained gels were then examined for differences in protein expression. We observed a cluster of four protein spots between 20-30 kDa, that was present in gels from transgenic negative mice and CASK FL mice, but was completely absent from the CASKΔ gels. This result was confirmed on four silver stained gels from each genotype and one additional set of coomassie stained gels (Fig. 3.9). All four spots were excised from the silver stained gels and sent for mass spectrometry analysis at The Ohio State University Mass Spectrometry Facility. Mass spectrometry analysis was able to identify one of the spots as the fast twitch Troponin T (TnT). This was confirmed by a second identification of the same spot from a Coomassie stained gel (Fig. 3.9). TnT is a ~38 kDa protein, but is known to undergo alternative splicing and proteolytic cleavage (Bouley et al., 2004; Filatov et al., 1999; Sangorrin et al., 2000). We confirmed the presence of a ~20 kDa TnT product in the pooled Tg- and CASK F.L. samples and its absence in the CASKΔ sample by western analysis of 1-D SDS-PAGE gels, using a monoclonal TnT antibody. However the presence of this TnT isoform on independent samples was not confirmed.

Finally, in analyzing the 2-D gels we observed several other spot differences besides the cluster mentioned above. Further experiments will be necessary to validate all the proteomic differences observed between the groups of mice, for example, there were three spots within the cluster that have yet to return peptide identifications.

Discussion

We have successfully generated two transgenic mouse models, CASK F.L. and CASKΔ, to begin an *in vivo* investigation into CASK protein function in mammalian skeletal muscle. The CASK F.L. mice are overexpressing the full-length CASK protein, while the CASKΔ mice overexpress the CaMK and L27 domains. Immunofluorescence data, combined with western analysis of microsome preparations, revealed that both of these proteins, upon overexpression, are localized to both the membrane and the cytoplasm. Furthermore, we found that overexpression of the CASK protein in skeletal muscle has led to an absence of the CASK protein at presynaptic locations of the NMJ, suggesting synaptic feedback. We then conducted a series of experiments to ascertain whether overexpression of either CASK protein affects the normal morphology of the skeletal muscle and/or neuromuscular junction. These experiments demonstrated that overexpression of the full-length or truncated CASK protein does not appear to affect the gross morphology of the skeletal muscle or NMJ. Furthermore, the contractile functions and strength of the skeletal muscle does not appear to be impaired in either line of transgenic mice. Immunofluorescence experiments were also utilized to examine whether overexpression of either CASK protein affects the cellular distribution of the known CASK interactor, Dlg, or other candidate interactors, including potassium channels Kir 2.2 and Kir 2.3, ErbB4 receptors, syndecan-3 and NMDA receptor subunits. Interestingly, the distribution of Dlg is not altered in either line of CASK transgenic mice; while the only candidate interactors that may be affected, are Girk2 and NR2B.

Finally, we conducted proteomic analysis, comparing the protein expression profiles of the skeletal muscle of Tg-, CASK F.L. and CASKΔ mice. These experiments are still underway, but there is some preliminary data suggests that overexpression of the CASKΔ protein may affect TnT post-mortem proteolysis.

As briefly discussed previously, the CASKΔ mice express a protein product that is ~ 65 kDa in size, which is significantly smaller than would be predicted to be encoded by the transgene that these mice possess. The transgene present in the CASKΔ mice is deleted only for the PDZ domain, which is 76 amino acids in size in the CASK protein, and would result in a protein of approximately ~100 kDa in size. Mass spectrometry analysis identified peptides covering the entire CASK protein sequence up to the PDZ domain, but did not identify any peptides that were not located in this region or did not match the CASK sequence. This data suggests that the CASKΔ protein most likely is intact up to the start of the PDZ domain, an assumption that is further supported by the fact that both the monoclonal and polyclonal CASK antibodies used in these analysis of the CASKΔ protein, for western and immunofluorescence analysis, are raised against an amino acids located between the CaMK domain and the PDZ domain. If the CASKΔ protein was somehow altered prior to the PDZ domain, it seems unlikely that both antibodies would still work efficiently. Several possible explanations may account for the truncated CASKΔ protein. First, it is possible that there is an error in the transgene DNA sequence that translates to a premature stop codon. Since this transgene was sequenced multiple times after the recombinant PCR to ensure sequence fidelity, this explanation seems unlikely. Also, primers located outside the PDZ domain still yield PCR products in genotyping experiments, suggesting that the entire transgene has been

incorporated into the mouse genome. Secondly, it is possible that the CASK protein is susceptible to proteolysis/cleavage at a location that is concurrent with the start of the PDZ domain, an explanation that would account for the same size band being present in Tg- protein homogenates.

The examination of CASK protein subcellular localizations at the motor unit in both lines of transgenic mice demonstrated that overexpression of CASK in skeletal muscle seems to result in an absence of the CASK protein from presynaptic locations. This phenomenon suggests that there is a feedback mechanism that exists between the postsynaptic membrane and presynaptic elements which involves CASK. Given that CASK is known to bind a variety of adhesion molecules it does seem possible that CASK might somehow be involved in linking the pre- and postsynaptic components of the NMJ. Furthermore, CASK has been shown by our lab to localize to the nucleus of C2C12 cells and MN-1 cells, as well as a subset of nuclei in mature mouse quadriceps muscle, which would also suggest CASK is capable of participating in signaling mechanisms at the NMJ (See Chapter 2). Further investigation will be required to determine the exact processes that are responsible for the absence of CASK protein at presynaptic locations in response to CASK overexpression in skeletal muscle.

We also demonstrated that overexpression of the both the CASK F.L. and CASKΔ proteins seems to result in an increased localization of the NR2B protein at both the membrane and in the cytoplasm. As mentioned previously, CASK has been shown to act in a ternary complex with both TBR-1 and CINAP, via its GK domain, in central nervous system synapses, to act as a co-activator of transcription of T-element containing genes, including NR2B (Hsueh et al., 2000; Wang et al., 2004a; Wang et al., 2004b). TBR-1 is

not present in skeletal muscle, but the CINAP protein is, suggesting that a version of this complex may exist in skeletal muscle. Our preliminary results suggest that perhaps CASK is acting promoting transcription of NR2B in skeletal muscle as well. However, one puzzling aspect to these results is the fact that NR2B appeared to upregulated in CASKΔ mice, lacking the GK domain, which has been shown to be necessary for binding CINAP. Since an investigation into the transcriptional properties of CASK in skeletal muscle has never been carried out, and given that our results are preliminary in nature, it is clear that further work will be required to confirm CASK's possible role in NR2B transcription. Furthermore, it is possible that CASK may not influence the transcription of NR2B, but that it may influence NR2B localization or stabilization by binding the protein, either directly or indirectly. Although CASK has not been shown to bind NR2B, homologues of hDlg/SAP97 have been shown to interact with this subunit.

The work presented in this chapter is the first *in vivo* characterization of CASK protein function in skeletal muscle utilizing transgenic mouse models. Interestingly, these analyses have yielded results that are contrary to previous experiments that have analyzed the overexpression of the CASK protein. In MDCK cells, which express CASK endogenously, an overexpressed mutant form of CASK, lacking its C-terminal half (similar to the CASKΔ protein), acts in a dominant negative fashion, resulting in mislocalization of the hDlg/SAP97 protein (Lee et al., 2002). Furthermore, separate studies demonstrate that this same CASK mutant causes Kir 2.2 potassium channels to redistribute from the basolateral membrane, resulting in intracellular accumulations of the Kir 2.2 protein in MDCK cells (Leonoudakis et al., 2004). In our analysis of the two CASK transgenic mouse models, we have found that neither Dlg, nor potassium channels

Kir 2.2 or Kir 2.3, were affected, despite the significant amount of overexpression of both CASK F.L. and CASKΔ proteins at the membrane and cytoplasm. These experiments therefore demonstrate that the CASK protein does not appear to influence the localization of Dlg or Kir 2.2, as has been suggested by *in vitro* experiments. Perhaps these results are specific for the CASK protein in skeletal muscle, or it is also possible that there are other Dlg isoforms or other potassium channels that are dependent on CASK for their localization in skeletal muscle. For instance, the results of this chapter demonstrate that possibility that the Girk2 potassium channel may be upregulated in CASK F.L. and CASKΔ mice; these results are preliminary and more work will be needed for confirmation. On the whole, these experiments underscore the importance of generating *in vivo* models, in various systems and varyious cell types, to determine the distinct physiologically relevant functions of these MAGUK proteins.

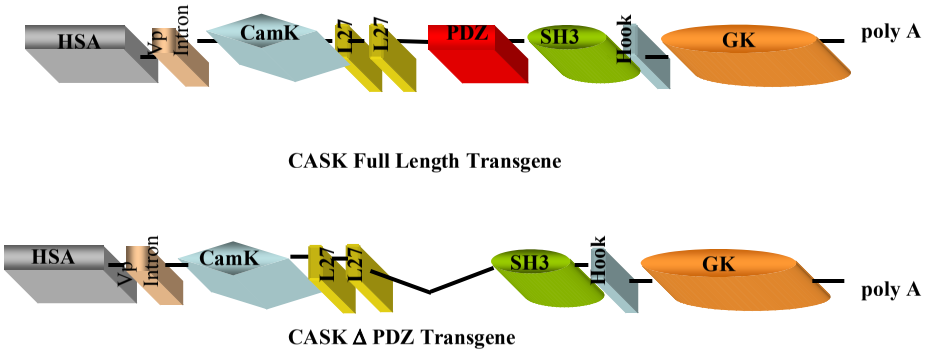

Figure 3.1: Schematic representation of the CASK F.L. and CASKΔ transgenic constructs and the protein domains that they encode

The transgenes used for the generation of CASK transgenic overexpressing mice were a full-length cDNA or a PDZ-domain deleted version of the cDNA expressed from the human skeletal actin (HSA) striated muscle-specific promoter. PDZ = PSD-95, Dlg, ZO-1; SH3 = Src homology 3; CaMK = Calcium/Calmodulin Kinase homology; GK = guanylate kinase-like, HSA = Human Skeletal Actin promoter.

Figure 3.2 A-D: Western analysis of CASK F.L. and CASKΔ protein

(A.)Western analysis was conducted on total skeletal muscle protein homogenates (quadriceps muscle and hindlimbs) from Tg-, CASK F.L. and CASKΔ mice. The protein from CASK F.L. and CASKΔ mice was diluted 1:10, as compared with Tg-. A CASK monoclonal antibody detected a band of the predicted 110 kDa size from both Tg- and CASK F.L. skeletal muscle. Additional protein products are observed in the CASK F.L. lane, a result that is most likely due to small amounts of degradation of the high levels of transgenic protein. The predicted size of the protein produced from the CASKΔ transgene should have been ~100 kDa, however western analysis detected a band of ~65 kDa. (B.) To further confirm the presence of the ~65 kDa protein in CASKΔ mice, western analysis was conducted on quadriceps muscles from individual transgenic negative and CASK F.L. and CASKΔ mice (1:10 dilution). The ~65 kDa protein was present in quadriceps muscle from four different CASKΔ transgenic positive mice. (C.) As another means of confirming the size of the protein produced from the CASKΔ transgene, COS cells were transfected with CASK F.L. and CASKΔ transgenes, contained in pcDNA3.1 vector. A band of 110 kDa in size, corresponding to the full-length CASK protein, was detected in microsome preparations from total skeletal muscle, untransfected COS cells, and COS cells transfected with pcDNA3.1-CASK F.L. or pcDNA-CASKΔ. An additional band of ~75 kDa was detected in all COS cells, which may corresponds to a predicted smaller CASK isoform. A band of ~65 kDa was only detected in COS cells transfected with pcDNA3.1-CASKΔ, corresponding to the same size protein observed *in vivo* in skeletal muscle. (D.) Western analysis of membrane protein-enriched microsome preparations from total skeletal muscle, using a CASK monoclonal antibody, demonstrates that both CASK F.L. and CASKΔ protein are associated with the membrane.

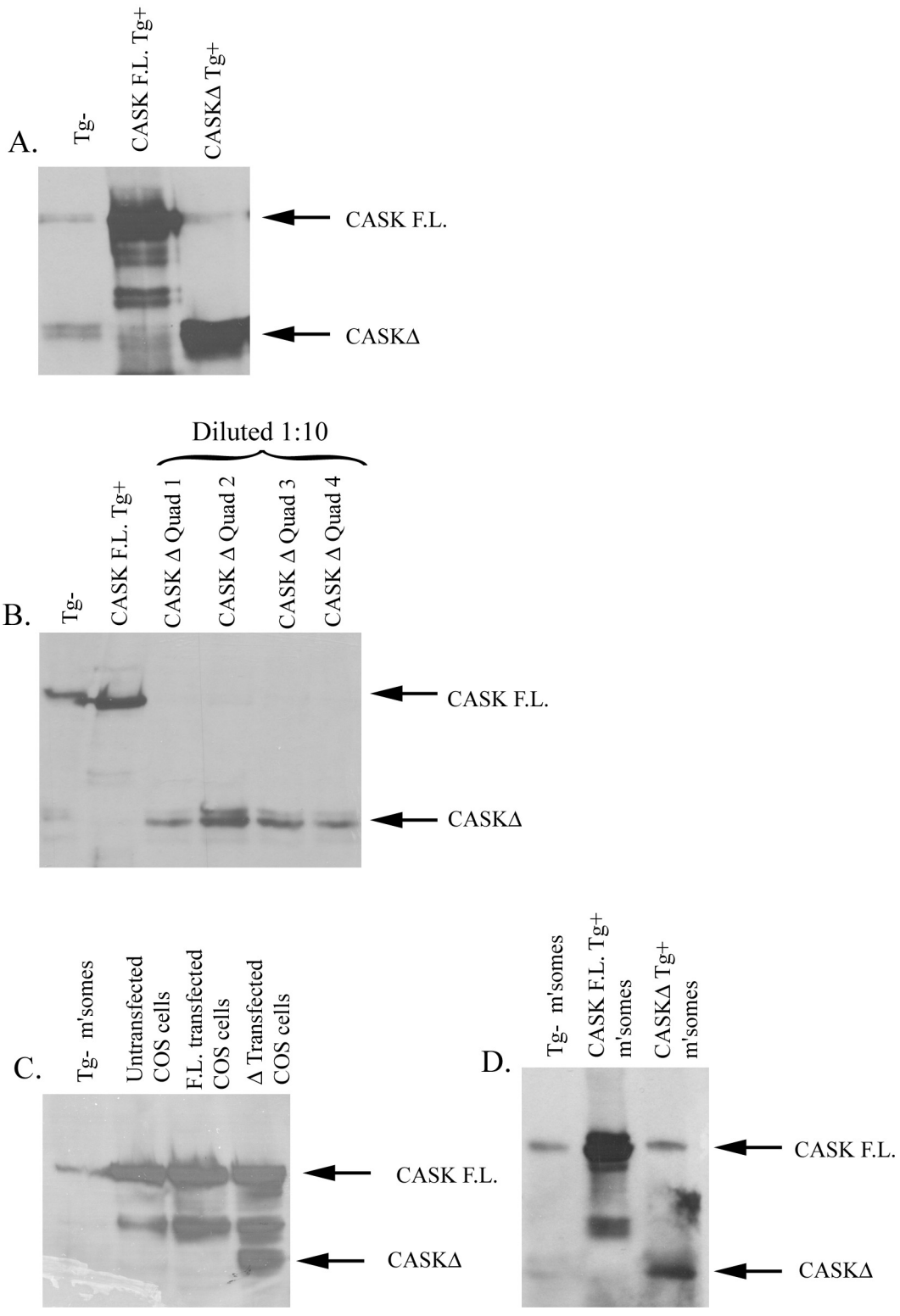

Figure 3.2 A-D Western analysis of CASK F.L. and CASKΔ protein

Figure 3.3: Overexpressed CASK protein is localized to both the membrane and cytoplasm in CASK F.L. and CASKΔ transgenic positive mouse skeletal muscle

An affinity-purified polyclonal antibody raised against CASK was used for immunohistochemical analysis of quadriceps, soleus, extensor digitorum longus (EDL), and tibialis anterior (TA) muscle from transgenic negative and transgenic positive mice. In skeletal muscle from transgenic negative mice, CASK localizes specifically to the neuromuscular junction. In skeletal muscle that is overexpressing the full-length CASK protein or a truncated CASK protein, CASK expression is seen around the membrane and in the cytoplasm. Bar = 50 μm

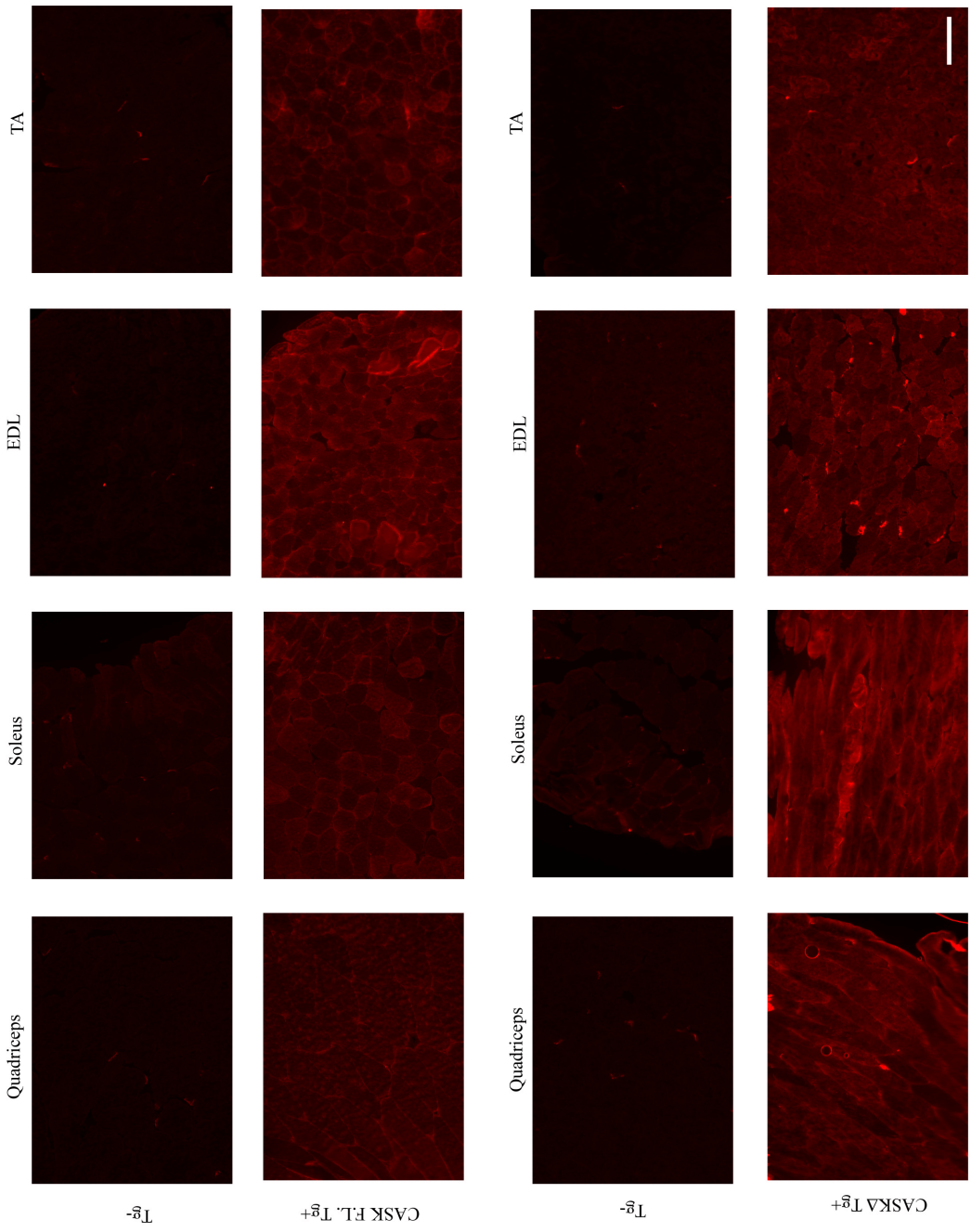

Figure 3.3

Figure 3.3 Overexpressed CASK protein is localized to both the membrane and cytoplasm in CASK F.L. and CASKΔ transgenic positive mouse skeletal muscle

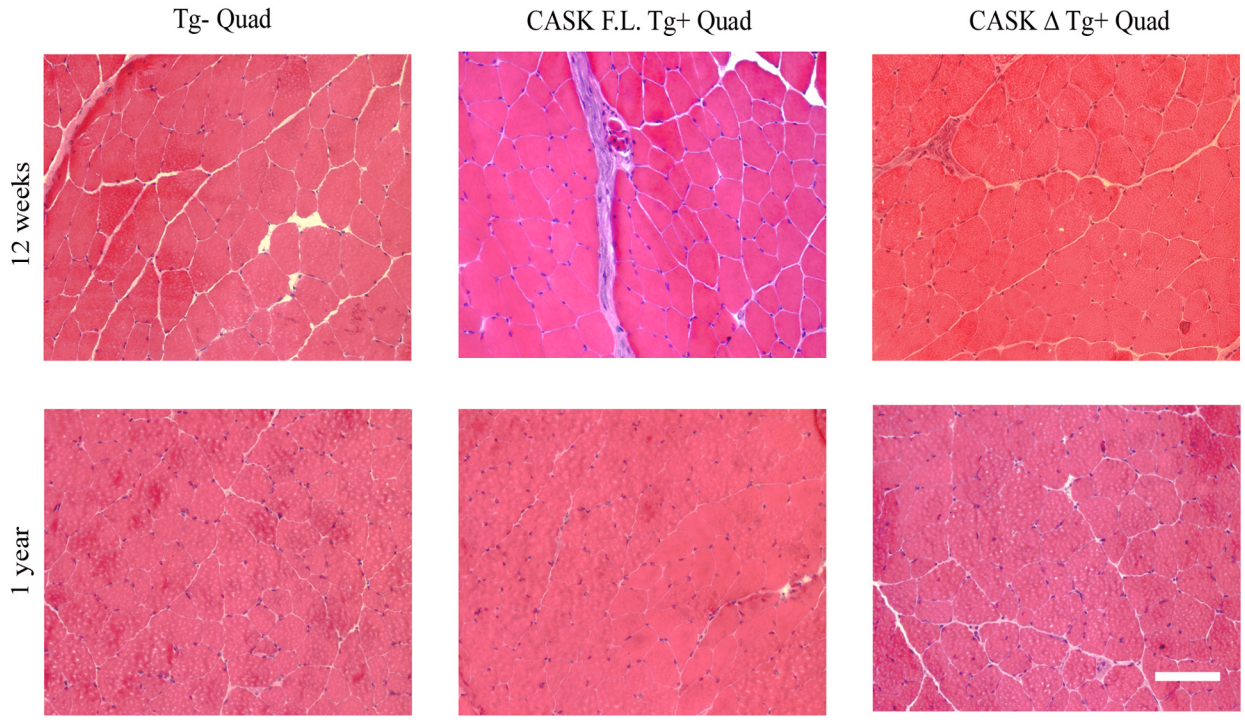

Figure 3.4: Morphology of CASK F.L. and CASKΔ transgenic positive quadriceps muscle

Hematoxylin and Eosin (H&E) staining of transgenic negative quadriceps muscle shows densely packed fibers with nuclei that localized to the periphery of the fiber. H&E staining of mouse quadriceps muscle from 12 week old and 1 year old mice overexpressing either CASK F.L. or CASKΔ protein display normal morphology. There are some centrally nucleated fibers visible in the CASKΔ mice, but counts of central nuclei demonstrate the percentages of centrally nucleated fibers are equivalent between all three genotypes. Bar = 50 μm

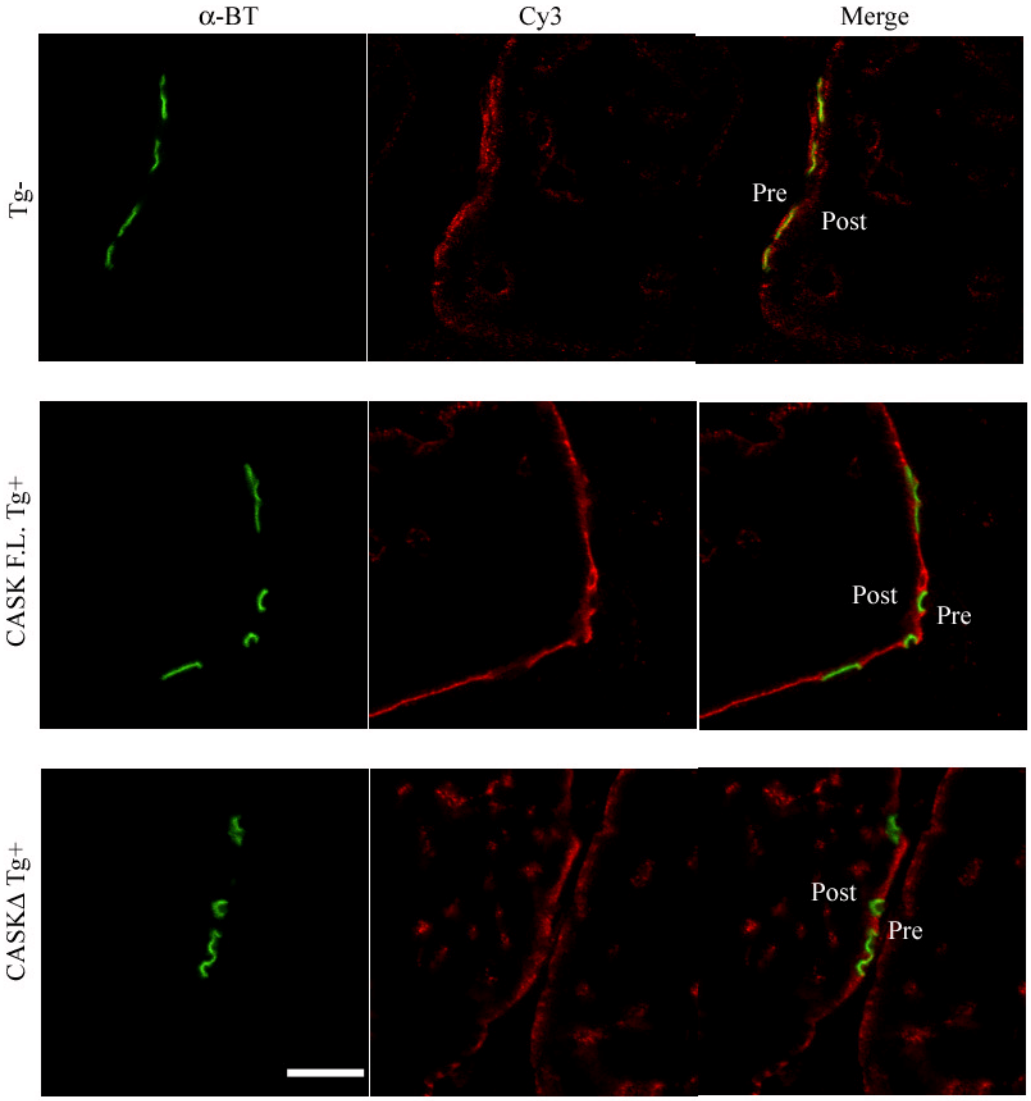

Figure 3.5: Confocal analysis of NMJs immunostained for CASK on quadriceps from Tg-, CASK F.L. and CASKΔ skeletal muscle

Immunofluorescence of fixed Tg-, CASK F.L. and CASKΔ quadriceps muscles followed by confocal microscopy show the localization of CASK (red) relative to Alexa 488 α-bungarotoxin-labeled AChRs (green). The third panel is a merged image of the red and green channels. In Tg- mice CASK immunolocalization is oberserved postsynaptically at the primary gutter and presynaptically. In CASK F.L. and CASKΔ mice CASK staining is observed postsynaptically, but there is no detectable presynaptic staining. Images shown are representative images and all images were taken at equal exposures. Bar = 25 nm

A.

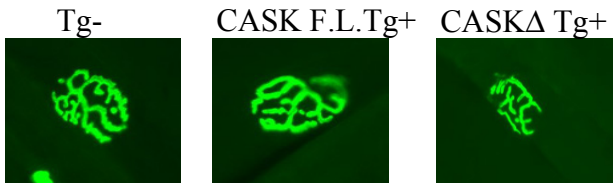

B.

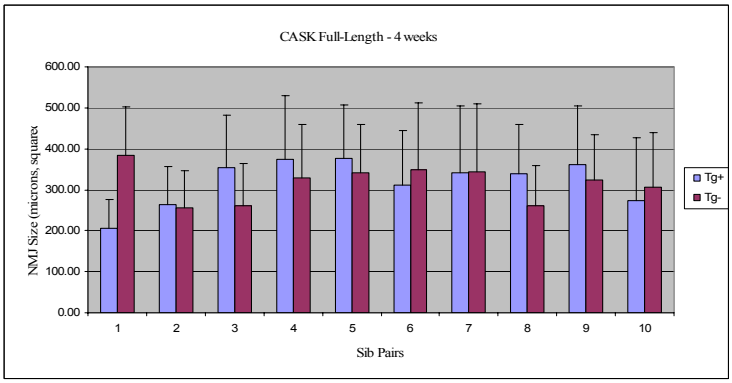

Continued

Figure 3.6 A-C: Analysis of NMJ size and morphology from quadriceps muscle of CASK F.L. and CASKΔ mice

In order to examine the morphology and size of the postsynaptic membrane of the NMJ, quadriceps muscle from CASK F.L. and CASKΔ mice were stained with fluorescently-conjugated α-bungarotoxin, which binds to AChR, and viewed en face. (A.) There were no gross differences in NMJ morphology oberserved between transgenic negative and CASK F.L. and CASKΔ mice at 4 and 8 weeks of age. Images shown are representative from 8 week old mice. (B.) NMJ measurements were made from ten Tg-/Tg+ pairs of CASK F.L. or CASKΔ mice, at both 4 and 8 weeks of age. This analysis revealed no differences in average NMJ size between Tg- and Tg+ mice, from either CASK transgenic line. NMJ sizes were determined by measuring the circumference of the en face NMJs and n>20 for each mouse. (C.) The NMJs of Tg- and CASKΔ mice were examined on an ultrastructural level using EM analysis. EM analysis revealed that the NMJs of CASKΔ mice Are unaffected on an ultrastructural level, as compared with Tg- mice. Bar, 1cm =1.6 mm

Figure 3.6 A-C continued

B.

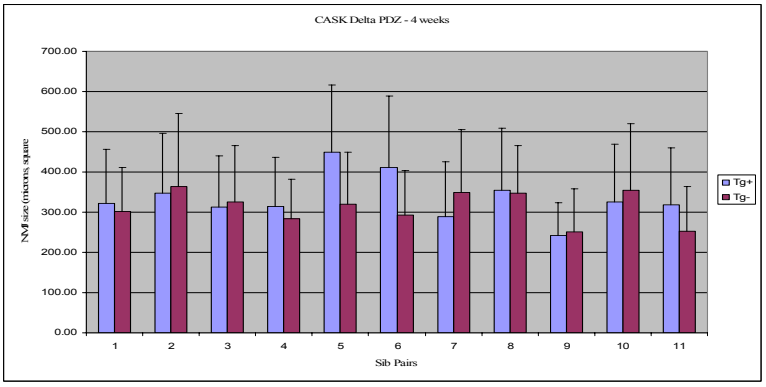

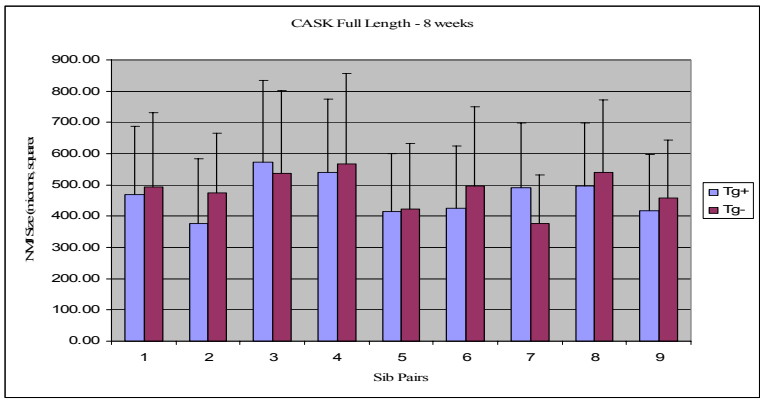

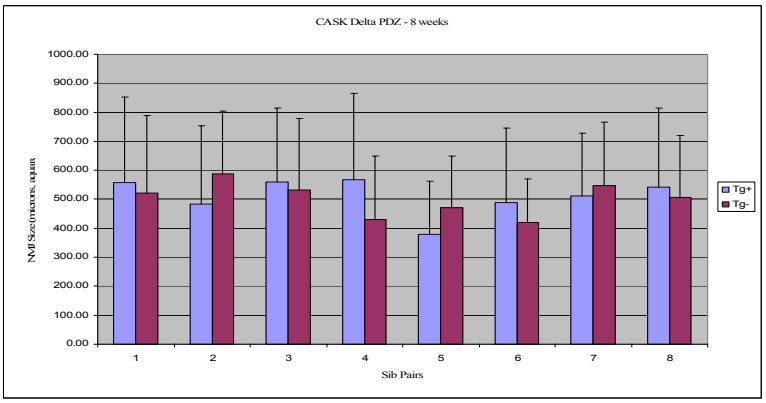

Continued

Figure 3.6 A-C continued

C.

Tg-

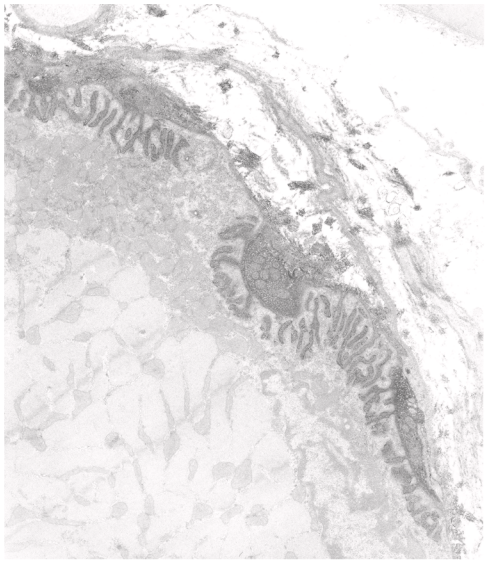

CASKΔ Tg+

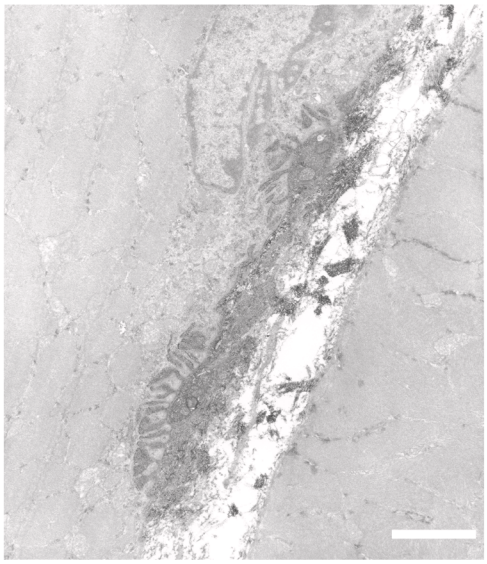

Figure 3.7: Functional analysis of CASK F.L. and CASKΔ mice.

(A.) The forelimb grip strength of 3 pairs of Tg-/Tg+ CASK F.L. or CASKΔ mice was examined at 2-3 months and at 6 months of age. These analyses demonstrate that the forelimb gripstrength, normalized to mouse weight, was not affected by overexpression of either CASK F.L. or CASKΔ protein. (B.) Physiological analysis was conducted to examine the maximum tetanic contraction from EDL muscles of Tg-, CASK F.L. and CASKΔ mice. These analyses revealed that the tetanic force, measured in mN and normalized to cross-sectional area of the fiber, showed no significant differences between any of the three genotypes.

Figure 3.7 A-B

A.

	Grip Strength (mN/g)	**Standard Deviation**
CASK F.L.		
8 weeks Tg-	8.47	0.29
8 weeks Tg+	8.60	0.36
6 months Tg-	7.58	1.50
6months Tg+	8.17	2.31
CASKΔ		
12 weeks Tg-	9.71	9.86
12 weeks Tg+	11.34	3.48
6 months Tg-	7.01	0.65
6 months Tg+	8.28	1.63

B.

	Wild-type	**CASK F.L.**	**CASKΔ**
N	6	5	5
Force (mN/mm2)	114.4633	112.154	102.62
SEM	6.561	3.140	4.402

	WT vs CASK FL	**WT vs CASKΔ**	**CASK F.L. vs CASKΔ**
p-Values	0.7735	0.1859	0.1159

Figure 3.8: Immunofluorescence analysis of Dlg and CASK candidate interactors in quadriceps muscle from CASK F.L. and CASKΔ mice.

In order to ascertain whether overexpression of CASK F.L. or CASKΔ protein affects localization of Dlg or CASK candidate protein interactors, immunohistochemical analysis was conducted on cross-sections of quadriceps muscle from Tg-, CASK F.L. and CASKΔ mice. Polyclonal antibodies to Dlg and the CASK candidate post-synaptic interactors, Girk2, Kir 2.2, Kir 2.3, ErbB4, NR2A and NR2B, and the heparan sulfate proteoglycan, Syndecan-3 (red) were used for detection of these proteins. Quadriceps sections were also stained with Alexa-488 α-bungarotoxin to label NMJs (green). Dlg, Girk2, Kir 2.2, Kir 2.3, ErbB4, NR2A and NR2B co-localized with AChRs in Tg- quadriceps. Syndecan-3 localized to satellite cell nuclei. There were no changes in protein localization observed for the Dlg, Kir 2.2, Kir 2.3, ErbB4, NR2A or Syndecan-3 proteins, in CASK F.L. or CASKΔ quadriceps muscle, as compared to Tg- quadriceps muscle. Immunohistochemical analysis of the Girk2 and NR2B protein suggests that these two proteins are slightly upregulated in response to overexpression of CASK F.L. or CASKΔ protein. Girk2 appears upregulated in the cytoplasm of CASK F.L. and CASKΔ mice, while NR2B appears upregulated at both the membrane and the cytoplasm of CASK F.L. and CASKΔ mice. For each antibody exposure times are equal between all three genotypes. Bar = 50 μm

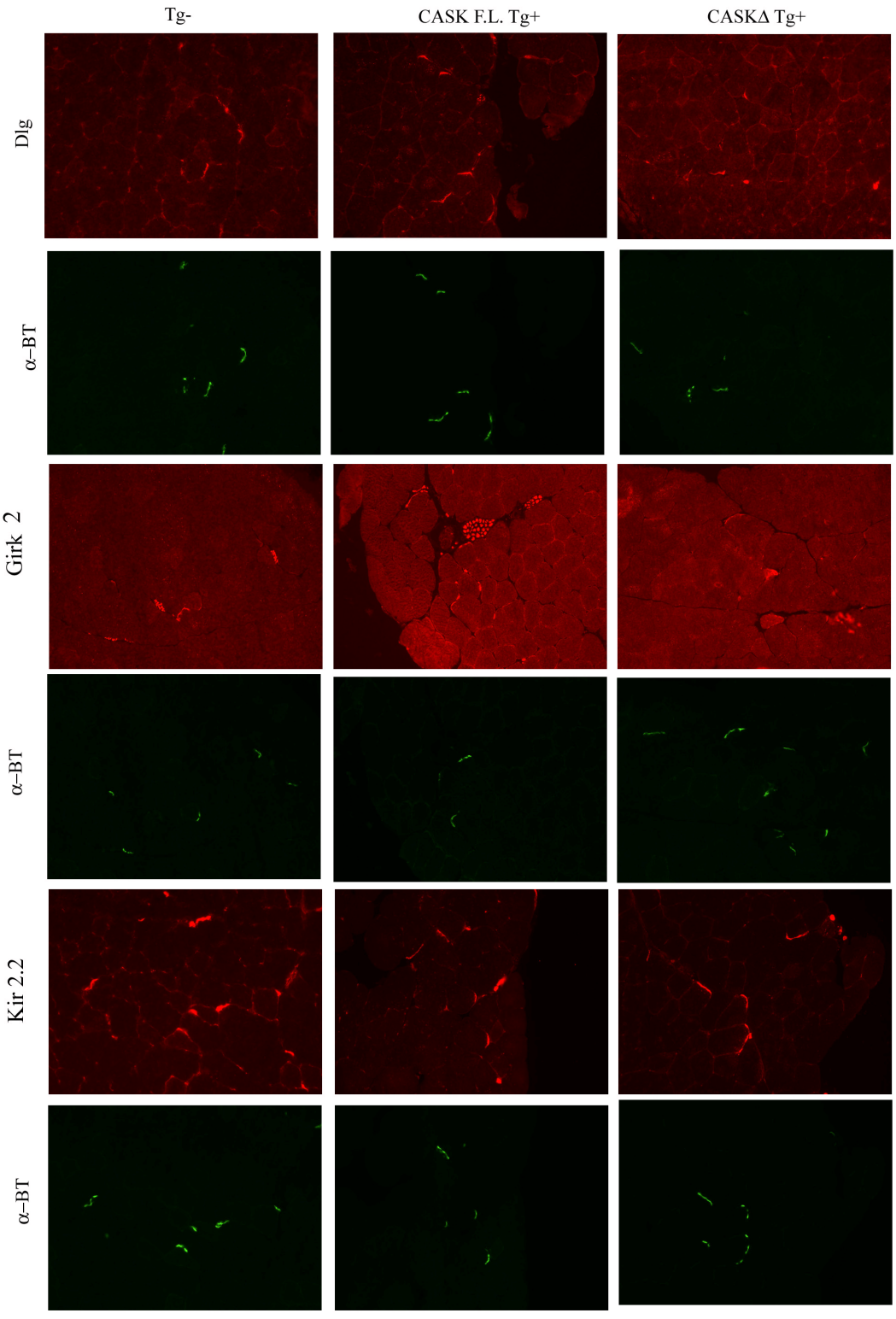

Continued

Figure 3.8 Immunofluorescence analysis of Dlg and CASK candidate interactors in quadriceps muscle from CASK F.L. and CASKΔ mice

Figure 3.8 continued

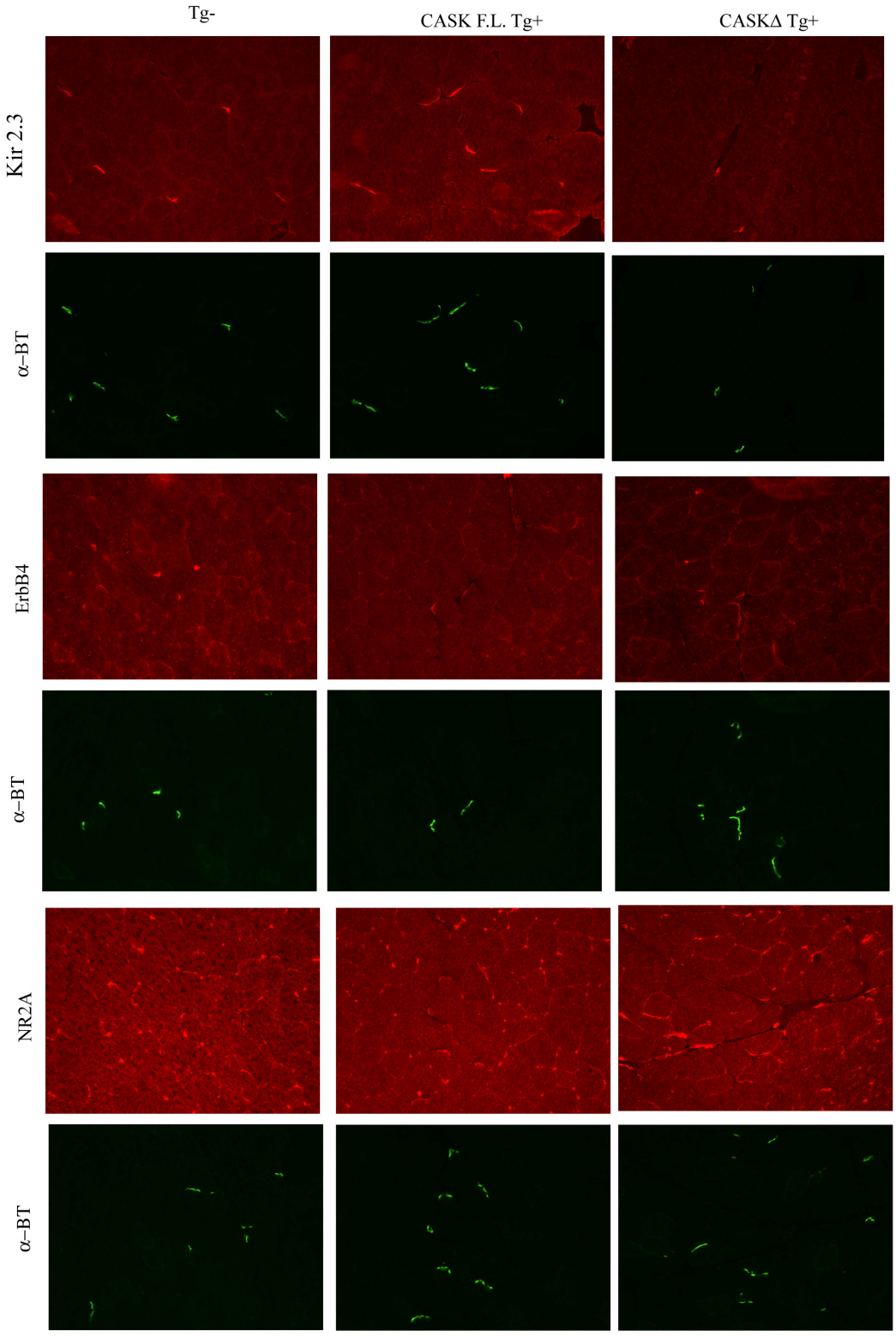

Continued

Figure 3.8 continued

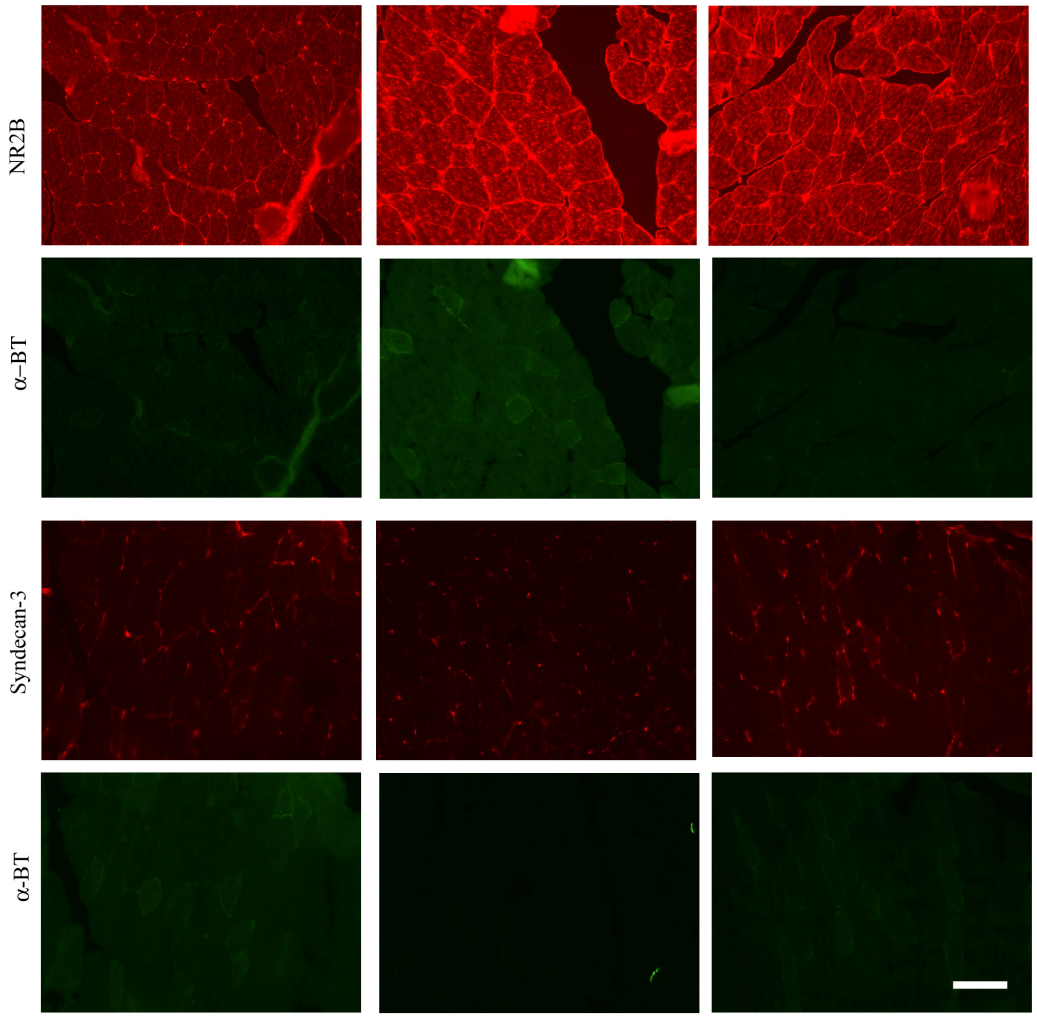

Figure 3.9: Proteomic analysis of CASK F.L. and CASKΔ skeletal muscle

Coomassie stained gels comparing global proteomic expression in Tg-, CASK F.L. and CASKΔ skeletal muscle. Total protein homogenates were first subjected to isoelectric focusing on pH 4-7 strips and then electrophoresed on SDS-PAGE, 8-16% gradient gels. Gels were Coomassie stained to detect any differences in protein expression. The protein spot that was sent to be analyzed by mass spectrometry analysis and identified as Troponin T is boxed in red.

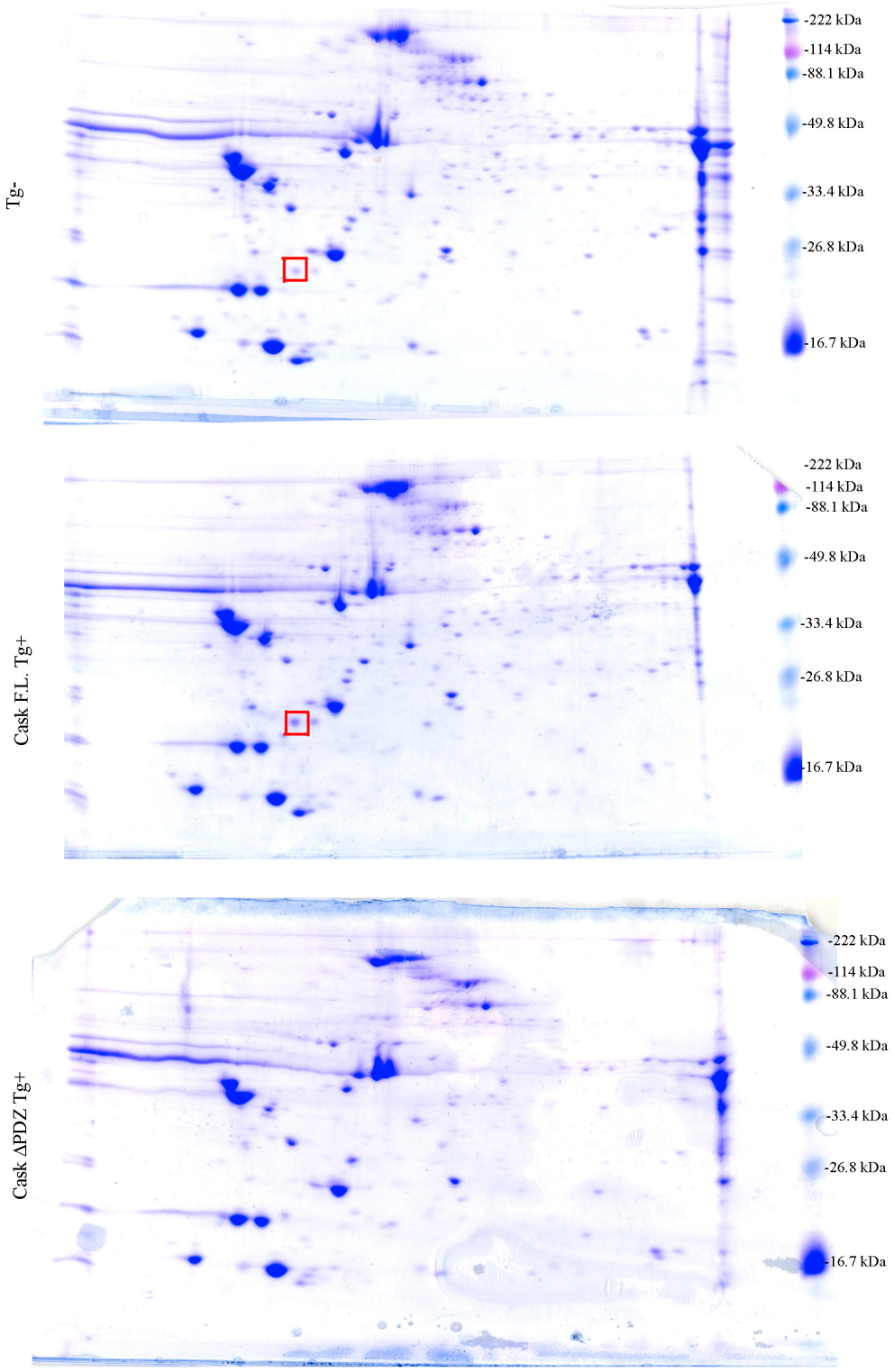

Figure 3.9 Proteomic analysis of CASK F.L. and CASKΔ skeletal muscle

CHAPTER 4

CLAUDIN-5 LOCALIZES TO THE LATERAL MEMBRANES OF CARDIOMYOCYTES AND IS ALTERED IN UTROPHIN/DYSTROPHIN-DEFICIENT CARDIOMYOPATHIC MICE

Introduction

Dilated cardiomyopathy (DCM) is characterized by dilation of the left or both ventricles and extensive areas of inflammation and fibrosis, resulting in impaired contraction of the heart. The causes of most cases of idiopathic DCM remain unknown, although mutations affecting cytoskeletal, sarcomeric, and other proteins in some rare familial cases, have recently been described (Reviewed in (Towbin and Bowles, 2002); (Bienengraeber et al., 2004)). The effects of these mutations on the molecular and cellular mechanisms that lead to dilation and heart failure are not understood; although recently, a number of studies in patients and animal models have demonstrated a connection between remodeling of cell junctions and cardiomyopathy (Barker et al., 2002; Ehler et al., 2001; Ferreira-Cornwell et al., 2002; Gutstein et al., 2003; Perriard et al., 2003).

Chapter 4 published with the permission of Journal of Molecular and Cellular Cardiology

In the heart, cardiomyocytes are joined end to end via intercalated discs, but are separated from each other laterally by extracellular matrix. Intercalated discs couple cells both mechanically and ionically through three types of cell junctions: adherens junctions, desmosomes, and gap junctions. Adherens junctions and desmosomes aid in the transmission of force through their linkage to the actin cytoskeleton and intermediate filaments. Gap junctions are communicating junctions composed of connexin protein subunits which form a permeable channel, that electrically couples adjacent cells and causes the heart to contract coordinately. Adherens junction, gap junction and desmosome proteins have been shown to be remodeled in several animal models of DCM (Barker et al., 2002; Ehler et al., 2001; Ferreira-Cornwell et al., 2002; Gutstein et al., 2003; Perriard et al., 2003).

Tight junctions are the main occluding cell junction which function as both an intramembrane and paracellular diffusion barrier, selectively regulating the movement of water and solutes at the lateral membranes of epithelial and endothelial cells. At the molecular level, tight junctions are complex structures composed of multiple adhesion molecules. The major components of these junctions are occludin, junctional adhesion molecule, and claudins (Reviewed in (Matter and Balda, 2003c; Sawada et al., 2003; Tsukita et al., 2001)). Although the tight junction has not been identified as a structure in cardiac muscle, the tight junction associated protein zonula occludens (ZO-1), which has been shown to interact with claudins, is present at both the intercalated discs and lateral membranes of cardiomyocytes (Barker et al., 2001; Barker et al., 2002; Itoh et al., 1999a; Kobayashi et al., 2002). Investigations of other tight junction proteins in the heart have not been carried out.

Claudins are integral membrane proteins containing four transmembrane domains and are the major structural component of tight junctions. The claudin-5 gene, located on chromosome 22q11, encodes a member of this claudin protein family and is expressed in every tissue examined to date (Matter and Balda, 2003b; Morita et al., 1999a; Morita et al., 1999b; Sirotkin et al., 1997; Tsukita and Furuse, 2000a; Tsukita and Furuse, 2000b). Also known as TMVCF (transmembrane protein deleted in velo-cardio-facial syndrome), deletion of claudin-5 can result in two autosomal disorders, velo-cardio facial syndrome and DiGeorge syndrome; the phenotypes include cleft palate, learning disabilities, facial dysmorphologies and conotruncal heart abnormalities (Epstein and Buck, 2000; Goldmuntz and Emanuel, 1997; Lindsay, 2001; Sirotkin et al., 1997). A claudin-5 knock-out in the mouse results in alterations of the blood brain barrier and death within 10 days of birth (Nitta et al., 2003). Notably, this claudin-5 deficiency did not result in a break down of tight junctions in brain; rather the tight junctions became more permeable to small molecules, a result that can be attributed to replacement of claudin-5 with occludin or another claudin protein.

We show by western and immunohistochemical analysis that claudin-5 protein is present in mouse cardiac muscle and localizes to the lateral membrane of cardiomyocytes. In order to examine the possible role of this tight junction protein in cardiomyopathy, we also determined claudin-5 protein levels and localization in two cardiomyopathic mouse models: dystrophin-deficient *mdx* mice and mice deficient for both dystrophin and the dystrophin homolog, utrophin (dko mice) (Bulfield et al., 1984; Deconinck et al., 1997b). The *mdx* mouse is the genotypic model for Duchenne muscular dystrophy (DMD) which is characterized in patients by progressive skeletal muscle

weakness and DCM (Emery, 1993; Towbin, 1998). Dko mice have more skeletal and cardiac muscle deficiencies than *mdx* mice and show all the clinical signs of DMD (Bulfield et al., 1984; Deconinck et al., 1997b). We have previously shown that *mdx* and dko hearts are characterized by degenerating cardiomyocytes, myocarditis, and fibrosis (Hainsey et al., 2003). Additionally, dko mice exhibit abnormal ECG patterns (Bia et al., 1999). We now demonstrate that claudin-5 protein levels are decreased at the lateral membranes of cardiomyocytes in dko hearts, but that claudin-5 protein levels and localization are unaltered in *mdx* hearts. In addition, microarray analysis of gene expression shows that claudin-5 mRNA is downregulated three-fold in dko hearts compared to *mdx* hearts. These data suggest that, in addition to remodeling that has been shown to occur at the intercalated disc, alteration of a cell junction protein at the lateral membrane of cardiomyocytes can also characterize cardiomyopathy**.**

Materials and Methods

Mice

Mdx; Utrn +/- mice with or without a Δ17-48 dystrophin transgene were mated to *mdx*;Utrn +/- mice to generate *mdx*;Utrn -/- (dko) and *mdx*,Utrn +/+ (*mdx*) mice and Δ17-48/dko. All mice were genotyped for the utrophin knockout allele and dystrophin transgenic status by PCR as previously described (Deconinck et al., 1997b; Rafael et al., 2000). Wild-type C57BL/10 (C57) mice were maintained as a separate inbred line. Mice were treated in accordance with the Institutional Laboratory Animal Care and Use Committee.

Immunblots

Hearts from 10 week-old C57, *mdx*, dko, and Δ17-48/dko mice were homogenized in Newcastle buffer (4M Urea, 75 mM Tris, pH 6.8, 3.8% SDS) and protein concentrations were determined using the Dc Protein Assay (Bio-Rad, Richmond, CA). Protein (100μg) was then run out on 8%,10%, or 12% SDS-Polyacrylamide gel electrophoresis (SDS-PAGE) gels at 80V. Proteins were then transferred from SDS-PAGE gels to nitrocellulose (Schleicher and Schuell Bioscience, Keene, NH) at 80 V for 45, 80 or 110 minutes using a wet transfer apparatus (Bio-Rad, Richmond, CA). Western blots were blocked in 5% nonfat milk in Tris-buffered saline plus 0.1% Tween-20 (TBST) and 1% normal goat serum (NGS) for one hour. Blots were then incubated with affinity purified polyclonal primary antibodies diluted in TBST and 1% NGS for two hours at the following dilutions: rabbit anti-claudin-5 (Zymed, San Francisco, CA) 1:250; rabbit anti-ZO-1 (Zymed) 1:250; rabbit anti-pan-cadherin (Sigma, St. Louis, MO) 1:400; rabbit anti-β-catenin (Sigma) 1:8000; rabbit anti-α-catenin (Sigma) 1:4000; rabbit anti-desmoplakin (Serotec, Oxford, UK) 1:200; rabbit anti-connexin-43 (Zymed) 1:500. Blots were then washed 3 x 15 minutes in TBST and incubated with horse-radish peroxidase (HRP)-conjugated goat anti-rabbit secondary antibody (Jackson Labs, West Grove, PA) for one hour at 1:10,000 in TBST plus 1% NGS. Enhanced chemiluminescence using the ECL plus kit (Amersham Pharmacia, Buckinghamshire, England) was used for detection of bound primary antibody. Each experiment was repeated at least three times with samples from at least two independent mice of each genotype. Claudin-5 analysis was performed on seven dko samples to confirm the data.

The blot shown in Figure 1A was over-exposed to show the dramatic difference in levels of claudin-5 protein between *mdx* and dko heart samples.

Immunohistochemistry

Immunohistochemistry was performed on unfixed 8 μm heart cryosections. Hearts were dissected from 10 week-old C57, *mdx* or dko mice and frozen in OCT (VWR, West Chester, PA) in liquid-nitrogen-cooled isopentane. Sections were blocked in 1% gelatin in potassium phosphate-buffered saline (KPBS) for 15 minutes. Following blocking, sections were washed and incubated in primary antibody for two hours at the following dilutions: rabbit anti-claudin-5 (Zymed) 1:10; rabbit anti-ZO-1 (Zymed) 1:250; rabbit anti-pan-cadherin (Sigma) 1:200; rabbit anti-β-catenin (Sigma) 1:1000; rabbit anti-α-catenin (Sigma) 1:500; rabbit anti-desmoplakin (Serotec) 1:100; rabbit anti-connexin-43 (Zymed) 1:400. Sections were then washed and incubated for one hour in Cy3-conjugated goat anti-rabbit (Jackson Immunoresearch), or Cy3-conjugated goat anti-rabbit plus FITC-conjugated goat anti-mouse IgG (for detection of degenerating myocytes). All antibodies were diluted in KPBS and 0.5% gelatin (KPBSG) plus 1% NGS. Images were obtained using a Nikon Eclipse E800 microscope (Nikon Corporation, Tokyo, Japan) with a SPOT-RT slider digital camera and SPOT software (Diagnostic Instruments, Inc., Sterling Heights, MI). Claudin-5 analysis was performed on seven dko samples to confirm the data. Confocal anaysis was conducted using a Zeiss 510 Meta laser scanning microscope (Carl Zeiss, Thornwood, New York). Images were taken using the 63x objective and 3x zoom.

Microarray analysis

DNA microarray analysis was run as three independent triplicates for *mdx* and dko hearts from eight week-old mice. DNA microarray methods were described previously (Porter et al., 2004; Porter et al., 2003b). Briefly, total RNA was extracted from hearts using TRIzol reagent (GibcoBRL, Rockville, MD). RNA pellets were resuspended at 1 µg RNA/µl DEPC-treated water and 8 µg was used in a reverse transcription reaction (SuperScript II; Life Technologies, Rockville, MD) to generate first strand cDNA. Double strand cDNA was synthesized and used in an *in vitro* transcription (IVT) reaction to generate biotinylated cRNA. Fragmented cRNA (15 µg) was used in a 300 µl hybridization cocktail containing herring sperm DNA and BSA as carrier molecules, spiked IVT controls, and buffering agents. A 200 µl aliquot of this cocktail was used for hybridization to Affymetrix (Santa Clara, CA) MG-U74Av2 microarrays for 16 hr at 45^{o} C. The manufacturer's standard post-hybridization wash, double-stain, and scanning protocols used an Affymetrix GeneChip Fluidics Station 400 and a Hewlett Packard Gene Array scanner.

Raw data from microarray scans were analyzed with both Affymetrix Microarray Suite (MAS) 5.0 and Robust Mutichip Average (RMA) algorithm (Irizarry et al., 2003) in ArrayAssist 2.0 (Iobion Informatics, La Jolla, CA). Transcripts absent from all samples were excluded from analysis. The MAS filter required that transcripts meet the criteria of: (a) consistent increase/decrease call across all replicate comparisons at a given time point, based upon Wilcoxon's signed rank test (algorithm assesses probe pair saturation, calculates a p value and determines increase, decrease, or no change calls) and (b)

average fold difference value ≥ 1.7. The RMA filter required that transcripts show an average fold difference value ≥ 1.7. Transcripts were defined as differentially expressed only if they passed filtering by both algorithms.

The microarray raw data series and .CEL files were posted on the National Center for Biotechnology Information (NCBI) Gene Expression Omnibus (GEO) database (http://www.ncbi.nlm.nih.gov/geo/), under series record accession number GSE1463.

Ultrastructural analysis

Whole hearts were dissected from *mdx* and dko mice, the apex of the left ventricle was removed, and immediately placed in fix (4% paraformaldehyde, 3% glutaraldhyde in 0.1M sodium phosphate buffer, pH 7.4) for one hour. The samples were then transferred to 3% glutaraldehyde in 0.1M sodium phosphate buffer, pH 7.4, overnight. Muscle was then washed 2 x 15 minutes in 0.1M sodium phosphate buffer. Samples were then post-fixed for 1.5 hours in 1% osmium tetraoxide in 0.1M sodium phosphate buffer. Following osmium fixation, sections were rinsed 3 x 5 minutes in phosphate buffer, dehydrated for 10 minutes in successive ethanol washes (50%,70%,80%, 95%, 100%, 100%), and rinsed for 15 minutes in propylene oxide. Cardiac samples were then infiltrated in 1:1 and 1:2 ratios of propylene oxide to Spurr resin (Ted Pella Inc., Redding, CA) for 1.5 hours and 2 hours, respectively. Finally, sections were embedded in Spurr resin at 60° C, overnight. Gold/silver 70-80 nm sections were cut on a Reichert UltracutE, stained with a 2% uranyl acetate plus Reynold's lead citrate and viewed using a Phillips CM12 transmission electron microscope. Ultrastructural analysis was performed on cardiac samples from three pairs of dko and *mdx* mice.

Results

Claudin-5 protein localizes to lateral cardiomyocyte membranes and cardiovasculature in heart.

Previous experiments have shown by northern blot analysis that claudin-5 mRNA is present in cardiac muscle (Morita et al., 1999a). To determine the presence of claudin-5 protein in heart, western analysis was performed using total heart protein homogenate from normal C57 10 week-old mice, using a polyclonal claudin-5 antibody. A band of the predicted 23 kDa size was detected in C57 total heart preparations (Fig. 4.1A) (Morita et al., 1999a; Tsukita and Furuse, 2000b). Immunohistochemical analysis on cryosections from C57 mice was conducted to determine the localization of claudin-5 in heart. Immunofluorescence revealed that claudin-5 localizes to the lateral membranes of C57 cardiomyocytes, where they associate with the extracellular matrix (Fig. 4.1B, C). Claudin-5 also localizes to the endothelia of cardiovasculature, but is not present at intercalated discs (Fig. 4.1C).

Claudin-5 protein is present in reduced amounts at cardiomyocyte membranes in utrophin/dystrophin deficient mice.

To determine whether claudin-5 is remodeled in animal models of cardiomyopathy, we next investigated whether claudin-5 retains normal levels and localization in dko and *mdx* cardiomyopathic hearts. Claudin-5 protein levels in *mdx* cardiac muscle appeared equivalent to C57 levels (Fig. 4.1A). In contrast, claudin-5 protein levels were dramatically decreased in dko heart as compared to C57 and *mdx* (Fig. 4.1A). In *mdx* mice, claudin-5 shows localization to the lateral membranes of cardiomyocytes and

cardiovasculature, similar to controls (Fig. 4.1C). However, in dko hearts, claudin-5 localization was significantly decreased at lateral membranes of cardiomyocytes, but not in cardiovasculature (Fig. 4.1C). Entire transverse sections of left ventricles from dko mice show a decrease in claudin-5 immunostaining, with any remaining localization appearing abnormally sparse (unpublished data [2004]). To confirm that claudin-5 remodeling is not occurring only in degenerating cardiomyocytes, immunolocalization of claudin-5 was performed in parallel with analyzing the uptake of serum proteins into the cytoplasm, which we have previously used to identify degenerating cardiomyocytes (Hainsey et al., 2003). This experiment showed that claudin-5 protein is also reduced at the lateral membranes of cardiomyocytes that are not degenerating (unpublished data [2003]). These western and immunohistochemical data demonstrate that claudin-5 protein levels are decreased in the dystrophic heart of dko mice and that this downregulation appears to precede membrane leakage.

To determine whether the absence of utrophin directly affects claudin-5, we performed western analysis with a claudin-5 antibody on heart protein homogenates from dko mice expressing a truncated dystrophin transgene that is able to prevent cardiomyopathic features (Δ17-48/dko) (Hainsey et al., 2003). Δ17-48/dko mice show levels of claudin-5 protein equivalent to those in *mdx* hearts (Fig. 4.1D). This data suggests that claudin-5 expression and localization is not directly dependent upon the presence of utrophin.

Intercalated disc cell junction proteins, and the tight junction protein, ZO-1, are not remodeled in dko cardiac muscle

Recent work has revealed that remodeling of intercalated disc cell junction proteins accompanies cardiomyopathy (Barker et al., 2002; Ehler et al., 2001; Ferreira-Cornwell et al., 2002; Gutstein et al., 2003; Perriard et al., 2003). We therefore wanted to determine whether expression or localization of these proteins is affected in the cardiomyopathic dko heart. Immunoblots were performed on cardiac muscle using affinity purified polyclonal antibodies to the adherens junction proteins, cadherin, β-catenin, and α-catenin; the gap junction protein, connexin-43; and the desmosome protein, desmoplakin. Western blot analysis of the same protein homogenates used for claudin immunoblots, revealed that the protein levels of these proteins were not changed in dko or *mdx*, as compared with C57 levels (Fig. 4.2A). Next, immunohistochemical analysis was performed using these same antibodies to detect any differences in the localization of these proteins between the cardiomyopathic models and controls. As expected, the localization of all of these cell junction proteins in C57 cardiac muscle are present at the intercalated disc (Fig. 4.2B). Immunohistochemistry revealed that the localization of adherens junction and desmosomal proteins were not altered in either *mdx* or dko cardiac muscle. The gap junction protein, connexin-43, may show minor alterations in localization, but western analysis showed no gross changes in protein levels.

Since claudin-5 is a tight junction protein, we also analyzed another tight junction associated protein, ZO-1, which is present at both the intercalated disc in cardiomyocytes and lateral membranes (Barker et al., 2001). Analysis of immunoblots demonstrated ZO-

1 protein levels in the dko heart were equivalent to C57 and *mdx* levels (Fig. 4.2A). Although ZO-1 protein levels were unaltered, there does appear to be a slight change in localization in the dko heart (Fig 4.2B). Levels of the tight junction protein occludin were also unaltered in immunoblots of *mdx* or dko heart samples (unpublished data [2003]). Overall, these results suggest that the decrease in claudin-5 expression observed in dko hearts is a specific change that occurs in cardiomyopathic dko cardiac muscle. Furthermore, it appears that cardiomyopathy in the dko heart does not result in remodeling of intercalated disc cell junction proteins, as has been found in other cardiomyopathic animal models; the dko mouse seems to exhibit protein remodeling at the lateral membrane.

Expression of the gene encoding claudin-5 is downregulated in hearts from dko mice

In a parallel experiment, we sought to determine gene expression differences between hearts from dko and *mdx* mice using DNA microarray analysis. Pooled mRNA samples from three mice of each genotype was used for each microarray experiment and the experiment was repeated with three different sets of mice to determine significant gene expression changes. Claudin-5 is three-fold downregulated in dko versus *mdx* hearts and is one of only 13 genes found to be differently expressed between hearts from mice of these genotypes (Table 4.1). Downregulation of claudin-5 transcript suggests that the reduced levels of protein in dko hearts are due, at least in part, to transcriptional regulation. The utrophin mRNA was shown to be downregulated in dko samples due to the insertion of the knockout cassette into this gene, showing the validity of the microarray analysis. Notably, only 13 genes were found to be differentially expressed in dko versus *mdx* hearts compared with 148 gene expression differences found between

dko and *mdx* limb muscle (unpublished data [2004]). Of the 13 expression differences found between dko and *mdx* hearts, only the claudin-5, *Acta1*, and *Tgtp* genes are changed exclusively in this microarray analysis. The other ten genes also show differences in gene expression in microarray experiments comparing either *mdx* versus dko limb muscle (unpublished data [2004]), and/or C57 versus *mdx* limb muscle, diaphragm, or heart (Porter et al., 2002; Porter et al., 2003a; Porter et al., 2004). These data suggest that claudin-5 is one of only three gene expression changes that specifically characterize the cardiomyopathy of dko mice, and are probably not involved in the common pathways observed in dystrophic skeletal and cardiac muscle such as degeneration, inflammation, and fibrosis.

The lateral membranes of cardiomyocytes in dko heart have an abnormal wavy appearance

Since western analysis and immunohistochemical analysis showed that claudin-5 protein was decreased in dko heart, while intercalated disc proteins appear unaffected, ultrastructural analysis was conducted to determine if there were any changes in the lateral membranes or intercalated discs in *mdx* and dko hearts. The structure of the intercalated disc showed no gross abnormalities in either *mdx* or dko hearts (Fig. 4.3). However, in dko hearts the lateral membranes were severely affected, as compared with *mdx*, exhibiting what appears to be a loss in the density of lateral membrane, as well as an abnormal wavy appearance (Fig. 4.3). This data provides further evidence that DCM in the dko mouse, a muscular dystrophy model, is characterized by abnormalities of the lateral membranes in cardiomyocytes.

Discussion

We now show by western and immunohistochemical data that the tight junction protein, claudin-5, is present in normal heart muscle at the lateral membrane of cardiomyocytes and in cardiovasculature. *Mdx* hearts show no differences in claudin-5 protein levels or localization as compared with C57. In contrast, claudin-5 protein levels in cardiomyopathic dko heart homogenates are greatly decreased compared with C57. Immunohistochemical analysis demonstrates that localization of claudin-5 at the lateral membranes of dko cardiomyocytes is also diminished compared to normal levels. This slight discrepancy between the levels of claudin-5 in dko heart detected by western and immunohistochemical analysis may be explained by the data that claudin-5 was detected in longer exposures of the immunoblot. Alternatively, it is also possible that the 23 kDa claudin-5 protein is cleaved, resulting in a fragment too small for detection by conventional western analysis. Interestingly, it has been shown that the dystrophin protein undergoes cleavage in a hamster model of cardiomyopathy, as well as in human patients with DCM (Toyo-Oka et al., 2004).

While the decrease in claudin-5 protein levels is clearly evident in the dko mouse, no obvious changes are observed in the *mdx* mouse. Decreased claudin-5 mRNA levels in dko compared to *mdx* hearts suggests transcriptional regulation may account for at least part of the observed differences in protein levels. This situation is comparable to a study of connexin expression in human congestive heart failure where connexin-43 protein levels were more reduced than transcript levels in patient versus control samples

(Dupont et al., 2001). The authors of this study conclude that post-transcriptional factors may also contribute to decreased connexin-43 protein. Studies of alterations of cell junction proteins in animal models have focused only on protein levels and have not analyzed levels of transcript (Ehler et al., 2001; Ferreira-Cornwell et al., 2002; Matsushita et al., 1999). Our data suggests the possibility that transcriptional regulation may also contribute to alterations of cell junction proteins in the rat ischemia model, and the MLP, TOT, and cadherin mouse models of cardiomyopathy.

The reasons for differences in cardiac phenotypes and claudin-5 changes between *mdx* and dko mice are not completely understood. As previously discussed, the dko mouse has a severe cardiomyopathy that includes histological abnormalities such as cardiomyocyte degeneration, myocarditis, fibrosis, physiological abnormalities that include tachycardia and an abnormal ECG pattern, and activation of the JNK1 cell signaling protein (Bia et al., 1999; Grady et al., 1997; Hainsey et al., 2003; Nakamura et al., 2001). The *mdx* mouse does exhibit some histological changes, as well as altered contractile properties; but overall, there are fewer detectable pathological changes than in the dko heart (Bia et al., 1999; Grady et al., 1997; Hainsey et al., 2003; Nakamura et al., 2001). For instance, *mdx* mice at 8 weeks of age do not show conduction abnormalities or similar signaling changes (Bia et al., 1999; Nakamura et al., 2001). Additionally, we show by ultrastructural analysis that the lateral membranes of cardiomyocytes have an abnormal appearance in dko, but not *mdx* mice. To our knowledge, ultrastructural abnormalities at the intercalated disc, but not at lateral membrane of cardiomyocytes have been observed in cardiomyopathic models (Arber et al., 1997; Ehler et al., 2001).

Dystrophin has been shown to play a mechanical role in skeletal and cardiac muscle by tethering the submembranous actin cytoskeleton to the membrane (Ahn and Kunkel, 1993; Straub and Campbell, 1997). Dystrophin and utrophin, which have different localization patterns in skeletal muscle and heart, appear to be functionally equivalent when localized in the correct pattern (Hainsey et al., 2003; Rafael et al., 1998b; Rafael et al., 2000; Tinsley et al., 1996). The loss of both proteins in mice, however, results in a phenotype much more severe than the addition of the two single mutants (Deconinck et al., 1997a; Deconinck et al., 1998). Dko mice have more skeletal and cardiac muscle deficiencies than *mdx* mice, show all the clinical signs of DMD, and survive for a maximum of 20 weeks (Deconinck et al., 1997b). Transgenic expression of dystrophin in dko hearts is able to prevent the cardiac pathology and these mice also show normal claudin-5 levels and localization (Hainsey et al., 2003); (Fig. 4.1D). Therefore, claudin-5 expression or localization is not directly dependent on utrophin, but rather the severity of the cardiomyopathy due to the loss of both utrophin and dystrophin.

Since utrophin relocalizes from the intercalated disc to low levels around the entire membrane of *mdx* cardiomyocytes, it is likely compensating, to some extent, for the loss of dystrophin, thereby slowing the progression of the disease pathology in these *mdx* mice (Rivier et al., 1999). Since we have only analyzed mice between eight and ten weeks of age, it is conceivable that changes in claudin-5 would be observed at a more advanced age in the *mdx* mouse, when pathology and functional deficits are more prominent. Alternatively, it is possible that claudin-5 alterations are specific to the dko mouse. Ultrastructural analysis conducted on two hearts from DMD patients that exhibited abnormal ECG patterns, shows that sarcolemmal changes were rare (Sanyal et

al., 1978). It is interesting that *mdx* mice and DMD patients, both of which lack only dystrophin, do not appear to show gross membrane alterations in non-degenerating cardiomyocytes. This suggests that in dko mice, it is the complete loss of the mechanical link, due to both dystrophin and utrophin deficiency, which is critical. This hypothesis is supported by the microarray data showing that the decrease in claudin-5 gene expression specifically characterizes dko hearts and is not a general change associated with dystrophic muscle. Claudin-5 is not contained in the much larger list of genes present in microarray data sets comparing either C57 versus *mdx* diaphragm, limb muscle, or heart, or *mdx* versus dko limb muscle (Porter et al., 2002; Porter et al., 2004; Porter et al., 2003b) (unpublished data [2004]).

Recently, studies in animal models have shown that many of the cell junction proteins present at intercalated discs are altered in DCM (Barker et al., 2002; Ehler et al., 2001; Ferreira-Cornwell et al., 2002; Gutstein et al., 2003; Perriard et al., 2003). Remodeling of cell junction proteins has been shown in two mouse models of the DCM: the muscle LIM protein (MLP) knockout mouse and the tropomodulin overexpressing transgenic (TOT) mouse. In both MLP knockout mice and TOT mice, adherens junction proteins were upregulated and gap junction proteins were downregulated (Ehler et al., 2001). Studies of transgenic mice overexpressing N-cadherin and E-cadherin in the heart both developed DCM, suggesting that modulation of cell junction protein levels can lead to cardiomyopathy in mice (Ferreira-Cornwell et al., 2002). Furthermore, experiments on rat myocardial infarcts showed that regions surrounding the infarct underwent gap junction remodeling as demonstrated by a decrease in expression and redistribution of connexin-43. Adherens junction and desmosomal proteins, cadherin and desmoplakin,

also showed decreased expression and localization changes (Matsushita et al., 1999). Similarly, cell junction proteins have also been shown to play a role in human DCM, as mutations in γ-catenin and the adherens junction-associated protein, metavinculin, cause cardiomyopathy (Maeda et al., 1997; Protonotarios et al., 2002). We have examined the levels and localization of these intercalated disc cell junction proteins in hearts of both *mdx* and dko mice and found them unaltered in comparison to C57. These data suggest that remodeling of proteins at the intercalated disc is not always associated with cardiomyopathic features.

The tight junction associated protein, ZO-1, has been shown to interact with the carboxy-terminus of claudins *in vitro* in epithelial cells and exhibits increased association with connexin-43 during gap junction remodeling in cardiomyocytes (Barker et al., 2002; Itoh et al., 1999a; Kobayashi et al., 2002). Our results demonstrate that ZO-1 levels in both *mdx* and dko hearts are normal; however, minor localization abnormalities of ZO-1 and connexin-43 might be present in dko hearts. Since the protein levels are unaffected, any differences in localization are subtle compared with claudin-5 abnormalities. Therefore, the changes that were observed in the claudin-5 protein seem to be specific to claudin-5, rather than a general feature of tight junction proteins in the dko heart. The alteration of claudin-5 at the lateral membranes of dko cardiomyocytes demonstrates that cell junction proteins not present at the intercalated disc can also be remodeled in response to cardiomyopathy. These observations provide novel insight into the molecular basis of DCM in an animal model of cardiomyopathy.

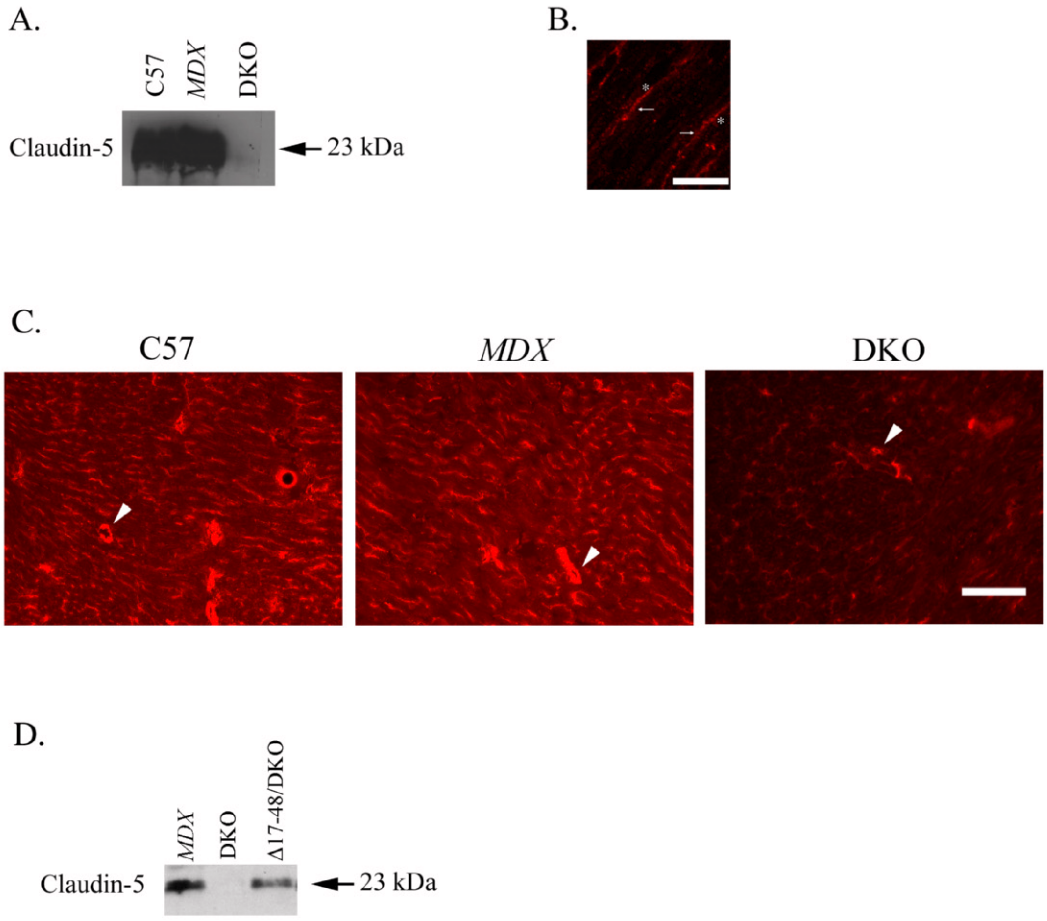

Figure 4.1 A-D: Claudin-5 protein levels and localization in C57, *mdx*, and dko heart.

A.) An affinity-purified polyclonal antibody raised against claudin-5 detects a band of 23 kDa on a western blot of total protein from C57 and *mdx* heart. The claudin-5 protein is detected at extremely low levels in heart homogenate from a dko mouse. B.) Single confocal section of C57 heart immunostained with this same antibody shows localization of claudin-5 protein to the lateral membranes of a cardiomyocyte (arrows). * shows the location of extracellular matrix separating adjacent cardiomyocytes. C.) Immunostaining of cross-sections from cardiac muscle detects localization of claudin-5 protein to the lateral membranes of cardiomyocytes in C57 and *mdx* heart, as well as the endothelia of cardiovasculature (arrows). In contrast, claudin-5 protein is present at lower levels in cardiomyocytes in dko heart; localization appears unaffected in cardiovasculature (arrow). All images were taken at equal exposures. Bar= 24 nm (B.) or 100 µm (C.) . D) Western analysis with an antibody against claudin-5 on protein homogenate from Δ17-48/dko heart shows levels equivalent to those seen in mdx heart samples in comparison to the decreased levels of claudin-5 observed in dko hearts.

Figure 4.2 A-B: Western and immunohistochemical analysis of adherens junction, gap junction, desmosomal and tight junction proteins

A.) Western analysis was conducted on total protein from C57, *mdx* and dko heart using affinity-purified polyclonal antibodies to the intercalated disc proteins, cadherin, α-catenenin, β-catenin, connexin-43,and desmoplakin I/II, as well as the tight junction protein, ZO-1. The Desmoplakin I/II antibody detects two alternatively spliced variants of the desmoplakin protein. Antibodies to all proteins detected bands of the predicted sizes (labeled on right of panels) and levels of all proteins were equivalent between all three genotypes. B.) Immunohistochemical analysis was also conducted with these same antibodies to determine if localization of these proteins was altered in *mdx* and dko heart. Cadherin, α-catenin, β-catenin, desmoplakin and connexin-43 localize to the intercalated disc, and ZO-1 localized to both intercalated discs and points of cell-matrix contact in normal mouse heart (C57). Localization of these proteins appeared unaltered in *mdx* and dko cardiac muscle, with the exception of connexin-43 and ZO-1 which may show slight alterations in localization. All images were taken at equal exposures. Bar = 60 μm

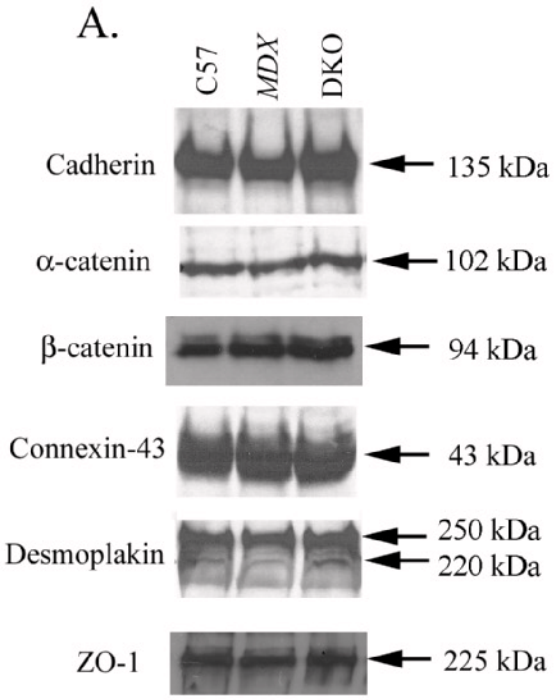

Continued

Figure 4.2 A-B Western and immunohistochemical analysis of adherens junction, gap junction, desmosomal and tight junction proteins

Figure 4.2 continued

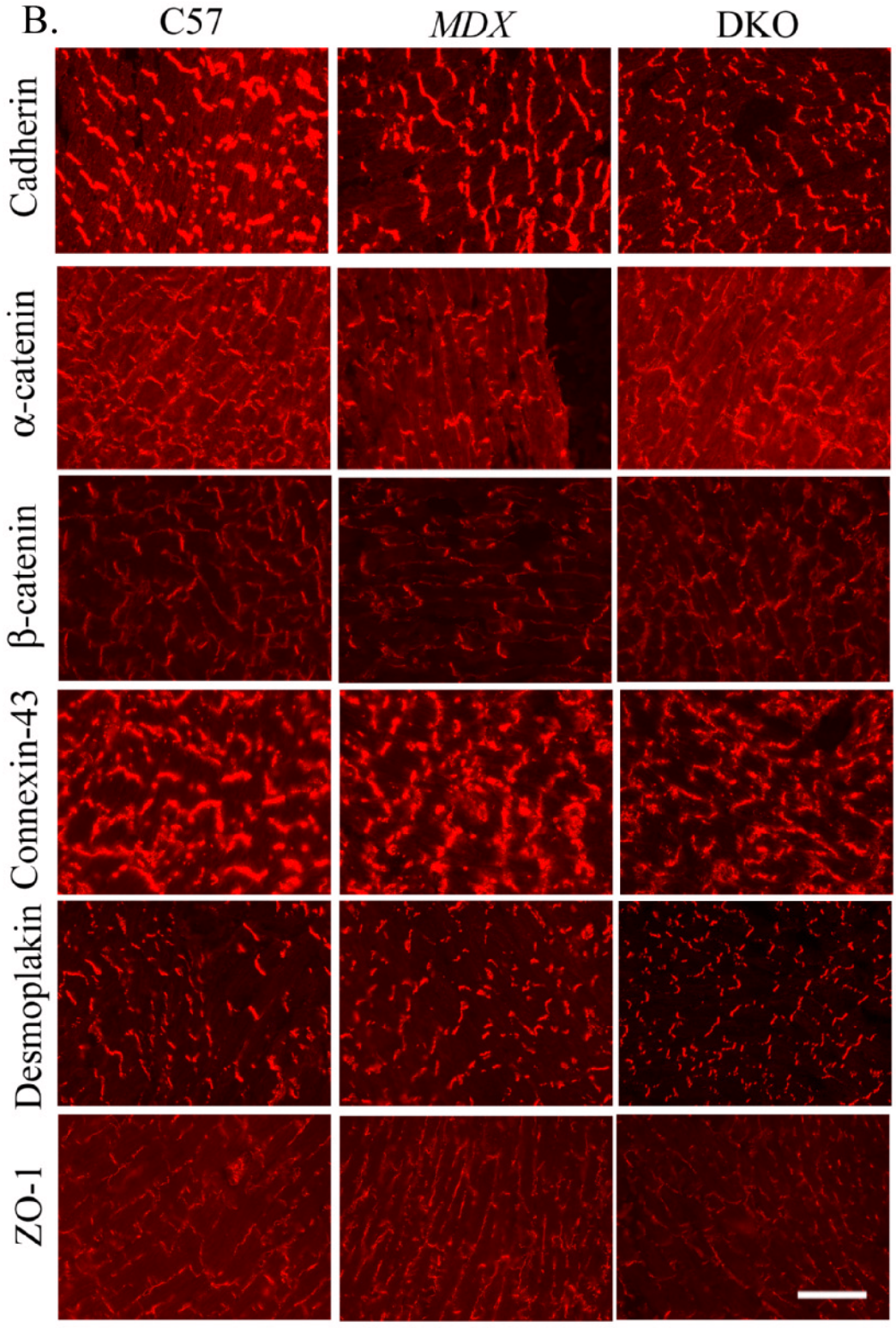

Table 4.1. Microarray analysis of dko vs. *mdx* heart gene expression differences.

Fold differences	Accession number	Gene name (symbol)
4.4	X13986	secreted phosphoprotein 1 (Spp1)
1.9	X16834	lectin, galactose binding, soluble 3 (Lgals3)
1.9	M70642	connective tissue growth factor (Ctgf)
1.7	X58198	H19 fetal liver mRNA (H19)
-2.2	M12347	Actin, alpha 1, skeletal muscle (Acta1)
-2.4	L38444	T-cell specific GTPase (Tgtp)
-2.7	Y12229	utrophin (Utrn)
-3.0	U82758	lung-specific membrane protein; claudin-5 (cldn5)
-3.0	M18237	gene model 460 (similar to immunoglobulin light chain variable region) (Gm460)
-3.1	M80423	IgK chain gene, C-region, 3
-3.2	U48716	Anti HIV-1 reverse transcriptase chain variablefrag mRNA
-3.7	U49915	Adipocyte, c1Q and collagen domain containing (Acdc)
-4.3	X04673	Adipsin (Adn)

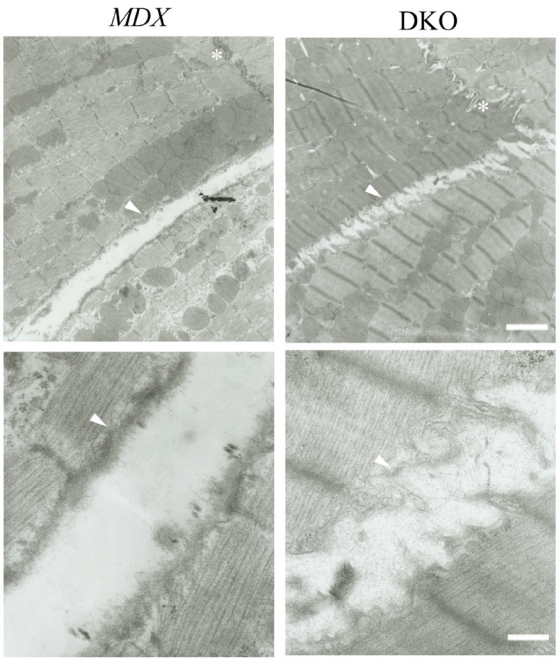

Figure 4.3: Ultrastructure of *mdx* and dko cardiomyocyte lateral membranes

Ultrastructural analysis was conducted on cardiac muscle sections from *mdx* and dko left ventricles. Intercalated discs in both *mdx* and dko hearts appear normal (asterisks). *Mdx* cardiomyocytes showed intact, straight lateral membranes, while dko heart lateral membranes appear to have a lack of density and exhibit an abnormal wavy appearance (arrows).
Bar: 1 cm = 1.6 μm (top panels) and 1 cm = 285 nm (bottom panels)

SUMMARY AND FUTURE PERSPECTIVES

The short-term goals of this dissertation were to gain new insights into the *in vivo* biological functions of the cell junction proteins, CASK and claudin-5, in striated muscle. Chapters 1-3 focused on the initial characterization of the CASK protein in skeletal muscle, including generation of the first transgenic mouse models of CASK in skeletal muscle. Chapter 4 examined the claudin-5 protein in normal cardiac muscle, followed by an assessment of claudin-5's expression and localization in two mouse models of cardiomyopathy.

Summary - Characterization of CASK in skeletal muscle

Overall, investigations into MAGUK proteins at the mammalian NMJ of skeletal muscle have been very limited. There has been some information gleaned from studies of Dlg at the *Drosophila* larval NMJ and our lab has shown that Dlg is present in skeletal muscle at the mammalian NMJ (Rafael et al., 1998a; Tejedor et al., 1997). However, to our knowledge, the only inquisition into MAGUK proteins at the mammalian NMJ, besides Dlg, were confined to studies of the Dlg homologue, PSD-95, and MAGI-1. Examination of the PSD-95 protein in skeletal muscle has been limited to *in vitro* experimentation in the C2C12 mouse myogenic cell line; examination of PSD-95 protein

in vivo at the NMJ has not been carried out. In contrast to PSD-95, MAGI-1 has been characterized *in vivo* in skeletal muscle, where it has been shown to interact with the MuSK receptor at the NMJ (Strochlic et al., 2001). Given the general lack of information regarding MAGUK proteins at the neuromuscular synaptic junction, we set about examining the CASK protein in skeletal muscle. Prior to the start of the work presented in this dissertation, the function of the CASK protein had been most extensively characterized in epithelial cell types and chemical synaptic junctions of the CNS. The only examination into the CASK protein in skeletal muscle consisted of northern analysis confirming the presence of CASK mRNA in skeletal muscle (Cohen et al., 1998). Our aim was to begin to delineate the *in vivo* functions of this MAGUK protein in skeletal muscle at the neuromuscular junction.

We show for the first time that the CASK protein is present in skeletal muscle and is specifically localized to the NMJ. Subcellularly at the NMJ, the CASK protein is localized to both postsynaptic and presynaptic locations. This localization is consistent with data from CNS synapses, where CASK expression has been also been demonstrated both pre- and postsynaptically (Hsueh et al., 1998; Kim and Sheng, 2004). We also identified hDlg/SAP97 as an *in vivo* binding partner for the CASK protein in skeletal muscle, providing evidence of a MAGUK scaffold at the NMJ, similar to what has been shown at synapses in the CNS. In the CNS, members of the MAGUK superfamily of proteins can form large macromolecular complexes, typically at sites of cell-cell contact, such as synapses. These complexes serve a multitude of functions, maintaining cell polarity, through the binding of the cell adhesion molecules, receptors and the cytoskeleton. Our data suggests that a similar scaffold is present at the NMJ. This work

has therefore contributed new knowledge regarding the molecular architecture of the NMJ, which is essential for a complete understanding of muscle physiology and synaptic transmission.

The work presented in Chapter 2 demonstrates that both CASK and Dlg are present in the mouse myogenic C2C12 cell line. Furthermore, the CASK-Dlg MAGUK scaffold is recruited to AChR complexes by a novel mechanism which is independent of the signaling pathways that cluster the AChR and utrophin-associated complexes. Neither CASK, nor Dlg, are recruited to AChR complexes in response to agrin or laminin treatment. We also demonstrate that both CASK and Dlg are capable of localizing to the nucleus. CASK localizes to the nucleus *in vivo* in skeletal muscle, as well as in C2C12 myoblasts and in MN-1 cells, a motor neuron neuroblastoma cell line. Dlg on the other hand, was only shown to localize to the nucleus of MN-1 cells. Overall, these data suggest that perhaps the CASK and Dlg proteins are not necessary for the initiation of NMJ formation, but rather are involved in maintaining and stabilizing NMJ architecture.

As previously discussed, the short term goal of the work presented in this dissertation is to gain a more advanced understanding of the *in vivo* function of the CASK protein in skeletal muscle at the neuromuscular junction and to that end, Chapter 3 describes the generation of two lines of CASK transgenic mice. The CASK F.L. and CASKΔ mice overexpress a full-length and truncated version of the CASK protein, respectively. Both the full-length CASK and the truncated CASK proteins are overexpressed at high levels in skeletal muscle and are localized to both the cytoplasm and the membrane. A series of histological and physiological tests suggest that overexpression of CASK F.L. or CASKΔ protein does not result in any morphologic or functional abnormalities of the skeletal

muscle or the NMJ. We also conducted immunohistochemical analysis to determine if the localization of the CASK interactor, Dlg, or any candidate interactors, were altered in response to CASK F.L. or CASKΔ overexpression. Interestingly, we found that the localization of the Dlg protein, a known *in vivo* interactor of CASK in skeletal muscle, is not affected in either line of CASK transgenic mice. Furthermore, the potassium channels Kir 2.2 and Kir 2.3, which exhibit localization changes *in vitro* in response to dominant negative CASK proteins, are also unaltered in CASK F.L. and CASKΔ mice. There were two candidate interactors, NR2B and Girk2, that appear to exhibit slight changes in localization in response to CASK protein overexpression, but further analysis is needed to confirm these results. Finally, 2-D gel analysis was conducted to compare the protein expression profiles between transgenic negative mice and CASK F.L. and CASKΔ mice. There were multiple protein differences observed between the genotypes, but only one protein spot was identified by mass spectrometry. This spot was identified at Troponin T, but the protein difference has not been confirmed by 1-D gel analysis.

Future Perspectives – Further defining the in vivo role of the CASK protein in skeletal muscle

The data presented in this thesis is the first investigation of CASK protein in skeletal muscle and represents only a small portion of the information necessary to realize the short and long-term goals discussed previously. Therefore, there are still some key questions regarding CASK protein function at the NMJ that remain unanswered. For example, what chemical or trophic signaling factors are responsible for recruiting CASK to the primary gutter of the NMJ? What is CASK's function in the skeletal muscle

nuclei? What other proteins are part of the CASK-Dlg scaffold at the NMJ? What would be the effect of CASK protein loss in skeletal muscle? These are all questions future work in our lab will attempt to answer.

One large focus of future work regarding CASK protein function in skeletal muscle, will involve identifying further *in vivo* binding partners of the protein. As demonstrated in Chapter 1, the CASK protein does interact with Dlg *in vivo* in skeletal muscle, but given CASK's multidomain structure and dynamic nature, there are likely binding partners yet to be identified. For example, we have not yet fully examined the possibility of a tripartite complex in skeletal muscle, similar to what is observed in epithelial cells and synapses of the CNS. Unpublished data produced from our laboratory has established via RT-PCR and western analysis that the Veli protein is present in skeletal muscle. Conversely, we have been unable to establish that the Mint protein is present in skeletal muscle. Since Mint may not be present in skeletal muscle, it is possible that the tripartite complex of skeletal muscle consists of Dlg-CASK-Veli; this would be analogous to the Dlg-CASK-Veli alternative tripartite complex that has been observed in brain (Borg et al., 1998; Butz et al., 1998). Further analysis of the Veli protein in skeletal muscle, including localization studies and immunoprecipitations, will be utilized to investigate the potential existence of a tripartite-like complex in skeletal muscle at the NMJ.

In epithelial cells and CNS synapses, CASK has also been shown to interact with a variety of adhesion molecules, such as syndecans and neurexins. The interactions of CASK with adhesion molecules present at the NMJ are potential binding partners that remain to be investigated. One candidate adhesion molecule interactor is perlecan, a

heparan sulfate proteoglycan, present in the extrasynaptic and in the postsynaptic membrane of the NMJ that has been shown to be involved in interactions with the extracellular matrix, as well as cell-cell interactions (Patton, 2003). Additionally, there are a variety of other adhesion molecules present in the postsynaptic membrane of the neuromuscular junction, including agrin and various isoforms of laminins and collagens. The results presented in Chapter 3 demonstrate that overexpression of CASK protein in skeletal muscle results in loss of presynaptic staining at the NMJ. This data seems to suggest that a feedback mechanism exists between the post- and presynaptic components of the NMJ, which involves CASK and/or its binding partners. Transmembrane adhesion molecules, such as perlecan, represent a class of proteins that could potentially be involved in such a feedback mechanism, given their association with intra- and extracellular molecules.

Finally, as a more global method for finding potential CASK binding partners, we will continue conducting proteomic analysis using 2-D gel analysis followed by silver staining and mass spectrometry analysis. As mentioned in Chapter 3, there were several spot differences that were unable to be identified by mass spectrometry analysis. Therefore, we plan to repeat the 2-D gel analysis and subject the spot differences to further mass spectrometry investigation. Furthermore, large-scale immunoprecipitations followed by proteomic analysis will also be used in the effort to identify direct and indirect CASK binding partners. Overall, the identification of CASK binding partners is indispensable for further exploring CASK protein function at the NMJ and for expanding our knowledge of NMJ architecture.

The CASK protein is localized both pre- and post-synaptically to the NMJ of skeletal muscle. Of course, there are some basic questions that still need to be addressed regarding the CASK protein on both sides of the motor unit. In terms of the post-synaptic localization, two of the questions we want to address are the *in vivo* developmental time course of CASK protein localization to the NMJ and the trophic/chemical/synaptic factors that recruit CASK to the NMJ. Understanding when CASK is recruited during the formation of the NMJ ultrastructure will also help aid in the delineation of CASK's function. In order to determine when CASK is recruited to the NMJ we will need to conduct immunohistochemical experiments, co-staining with both CASK and α-bungarotoxin, beginning at day E. 12-13; aneural clustering of AChRs begins at day E. 14.5 and nerve-induced clusters form around day E.16.5-18.5 (Luo et al., 2003). Co-staining with a fluorescently-conjugated α-bungarotoxin, which binds to AChRs, will help to answer when the CASK protein is recruited to the postsynaptic apparatus, in relation to when AChR are recruited to the postsynaptic apparatus. If CASK is recruited to the NMJ after the clustering of AChR and formation of the postsynaptic apparatus, this would lend further support to the suggestion that the CASK protein is involved in maintaining and stabilizing the NMJ after postsynaptic formation. This observation would also suggest that CASK is recruited by a secondary signal that is activated and/or produced in response to synaptic transmission, which is only possible after clustering of the AChRs. A second possibility is that CASK is recruited to the NMJ concurrently with AChR, which would suggest that CASK is in some respect involved in the initiation/establishment of NMJ postsynaptic architecture. This result would be in conflict with the results obtained in C2C12 cells, which are able to form an aneural

pseudo-neuromuscular junction without recruitment of the CASK protein. However, these results were obtained *in vitro*, which may not recapitulate the *in vivo* situation. We would also need to conduct these same experiments for the Dlg protein, for the same reasons discussed in regards to the CASK protein. Additionally, determining when Dlg is recruited to the NMJ will aid in understanding when CASK and Dlg are recruited in relation to each other. Finally, as a compliment to these protein localization experiments, we may also want to conduct *in situ* hybridization experiments on embryos to determine when and where CASK mRNA is being produced in skeletal muscle.

In order to further enhance our understanding of CASK protein localization at the postsynaptic membrane of the NMJ, we will also attempt to determine the signaling or trophic factors responsible for recruiting CASK to the postsynaptic apparatus. As discussed in Chapter 2, experiments conducted in C2C12 cells suggest that CASK, as well as Dlg, are recruited to the postsynaptic apparatus by a mechanism that is independent of that which recruits and clusters AChR and members of the utrophin-associated complex. There are two possible mechanisms by which CASK may be recruited to the NMJ. As discussed earlier, it is feasible that formation of the postsynaptic apparatus (which occurs after agrin-induced clustering of AChR) and subsequent synaptic transmission initiates a signaling cascade that results in recruitment and clustering of the CASK protein. These signaling factors would be missing in our agrin clustering experiments, which were conducted in the absence of neural input. For example, one well characterized signaling pathway that is initiated after formation of the postsynaptic apparatus is the MuSK signaling pathway. One way to determine if CASK is recruited in response to this signaling cascade is to examine CASK protein localization

in mouse models that are knocked-out for various components of the signaling pathways. For instance, the Src kinases, Src, Fyn and YES, are initiated via the MuSK signaling cascade and there are knockout mouse models of each of these kinases (Smith et al., 2001). Each of the knockout mouse models still form intact NMJs, but exhibit AChR clusters that are less stable than those of wild-type mice.

Another mechanism that would result in clustering of CASK at the postsynaptic membrane is the possibility that a trophic factor, other than agrin or laminin, is released from the nerve and is responsible for CASK clustering. Besides agrin and laminin, there are other factors such as heparin-binding growth associated molecule, fibroblast growth factor, and midkine, which have been shown to induce AChR clustering *in vitro* (Luo et al., 2003). In order to determine whether one of these trophic factors results in co-clustering of CASK with AChR we would simply need to conduct experiments very similar to the agrin and laminin clustering experiments presented in Chapter 2. Finally, if none of the experiments presented above produce a mechanism for CASK clustering, it would be necessary to conduct experiments that would identify novel trophic factors. One possible way in which we might be able to answer this question is to conduct co-culture experiments with C2C12 cells and a motor neuron cell line, such as MN-1 cell line, which we have been successful in growing in culture. If co-clustering of MN-1 cells with C2C12 myotubes resulted in clustering of CASK with AChR, this would suggest that there is some trophic factor released from the MN-1 cell that produces this result. In order to isolate the trophic factor necessary for CASK clustering, the media would be collected and subjected to various biochemical fractionation and purification studies.

Another aspect of the CASK protein at the NMJ which needs to be addressed is its presynaptic localization. The work of this thesis demonstrates via confocal micrsocopy and transgenic mouse models that CASK is localized to the presynaptic side of the NMJ and that overexpression of the CASK protein on the skeletal muscle side of the NMJ causes a loss of CASK from presynaptic locales (Chapters 1 and 3). Although our laboratory does not plan to focus on the presynaptic functions of the CASK protein, the results obtained from our transgenic mouse models dictate that we gain some basic information on CASK's localization and expression on the presynaptic side of the motor unit. We have not yet demonstrated whether the presynaptic staining observed *in vivo* is due to expression of CASK protein in the motor neuron or the Schwann cell. Our laboratory has demonstrated that CASK is expressed in the MN-1 motor neuron cell line, but this needs to be confirmed *in vivo*. We will be able to answer this question by performing immunohistochemical analysis followed by confocal microscopy on mouse quadriceps muscle co-stained with a CASK and antibodies specific to the motor neuron, such as synaptophysin, or an antibody specific to Schwann cells such as S-100 (Trinidad et al., 2000). Furthermore, once we determine the precise presynaptic location of CASK, we will also need to conduct western analysis of isolated motor neurons or Schwann cells to corroborate the immunohistochemical data in wild-type mice and to confirm the loss of CASK protein expression in motor neurons or Schwann cells of CASK F.L. and CASKΔ mice.

In Chapters 1 and 2, we demonstrate that CASK is localized to a subset of nuclei *in vivo* in adult skeletal muscle and is localized almost exclusively to the nucleus of C2C12 cell myoblasts. Further work in our laboratory will attempt to dissect the possible

functions of CASK in skeletal muscle nuclei. There are two possible explanations that may account for the observed nuclear localization of the CASK protein. First, as discussed earlier, CASK has been shown to act as a co-activator of transcription in synapses of the CNS. If the CASK protein is performing this same function in skeletal muscle, this may account for its nuclear localization. Secondly, it is possible that the nuclear staining we observe *in vivo* in adult skeletal muscle is nuclei of satellite cells. It is difficult to discern the nuclei of muscle fibers from the nuclei of satellite cells, as both are located on the periphery of the muscle fiber. Therefore, the first task would be to discern which subset of nuclei exhibits CASK protein expression. The most direct way to accomplish this is to conduct double immunohistochemical analysis with a CASK antibody and an antibody to a marker for satellite cells, such as syndecan-3, which we have used successfully in our laboratory (See Chapter 3). If the CASK nuclear staining is concomitant with satellite cell nuclei, this would suggest that perhaps CASK is involved in the development and regeneration of muscle fibers. This hypothesis is supported by the fact that CASK staining is seen in the centrally located nuclei of regenerating fibers in *mdx* mice; regenerating fibers arise from the differentiation of satellite cells. This is also an attractive model given the interaction of CASK with various syndecan proteins in other cell types (Cohen et al., 1998; Cornelison et al., 2001; Hsueh et al., 1998). If CASK staining is not co-localized with satellite cell markers, this would suggest that CASK is present in the nuclei of adult muscle fibers, where it could potentially act as a transcription factor (transcriptional activity would also be possible in satellite cell nuclei). In order to pursue CASK's possible involvement in transcription, we would first attempt to find the *in vivo* binding partners of CASK in the nucleus. Immunoprecipitations from

nuclear preparations of adult skeletal muscle, followed by SDS-PAGE, silver staining and mass spectrometry, would be one way to achieve this goal. Furthermore, one possible candidate interactor of CASK in the nucleus that we could test directly via immunoprecipitations is CINAP, a putative nucleosome assembly protein; CINAP interacts with CASK in the CNS and is present in skeletal muscle (Hsueh et al., 2000; Wang et al., 2004a; Wang et al., 2004b). CASK and any identified nuclear binding partners could then be examined for transcriptional activities using gel shift assays and/or reporter construct assays *in vitro* in C2C12 cells. Another avenue that may be pursued is to perform microarray analysis comparing mRNA profiles between transgenic negative mice and CASK F.L. and CASKΔ mice. This could potentially identify transcriptional targets of the CASK protein and any other RNA expression changes that might occur in response to CASK protein overexpression in skeletal muscle.

Chapter 3 of this thesis discusses the generation of the first transgenic mouse models of CASK protein function in skeletal muscle. We plan to further expand on these initial mouse studies by generating conditional knock-outs of the CASK protein in skeletal muscle. Briefly, we will generate a CASK construct containing a Neo cassette flanked by exonic and intronic genomic CASK DNA sequence, which will be cloned into a ploxPFlpneo vector. The ploxPFFlpneo vector contains Lox P sites necessary for the generation of conditional knock-outs. The CASK-Neo construct flanked by the Lox P sites (CASK-Neo-LoxP) will then be excised from the vector and used for the electroporation of ES cells. ES cells in which the inserted CASK-Neo-LoxP DNA has undergone homologous recombination with the endogenous genomic CASK sequence will be selected for with G418. These ES cells will then be used to generate chimeric

mice, which will in turn be used to generate mice that are homozygous for the CASK-Neo-LoxP insertion. Next, we will generate conditional knockouts by mating these mice to Cre transgenic mice in which the Cre recombinase gene is under the control of the MCK muscle specific promoter. The Cre recombinase will cause the CASK sequence contained within the Lox P sites to be excised, generating mice that are null for CASK protein function in skeletal muscle. These mice will be useful in the further characterization of the function of the CASK protein in skeletal muscle. Also, we currently have obtained an ES cell line that is knocked-out for the CASK gene via a gene trap Lac-Z locus. We have confirmed the absence of any CASK protein in these cells by western analysis (JLS and JRF, unpublished data). These CASK knock-out ES cells will be differentiated to myoblasts and/or myotubes and will be subjected to *in vitro* analyses while we are waiting for the conditional knock-out mice to be generated.

As discussed in Chapter 3, overexpression of the CASKΔ protein did not result in any morphologic or physiological abnormalities. This is most likely due to the presence of endogenous protein and/or compensation of CASK protein function by other MAGUK proteins of the NMJ, such as Dlg. Therefore, the generation of conditional CASK knock-outs will be able to more concisely determine the function of CASK protein in skeletal muscle. These mice will be examined using the same basic methods used to investigate the CASK F.L. and CASKΔ mice. Two important questions that will be addressed using these mice is whether loss of CASK protein affects NMJ architecture or affects the localization of CASK binding partners. Furthermore, we will also be generating conditional Dlg knock-out mice, which will be mated to the CASK conditional knock-outs, in order to address any functional redundancy that may exist between the two

proteins. Any phenotypes observed in the CASK conditional knock-outs will be confirmed through rescue experiments using the CASK F.L. and/or CASKΔ mice. Overall, the generation of conditional knock-outs, in addition to the results of the experiments discussed above, will result in a more concise and thorough knowledge of CASK protein function in skeletal muscle.

Summary - Characterization of claudin-5 in cardiomyocytes of normal heart muscle and two mouse models of cardiomyopathy

In addition to the examination of the cell junction protein CASK, this thesis also investigated the claudin-5 cell junction protein. Prior to the studies presented here, claudin-5 had not been investigated in the heart, despite the fact that mutations in the gene result in cardiomyopathic pathology associated with DiGeorge and velo-cardio-facial syndromes. Remodeling of cell junction proteins of the intercalated disc has recently been associated with DCM (Perriard et al., 2003). As stated previously, many neuromuscular diseases, including muscular dystrophies, include cardiac pathologies that remain to be investigated if a full treatment of these diseases is to be achieved. We therefore investigated claudin-5 in normal heart muscle and in heart muscle of *mdx* and dko mice, two mouse models of Duchenne muscular dystrophy. Immuonfluorescent and western analysis demonstrated that claudin-5 protein is expressed in wild-type cardiac muscle and is specifically localized to the lateral membranes of cardiomyocytes. Interestingly, claudin-5 mRNA and protein levels were decreased in cardiac muscle of dko muscle, but not *mdx* cardiac muscle, as compared to normal cardiac muscle. Furthermore, expression and localization of intercalated disc proteins are not altered in

dko mice. Electron micrograph analysis also reveals that the lateral membranes of dko cardiomyocytes exhibit an abnormal wavy appearance, as compared to lateral membranes of normal and *mdx* cardiomyocytes. Overall, these results suggest that alterations of the lateral membranes are associated with cardiomyopathy in the dko mouse.

Future perspectives – Further assessing claudin-5 protein in dko mice and other mouse models of cardiomyopathy

Our analysis of claudin-5 in *mdx* and dko mice demonstrated that the protein was decreased in cardiac muscle from dko mice. The major question that still needs resolved is whether claudin-5 protein changes are exclusive to dko mice or are a more general side effect associated with other models of cardiomyopathy. Our results in the *mdx* mice suggest that claudin-5 changes are specifically associated with dko mice. However, as discussed in Chapter 4, our experiments were only conducted on mice which were 8-10 weeks of age (as dko mice die by 12 weeks of age). One question that still remains unresolved is whether claudin-5 levels are affected in *mdx* mice at a more advanced age, when cardiomyopathic features are more severe. Therefore, we will analyze claudin-5 expression and localization in *mdx* mice at several different ages, up until 1.5-2 years of age. Another approach that will be used to answer this question is to examine claudin-5 protein expression and localization in human patients with DCM. Our lab, in collaboration with Dr. Phil Binkley, has heart samples from over 50 patients with different forms of DCM which will be ultilized to analyze claudin-5 expression and localization. Furthermore, since the intercalated disc protein remodeling that has been observed in mouse models has not been investigated in human samples, we will also

examine these proteins in the human DCM samples. These experiments will begin to answer more definitively whether claudin-5 protein changes are found specifically in dko mice or are a more general feature of advanced DCM. As a complement to these investigations, we will also examine whether the claudin-5 protein alterations occur prior to or after the onset of cardiomyopathy in the dko mouse. This will be accomplished by conducting western and immunohistochemical analysis of dko hearts at 1 week of age through 12 weeks of age. These experiments will address whether claudin-5 protein may play causative role in the dko cardiomyopathy, or a secondary effect that results from the breakdown of membrane architecture caused from loss of dystrophin and utrophin.

Eventually, we may also want to identify *in vivo* binding partners for the claudin-5 protein in cardiac muscle, to gain insight into the lateral membrane architecture. As claudin-5 is a component of tight junction proteins in endothelial cells, it will be interesting to see if, in cardiomyocytes, claudin-5 is binding other proteins that are typically found at tight junctions, such as the ZO proteins. If this is the case, perhaps this claudin-5 protein complex may perform a function analogous to that of endothelial cell tight junctions, regulating diffusion into cardiomyocytes. In this instance, it is possible that loss of claudin-5 may contribute to cardiomyopathy by affecting cardiomyocyte homeostasis, allowing diffusion of detrimental molecules into the intracellular compartment of cardiomyocytes. If these experiments suggest that loss of claudin-5 results in disease progression in the dko mouse or other cardiomyopathic models, it may eventually lead to our long-term goal of a treatment for cardiomyopathies associated with neuromuscular diseases.

LIST OF REFERENCES

Adams, M. E., Mueller, H. A., and Froehner, S. C. (2001). In vivo requirement of the {alpha}-syntrophin PDZ domain for the sarcolemmal localization of nNOS and aquaporin-4. J Cell Biol *155*, 113-122.

Ahn, A. H., and Kunkel, L. M. (1993). The structural and functional diversity of dystrophin. Nat Genet *3*, 283-291.

Amalfitano, A. A., Rafael, J. A., and Chamberlain, J. S. (1997). Structure and mutation of the dystrophin gene. In Dystrophin: Gene, Protein, and Cell Biology, J. Lucy, and S. C. Brown, eds. (Cambridge University Press).

Anderson, J. M. (1996). Cell signalling: MAGUK magic. Curr Biol *6*, 382-384.

Arber, S., Hunter, J., Ross, J. J., Hongo, M., Sansig, G., Borg, J., Perriard, J., Chien, K., and Caroni, P. (1997). MLP-deficient mice exhibit a disruption of cardiac cytoarchitectural organization, dilated cardiomyopathy, and heart failure. CELL *88*, 393-403.

Balda, M. S., Whitney, J. A., Flores, C., Gonzalez, S., Cereijido, M., and Matter, K. (1996). Functional dissociation of paracellular permeability and transepithelial electrical resistance and disruption of the apical-basolateral intramembrane diffusion barrier by expression of a mutant tight junction membrane protein. J Cell Biol *134*, 1031-1049.

Banks, G. B., Fuhrer, C., Adams, M. E., and Froehner, S. C. (2003). The postsynaptic submembrane machinery at the neuromuscular junction: requirement for rapsyn and the utrophin/dystrophin-associated complex. J Neurocytol *32*, 709-726.

Barker, R. J., Price, R. L., and Gourdie, R. G. (2001). Increased co-localization of connexin43 and ZO-1 in dissociated adult myocytes. Cell Commun Adhes *8*, 205-208.

Barker, R. J., Price, R. L., and Gourdie, R. G. (2002). Increased association of ZO-1 with connexin43 during remodeling of cardiac gap junctions. Circ Res *90*, 317-324.

Bass, M. D., and Humphries, M. J. (2002). Cytoplasmic interactions of syndecan-4 orchestrate adhesion receptor and growth factor receptor signalling. Biochem J *368*, 1-15.

Bassand, P., Bernard, A., Rafiki, A., Gayet, D., and Khrestchatisky, M. (1999). Differential interaction of the tSXV motifs of the NR1 and NR2A NMDA receptor subunits with PSD-95 and SAP97. EUROPEAN JOURNAL OF NEUROSCIENCE *11*, 2031-2043.

Benmerah, A., Scott, M., Poupon, V., and Marullo, S. (2003). Nuclear functions for plasma membrane-associated proteins? Traffic *4*, 503-511.

Bernfield, M., Hinkes, M. T., and Gallo, R. L. (1993). Developmental expression of the syndecans: possible function and regulation. Dev Suppl, 205-212.

Bernfield, M., Kokenyesi, R., Kato, M., Hinkes, M. T., Spring, J., Gallo, R. L., and Lose, E. J. (1992). Biology of the syndecans: a family of transmembrane heparan sulfate proteoglycans. Annu Rev Cell Biol *8*, 365-393.

Bia, B., Cassidy, P., Young, M., Rafael, J., Leighton, B., Davies, K., Radda, G., and Clarke, K. (1999). Decreased myocardial nNOS, increased iNOS and abnormal ECGs in mouse models of Duchenne muscular dystrophy. Journal of Molecular and Cellular Cardiology *31*, 1857-1862.

Biederer, T., and Sudhof, T. C. (2001). CASK and protein 4.1 support F-actin nucleation on neurexins. J Biol Chem *276*, 47869-47876.

Bienengraeber, M., Olson, T. M., Selivanov, V. A., Kathmann, E. C., O'Cochlain, F., Gao, F., Karger, A. B., Ballew, J. D., Hodgson, D. M., Zingman, L. V.*, et al.* (2004). ABCC9 mutations identified in human dilated cardiomyopathy disrupt catalytic KATP channel gating. Nat Genet *36*, 382-387. Epub 2004 Mar 2021.

Boonyapisit, K., Kaminski, H. J., and Ruff, R. L. (1999). Disorders of neuromuscular junction ion channels. Am J Med *106*, 97-113.

Borg, J. P., Straight, S. W., Kaech, S. M., de Taddeo-Borg, M., Kroon, D. E., Karnak, D., Turner, R. S., Kim, S. K., and Margolis, B. (1998). Identification of an evolutionarily conserved heterotrimeric protein complex involved in protein targeting. J Biol Chem *273*, 31633-31636.

Bossinger, O., Klebes, A., Segbert, C., Theres, C., and Knust, E. (2001). Zonula adherens formation in Caenorhabditis elegans requires dlg-1, the homologue of the Drosophila gene discs large. Dev Biol *230*, 29-42.

Bouley, J., Chambon, C., and Picard, B. (2004). Mapping of bovine skeletal muscle proteins using two-dimensional gel electrophoresis and mass spectrometry. Proteomics *4*, 1811-1824.

Braun, A. P., and Schulman, H. (1995). The multifunctional calcium/calmodulin-dependent protein kinase: from form to function. Annu Rev Physiol *57*, 417-445.

Brenman, J. E., Chao, D. S., Gee, S. H., McGee, A. W., Craven, S. E., Santillano, D. R., Wu, Z., Huang, F., Xia, H., Peters, M. F.*, et al.* (1996). Interaction of nitric oxide synthase with the postsynaptic density protein PSD-95 and alpha1-syntrophin mediated by PDZ domains. Cell *84*, 757-767.

Brenman, J. E., Topinka, J. R., Cooper, E. C., McGee, A. W., Rosen, J., Milroy, T., Ralston, H. J., and Bredt, D. S. (1998). Localization of postsynaptic density-93 to dendritic microtubules and interaction with microtubule-associated protein 1A. J Neurosci *18*, 8805-8813.

Buckley, K., and Kelly, R. B. (1985). Identification of a transmembrane glycoprotein specific for secretory vesicles of neural and endocrine cells. J Cell Biol *100*, 1284-1294.

Buday, L. (1999). Membrane-targeting of signalling molecules by SH2/SH3 domain-containing adaptor proteins. Biochim Biophys Acta *1422*, 187-204.

Bulfield, G., Siller, W. G., Wight, P. A., and Moore, K. J. (1984). X chromosome-linked muscular dystrophy (mdx) in the mouse. Proc Natl Acad Sci U S A *81*, 1189-1192.

Bulfone, A., Smiga, S. M., Shimamura, K., Peterson, A., Puelles, L., and Rubenstein, J. L. (1995). T-brain-1: a homolog of Brachyury whose expression defines molecularly distinct domains within the cerebral cortex. Neuron *15*, 63-78.

Bulfone, A., Wang, F., Hevner, R., Anderson, S., Cutforth, T., Chen, S., Meneses, J., Pedersen, R., Axel, R., and Rubenstein, J. L. (1998). An olfactory sensory map develops in the absence of normal projection neurons or GABAergic interneurons. Neuron *21*, 1273-1282.

Buonanno, A., and Fischbach, G. D. (2001). Neuregulin and ErbB receptor signaling pathways in the nervous system. Curr Opin Neurobiol *11*, 287-296.

Burden, S. J. (1998). The formation of neuromuscular synapses. Genes Dev *12*, 133-148.

Burgoyne, R. D., and Clague, M. J. (2003). Calcium and calmodulin in membrane fusion. Biochim Biophys Acta *1641*, 137-143.

Bushby, K. M., Cleghorn, N. J., Curtis, A., Haggerty, I. D., Nicholson, L. V., Johnson, M. A., Harris, J. B., and Bhattacharya, S. S. (1991). Identification of a mutation in the promoter region of the dystrophin gene in a patient with atypical Becker muscular dystrophy. Hum Genet *88*, 195-199.

Butz, S., Okamoto, M., and Sudhof, T. C. (1998). A tripartite protein complex with the potential to couple synaptic vesicle exocytosis to cell adhesion in brain. Cell *94*, 773-782.

Cai, C., Coleman, S. K., Niemi, K., and Keinanen, K. (2002). Selective binding of synapse-associated protein 97 to GluR-A alpha-amino-5-hydroxy-3-methyl-4-isoxazole propionate receptor subunit is determined by a novel sequence motif. J Biol Chem *277*, 31484-31490.

Carey, D. J. (1997). Syndecans: multifunctional cell-surface co-receptors. Biochem J *327 (Pt 1)*, 1-16.

Caruana, G. (2002). Genetic studies define MAGUK proteins as regulators of epithelial cell polarity. Int J Dev Biol *46*, 511-518.

Caruana, G., and Bernstein, A. (2001). Craniofacial dysmorphogenesis including cleft palate in mice with an insertional mutation in the discs large gene. Mol Cell Biol *21*, 1475-1483.

Chetkovich, D. M., Bunn, R. C., Kuo, S. H., Kawasaki, Y., Kohwi, M., and Bredt, D. S. (2002). Postsynaptic targeting of alternative postsynaptic density-95 isoforms by distinct mechanisms. J Neurosci *22*, 6415-6425.

Cho, K., Hunt, C., and Kennedy, M. (1992). The rat brain postsynaptic density fraction contains a homolog of the Drosophila discs-large tumor suppressor protein. NEURON *9*, 929-942.

Cohen, A. R., Woods, D. F., Marfatia, S. M., Walther, Z., Chishti, A. H., Anderson, J. M., and Wood, D. F. (1998). Human CASK/LIN-2 binds syndecan-2 and protein 4.1 and localizes to the basolateral membrane of epithelial cells. J Cell Biol *142*, 129-138.

Colledge, M., Dean, R. A., Scott, G. K., Langeberg, L. K., Huganir, R. L., and Scott, J. D. (2000). Targeting of PKA to glutamate receptors through a MAGUK-AKAP complex. Neuron *27*, 107-119.

Cornelison, D. D., Filla, M. S., Stanley, H. M., Rapraeger, A. C., and Olwin, B. B. (2001). Syndecan-3 and syndecan-4 specifically mark skeletal muscle satellite cells and are implicated in satellite cell maintenance and muscle regeneration. Dev Biol *239*, 79-94.

Craven, S., and Bredt, D. (1998). PDZ proteins organize synaptic signaling pathways. CELL *93*, 495-498.

Daniels, D. L., Cohen, A. R., Anderson, J. M., and Brunger, A. T. (1998). Crystal structure of the hCASK PDZ domain reveals the structural basis of class II PDZ domain target recognition. Nat Struct Biol *5*, 317-325.

DeChiara, T. M., Bowen, D. C., Valenzuela, D. M., Simmons, M. V., Poueymirou, W. T., Thomas, S., Kinetz, E., Compton, D. L., Rojas, E., Park, J. S*., et al.* (1996). The receptor tyrosine kinase MuSK is required for neuromuscular junction formation in vivo. Cell *85*, 501-512.

Deconinck, A. E., Potter, A. C., Tinsley, J. M., Wood, S. J., Vater, R., Young, C., Metzinger, L., Vincent, A., Slater, C. R., and Davies, K. E. (1997a). Postsynaptic abnormalities at the neuromuscular junctions of utrophin- deficient mice. J Cell Biol *136*, 883-894.

Deconinck, A. E., Rafael, J. A., Skinner, J. A., Brown, S. C., Potter, A. C., Metzinger, L., Watt, D. J., Dickson, J. G., Tinsley, J. M., and Davies, K. E. (1997b). Utrophin-dystrophin-deficient mice as a model for Duchenne muscular dystrophy. Cell *90*, 717-727.

Deconinck, N., Rafael, J. A., Beckers-Bleukx, G., Kahn, D., Deconinck, A. E., Davies, K. E., and Gillis, J. M. (1998). Consequences of the combined deficiency in dystrophin and utrophin on the mechanical properties and myosin composition of some limb and respiratory muscles of the mouse. Neuromuscul Disord *8*, 362-370.

Dimitratos, S., Woods, D., and Bryant, P. (1997). Camguk, Lin-2, and CASK: novel membrane-associated guanylate kinase homologs that also contain CaM kinase domains. MECHANISMS OF DEVELOPMENT *63*, 127-130.

Dobrosotskaya, I., Guy, R., and James, G. (1997a). MAGI-1, a membrane-associated guanylate kinase with a unique arrangement of protein-protein interaction domains. JOURNAL OF BIOLOGICAL CHEMISTRY *272*, 31589-31597.

Dobrosotskaya, I., Guy, R. K., and James, G. L. (1997b). MAGI-1, a membrane-associated guanylate kinase with a unique arrangement of protein-protein interaction domains. J Biol Chem *272*, 31589-31597.

Doerks, T., Bork, P., Kamberov, E., Makarova, O., Muecke, S., and Margolis, B. (2000). L27, a novel heterodimerization domain in receptor targeting proteins Lin-2 and Lin-7. Trends Biochem Sci *25*, 317-318.

Dong, H., RJ., O. B., Fung, E., Lanahan, A., Worley, P., and Huganir, R. (1997). GRIP: a synaptic PDZ domain-containing protein that interacts with AMPA receptors. NATURE *386*, 279-284.

Doyle, D. A., Lee, A., Lewis, J., Kim, E., Sheng, M., and MacKinnon, R. (1996). Crystal structures of a complexed and peptide-free membrane protein-binding domain: molecular basis of peptide recognition by PDZ. Cell *85*, 1067-1076.

Dupont, E., Matsushita, T., Kaba, R. A., Vozzi, C., Coppen, S. R., Khan, N., Kaprielian, R., Yacoub, M. H., and Severs, N. J. (2001). Altered connexin expression in human congestive heart failure. J Mol Cell Cardiol *33*, 359-371.

Ehler, E., Horowits, R., Zuppinger, C., Price, R. L., Perriard, E., Leu, M., Caroni, P., Sussman, M., Eppenberger, H. M., and Perriard, J. C. (2001). Alterations at the intercalated disk associated with the absence of muscle LIM protein. J Cell Biol *153*, 763-772.

Emery, A. E. H. (1993). Duchenne Muscular Dystrophy, Second Edition edn (Oxford, Oxford University Press).

Epstein, J. A., and Buck, C. A. (2000). Transcriptional regulation of cardiac development: implications for congenital heart disease and DiGeorge syndrome. Pediatr Res *48*, 717-724.

Falls, D. L. (2003a). Neuregulins and the neuromuscular system: 10 years of answers and questions. J Neurocytol *32*, 619-647.

Falls, D. L. (2003b). Neuregulins: functions, forms, and signaling strategies. Exp Cell Res *284*, 14-30.

Fanning, A., and Anderson, J. (1999). PDZ domains: fundamental building blocks in the organization of protein complexes at the plasma membrane. JOURNAL OF CLINICAL INVESTIGATION *103*, 767-772.

Farquhar, M. G., and Palade, G. E. (1963). Junctional complexes in various epithelia. J Cell Biol *17*, 375-412.

Feng, W., Long, J. F., Fan, J. S., Suetake, T., and Zhang, M. (2004). The tetrameric L27 domain complex as an organization platform for supramolecular assemblies. Nat Struct Mol Biol *11*, 475-480.

Ferguson, E. L., and Horvitz, H. R. (1985). Identification and characterization of 22 genes that affect the vulval cell lineages of the nematode Caenorhabditis elegans. Genetics *110*, 17-72.

Ferreira-Cornwell, M. C., Luo, Y., Narula, N., Lenox, J. M., Lieberman, M., and Radice, G. L. (2002). Remodeling the intercalated disc leads to cardiomyopathy in mice misexpressing cadherins in the heart. J Cell Sci *115*, 1623-1634.

Fertuck, H. C., and Salpeter, M. M. (1976). Quantitation of junctional and extrajunctional acetylcholine receptors by electron microscope autoradiography after 125I-alpha-bungarotoxin binding at mouse neuromuscular junctions. J Cell Biol *69*, 144-158.

Filatov, V. L., Katrukha, A. G., Bulargina, T. V., and Gusev, N. B. (1999). Troponin: structure, properties, and mechanism of functioning. Biochemistry (Mosc) *64*, 969-985.

Firestein, B. L., and Rongo, C. (2001). DLG-1 is a MAGUK similar to SAP97 and is required for adherens junction formation. Mol Biol Cell *12*, 3465-3475.

Fuh, G., Pisabarro, M. T., Li, Y., Quan, C., Lasky, L. A., and Sidhu, S. S. (2000). Analysis of PDZ domain-ligand interactions using carboxyl-terminal phage display. J Biol Chem *275*, 21486-21491.

Furuse, M., Fujimoto, K., Sato, N., Hirase, T., and Tsukita, S. (1996). Overexpression of occludin, a tight junction-associated integral membrane protein, induces the formation of intracellular multilamellar bodies bearing tight junction-like structures. J Cell Sci *109 (Pt 2)*, 429-435.

Furuse, M., Fujita, K., Hiiragi, T., Fujimoto, K., and Tsukita, S. (1998a). Claudin-1 and -2: novel integral membrane proteins localizing at tight junctions with no sequence similarity to occludin. J Cell Biol *141*, 1539-1550.

Furuse, M., Hirase, T., Itoh, M., Nagafuchi, A., Yonemura, S., and Tsukita, S. (1993). Occludin: a novel integral membrane protein localizing at tight junctions. J Cell Biol *123*, 1777-1788.

Furuse, M., Sasaki, H., Fujimoto, K., and Tsukita, S. (1998b). A single gene product, claudin-1 or -2, reconstitutes tight junction strands and recruits occludin in fibroblasts. J Cell Biol *143*, 391-401.

Garcia, R. A., Vasudevan, K., and Buonanno, A. (2000). The neuregulin receptor ErbB-4 interacts with PDZ-containing proteins at neuronal synapses. Proc Natl Acad Sci U S A *97*, 3596-3601.

Gardoni, F., Mauceri, D., Fiorentini, C., Bellone, C., Missale, C., Cattabeni, F., and Di Luca, M. (2003). CaMKII-dependent phosphorylation regulates SAP97/NR2A interaction. J Biol Chem *278*, 44745-44752.

Garner, C. C., Nash, J., and Huganir, R. L. (2000). PDZ domains in synapse assembly and signalling. Trends Cell Biol *10*, 274-280.

Gerber, S. H., and Sudhof, T. C. (2002). Molecular determinants of regulated exocytosis. Diabetes *51 Suppl 1*, S3-11.

Getsios, S., Huen, A. C., and Green, K. J. (2004). Working out the strength and flexibility of desmosomes. Nat Rev Mol Cell Biol *5*, 271-281.

Glass, D. J., Bowen, D. C., Stitt, T. N., Radziejewski, C., Bruno, J., Ryan, T. E., Gies, D. R., Shah, S., Mattsson, K., Burden, S. J.*, et al.* (1996). Agrin acts via a MuSK receptor complex. Cell *85*, 513-523.

Glass, D. J., and Yancopoulos, G. D. (1997). Sequential roles of agrin, MuSK and rapsyn during neuromuscular junction formation. Curr Opin Neurobiol *7*, 379-384.

Godfrey, E. W., Nitkin, R. M., Wallace, B. G., Rubin, L. L., and McMahan, U. J. (1984). Components of Torpedo electric organ and muscle that cause aggregation of acetylcholine receptors on cultured muscle cells. J Cell Biol *99*, 615-627.

Goldmuntz, E., and Emanuel, B. S. (1997). Genetic disorders of cardiac morphogenesis. The DiGeorge and velocardiofacial syndromes. Circ Res *80*, 437-443.

Gonzalez-Mariscal, L., Islas, S., Contreras, R. G., Garcia-Villegas, M. R., Betanzos, A., Vega, J., Diaz-Quinonez, A., Martin-Orozco, N., Ortiz-Navarrete, V., Cereijido, M., and Valdes, J. (1999). Molecular characterization of the tight junction protein ZO-1 in MDCK cells. Exp Cell Res *248*, 97-109.

Grady, R. M., Teng, H., Nichol, M. C., Cunningham, J. C., Wilkinson, R. S., and Sanes, J. R. (1997). Skeletal and cardiac myopathies in mice lacking utrophin and dystrophin: a model for Duchenne muscular dystrophy. Cell *90*, 729-738.

Grozdanovic, Z., and Gossrau, R. (1998). Co-localization of nitric oxide synthase I (NOS I) and NMDA receptor subunit 1 (NMDAR-1) at the neuromuscular junction in rat and mouse skeletal muscle. Cell Tissue Res *291*, 57-63.

Gutstein, D. E., Liu, F. Y., Meyers, M. B., Choo, A., and Fishman, G. I. (2003). The organization of adherens junctions and desmosomes at the cardiac intercalated disc is independent of gap junctions. J Cell Sci *116*, 875-885.

Hack, A. A., Ly, C. T., Jiang, F., Clendenin, C. J., Sigrist, K. S., Wollmann, R. L., and McNally, E. M. (1998). Gamma-sarcoglycan deficiency leads to muscle membrane defects and apoptosis independent of dystrophin. J Cell Biol *142*, 1279-1287.

Hainsey, T. A., Senapati, S., Kuhn, D. E., and Rafael, J. A. (2003). Cardiomyopathic features associated with muscular dystrophy are independent of dystrophin absence in cardiovasculature. Neuromuscul Disord *13*, 294-302.

Hanada, T., Lin, L., Tibaldi, E. V., Reinherz, E. L., and Chishti, A. H. (2000). GAKIN, a novel kinesin-like protein associates with the human homologue of the Drosophila discs large tumor suppressor in T lymphocytes. J Biol Chem *275*, 28774-28784.

Harris, B. Z., Venkatasubrahmanyam, S., and Lim, W. A. (2002). Coordinated folding and association of the LIN-2, -7 (L27) domain. An obligate heterodimerization involved in assembly of signaling and cell polarity complexes. J Biol Chem *277*, 34902-34908.

Hata, Y., Butz, S., and Sudhof, T. (1996a). CASK: a novel dlg/PSD95 homolog with an N-terminal calmodulin-dependent protein kinase domain identified by interaction with neurexins. JOURNAL OF NEUROSCIENCE *16*, 2488-2494.

Hata, Y., Butz, S., and Sudhof, T. (1996b). CASK: a novel dlg/PSD95 homolog with an N-terminal calmodulin-dependent protein kinase domain identified by interaction with neurexins. JOURNAL OF NEUROSCIENCE *16*, 2488-2494.

Hata, Y., Nakanishi, H., and Takai, Y. (1998). Synaptic PDZ domain-containing proteins. NEUROSCIENCE RESEARCH *32*, 1-7.

Hauser, M. A., Amalfitano, A., Kumar-Singh, R., Hauschka, S. D., and Chamberlain, J. S. (1997). Improved adenoviral vectors for gene therapy of Duchenne muscular dystrophy. Neuromuscul Disord *7*, 277-283.

Hevner, R. F., Shi, L., Justice, N., Hsueh, Y., Sheng, M., Smiga, S., Bulfone, A., Goffinet, A. M., Campagnoni, A. T., and Rubenstein, J. L. (2001). Tbr1 regulates differentiation of the preplate and layer 6. Neuron *29*, 353-366.

Hoover, K. B., and Bryant, P. J. (2000). The genetics of the protein 4.1 family: organizers of the membrane and cytoskeleton. Curr Opin Cell Biol *12*, 229-234.

Horvitz, H. R., and Sulston, J. E. (1980). Isolation and genetic characterization of cell-lineage mutants of the nematode Caenorhabditis elegans. Genetics *96*, 435-454.

Hoskins, R., Hajnal, A. F., Harp, S. A., and Kim, S. K. (1996). The C. elegans vulval induction gene lin-2 encodes a member of the MAGUK family of cell junction proteins. Development *122*, 97-111.

Hsueh, Y. P., and Sheng, M. (1999a). Regulated expression and subcellular localization of syndecan heparan sulfate proteoglycans and the syndecan-binding protein CASK/LIN-2 during rat brain development. J Neurosci *19*, 7415-7425.

Hsueh, Y. P., and Sheng, M. (1999b). Requirement of N-terminal cysteines of PSD-95 for PSD-95 multimerization and ternary complex formation, but not for binding to potassium channel Kv1.4. J Biol Chem *274*, 532-536.

Hsueh, Y. P., Wang, T. F., Yang, F. C., and Sheng, M. (2000). Nuclear translocation and transcription regulation by the membrane-associated guanylate kinase CASK/LIN-2. Nature *404*, 298-302.

Hsueh, Y. P., Yang, F. C., Kharazia, V., Naisbitt, S., Cohen, A. R., Weinberg, R. J., and Sheng, M. (1998). Direct interaction of CASK/LIN-2 and syndecan heparan sulfate proteoglycan and their overlapping distribution in neuronal synapses. J Cell Biol *142*, 139-151.

Ibraghimov-Beskrovnaya, O., Ervasti, J. M., Leveille, C. J., Slaughter, C. A., Sernett, S. W., and Campbell, K. P. (1992). Primary structure of dystrophin-associated glycoproteins linking dystrophin to the extracellular matrix. Nature *355*, 696-702.

Ichtchenko, K., Nguyen, T., and Sudhof, T. C. (1996). Structures, alternative splicing, and neurexin binding of multiple neuroligins. J Biol Chem *271*, 2676-2682.

Ide, N., Hirao, K., Hata, Y., Takeuchi, M., Irie, M., Yao, I., Deguchi, M., Toyoda, A., Nishioka, H., Mizoguchi, A., and Takai, Y. (1998). Molecular cloning and characterization of rat lin-10. Biochem Biophys Res Commun *243*, 634-638.

Im, Y. J., Lee, J. H., Park, S. H., Park, S. J., Rho, S. H., Kang, G. B., Kim, E., Eom, S. H., Sheng, M., Karthikeyan, S.*, et al.* (2003a). Crystal structure of the Shank PDZ-ligand complex reveals a class I PDZ interaction and a novel PDZ-PDZ dimerization

Im, Y. J., Park, S. H., Rho, S. H., Lee, J. H., Kang, G. B., Sheng, M., Kim, E., and Eom, S. H. (2003b). Crystal structure of GRIP1 PDZ6-peptide complex reveals the structural basis for class II PDZ target recognition and PDZ domain-mediated multimerization. J Biol Chem *278*, 8501-8507.

Irizarry, R. A., Bolstad, B. M., Collin, F., Cope, L. M., Hobbs, B., and Speed, T. P. (2003). Summaries of Affymetrix GeneChip probe level data. Nucleic Acids Res *31*, e15.

Itoh, M., Furuse, M., Morita, K., Kubota, K., Saitou, M., and Tsukita, S. (1999a). Direct binding of three tight junction-associated MAGUKs, ZO-1, ZO-2, and ZO-3, with the COOH termini of claudins. J Cell Biol *147*, 1351-1363.

Itoh, M., Morita, K., and Tsukita, S. (1999b). Characterization of ZO-2 as a MAGUK family member associated with tight as well as adherens junctions with a binding affinity to occludin and alpha catenin. JOURNAL OF BIOLOGICAL CHEMISTRY *274*, 5981-5986.

Kaech, S. M., Whitfield, C. W., and Kim, S. K. (1998). The LIN-2/LIN-7/LIN-10 complex mediates basolateral membrane localization of the C. elegans EGF receptor LET-23 in vulval epithelial cells. Cell *94*, 761-771.

Kay, B. K., Williamson, M. P., and Sudol, M. (2000). The importance of being proline: the interaction of proline-rich motifs in signaling proteins with their cognate domains. Faseb J *14*, 231-241.

Kim, E., Cho, K. O., Rothschild, A., and Sheng, M. (1996). Heteromultimerization and NMDA receptor-clustering activity of Chapsyn-110, a member if the PSD-95 family of proteins. Neuron *17*, 103-113.

Kim, E., Naisbitt, S., Hsueh, Y. P., Rao, A., Rothschild, A., Craig, A. M., and Sheng, M. (1997). GKAP, a novel synaptic protein that interacts with the guanylate kinase-like domain of the PSD-95/SAP90 family of channel clustering molecules. J Cell Biol *136*, 669-678.

Kim, E., Niethammer, M., Rothschild, A., Jan, Y., and Sheng, M. (1995). Clustering of Shaker-type K+ channels by interaction with a family of membrane-associated guanylate kinases. NATURE *378*, 85-88.

Kim, E., and Sheng, M. (2004). PDZ domain proteins of synapses. Nat Rev Neurosci *5*, 771-781.

Kim, S. K., and Horvitz, H. R. (1990). The Caenorhabditis elegans gene lin-10 is broadly expressed while required specifically for the determination of vulval cell fates. Genes Dev *4*, 357-371.

Kispert, A., and Hermann, B. G. (1993). The Brachyury gene encodes a novel DNA binding protein. Embo J *12*, 4898-4899.

Kispert, A., Koschorz, B., and Herrmann, B. G. (1995). The T protein encoded by Brachyury is a tissue-specific transcription factor. Embo J *14*, 4763-4772.

Kistner, U., Wenzel, B., Veh, R., C., C.-L., Garner, A., Appeltauer, U., Voss, B., Gundelfinger, E., and Garner, C. (1993). SAP90, a rat presynaptic protein related to the product of the Drosophila tumor suppressor gene dlg-A. JOURNAL OF BIOLOGICAL CHEMISTRY *268*, 4580-4583.

Kobayashi, J., Inai, T., and Shibata, Y. (2002). Formation of tight junction strands by expression of claudin-1 mutants in their ZO-1 binding site in MDCK cells. Histochem Cell Biol *117*, 29-39. Epub 2002 Jan 2008.

Kohu, K., Ogawa, F., and Akiyama, T. (2002). The SH3, HOOK and guanylate kinase-like domains of hDLG are important for its cytoplasmic localization. Genes Cells *7*, 707-715.

Koonin, E. V., Woods, D. F., and Bryant, P. J. (1992). dlg-R proteins: modified guanylate kinases. Nat Genet *2*, 256-257.

Kornau, H., Schenker, L., Kennedy, M., and Seeburg, P. (1995). Domain interaction between NMDA receptor subunits and the postsynaptic density protein PSD-95. SCIENCE *269*, 1737-1740.

Kornau, H., Seeburg, P., and Kennedy, M. (1997). Interaction of ion channels and receptors with PDZ domain proteins. CURRENT OPINION IN NEUROBIOLOGY *7*, 368-373.

Kortvely, E., and Gulya, K. (2004). Calmodulin, and various ways to regulate its activity. Life Sci *74*, 1065-1070.

Kuhlendahl, S., Spangenberg, O., Konrad, M., Kim, E., and Garner, C. C. (1998). Functional analysis of the guanylate kinase-like domain in the synapse-associated protein SAP97. Eur J Biochem *252*, 305-313.

Lapierre, L. A. (2000). The molecular structure of the tight junction. Adv Drug Deliv Rev *41*, 255-264.

Laprise, P., Viel, A., and Rivard, N. (2004). Human homolog of disc-large is required for adherens junction assembly and differentiation of human intestinal epithelial cells. J Biol Chem *279*, 10157-10166.

Laverty, H., and Wilson, J. (1998). Murine CASK is disrupted in a sex-linked cleft palate mouse mutant. GENOMICS *53*, 29-41.

Lee, O. K., Frese, K. K., James, J. S., Chadda, D., Chen, Z. H., Javier, R. T., and Cho, K. O. (2003). Discs-Large and Strabismus are functionally linked to plasma membrane formation. Nat Cell Biol *5*, 987-993.

Lee, S., Fan, S., Makarova, O., Straight, S., and Margolis, B. (2002). A novel and conserved protein-protein interaction domain of mammalian Lin-2/CASK binds and recruits SAP97 to the lateral surface of epithelia. Mol Cell Biol *22*, 1778-1791.

Leonard, A. S., Davare, M. A., Horne, M. C., Garner, C. C., and Hell, J. W. (1998). SAP97 is associated with the alpha-amino-3-hydroxy-5-methylisoxazole-4-propionic acid receptor GluR1 subunit. J Biol Chem *273*, 19518-19524.

Leonoudakis, D., Conti, L. R., Radeke, C. M., McGuire, L. M., and Vandenberg, C. A. (2004). A multiprotein trafficking complex composed of SAP97, CASK, Veli, and Mint1 is associated with inward rectifier Kir2 potassium channels. J Biol Chem *279*, 19051-19063.

Leonoudakis, D., Mailliard, W., Wingerd, K., Clegg, D., and Vandenberg, C. (2001). Inward rectifier potassium channel Kir2.2 is associated with synapse-associated protein SAP97. J Cell Sci *114*, 987-998.

Lin, L., Sahr, K., and Chishti, A. (1997). Identification of the mouse homologue of human discs large and rat SAP97 genes. BIOCHIMICA ET BIOPHYSICA ACTA *1362*, 1-5.

Lin, R. C., and Scheller, R. H. (2000). Mechanisms of synaptic vesicle exocytosis. Annu Rev Cell Dev Biol *16*, 19-49.

Lindsay, E. A. (2001). Chromosomal microdeletions: dissecting del22q11 syndrome. Nat Rev Genet *2*, 858-868.

Lisman, J., Schulman, H., and Cline, H. (2002). The molecular basis of CaMKII function in synaptic and behavioural memory. Nat Rev Neurosci *3*, 175-190.

Loeb, J. A. (2003). Neuregulin: an activity-dependent synaptic modulator at the neuromuscular junction. J Neurocytol *32*, 649-664.

Luck, G., Hoch, W., Hopf, C., and Blottner, D. (2000). Nitric Oxide Synthase (NOS-1) Coclustered With Agrin-Induced AChR-Specializations on Cultured Skeletal Myotubes. Mol Cell Neurosci *16*, 269-281.

Lue, R., Brandin, E., Chan, E., and Branton, D. (1996). Two independent domains of hDlg are sufficient for subcellular targeting: the PDZ1-2 conformational unit and an alternatively spliced domain. JOURNAL OF CELL BIOLOGY *135*, 1125-1137.

Lue, R., Marfatia, S., Branton, D., and Chishti, A. (1994a). Cloning and characterization of hdlg: the human homologue of the Drosophila discs large tumor suppressor binds to protein 4.1. PROCEEDINGS OF THE NATIONAL ACADEMY OF SCIENCES OF THE UNITED STATES *91*, 9818-9822.

Lue, R. A., Marfatia, S. M., Branton, D., and Chishti, A. H. (1994b). Cloning and characterization of hdlg: the human homologue of the Drosophila discs large tumor suppressor binds to protein 4.1. Proc Natl Acad Sci U S A *91*, 9818-9822.

Lumeng, C., Phelps, S., Crawford, G. E., Walden, P. D., Barald, K., and Chamberlain, J. S. (1999). Interactions between beta 2-syntrophin and a family of microtubule-associated serine/threonine kinases. Nat Neurosci *2*, 611-617.

Luo, Z., Wang, Q., Dobbins, G. C., Levy, S., Xiong, W. C., and Mei, L. (2003). Signaling complexes for postsynaptic differentiation. J Neurocytol *32*, 697-708.

MacLennan, P. A., and Edwards, R. H. (1990). Protein turnover is elevated in muscle of mdx mice in vivo. Biochem J *268*, 795-797.

Madhavan, R., and Peng, H. B. (2003). A synaptic balancing act: local and global signaling in the clustering of ACh receptors at vertebrate neuromuscular junctions. J Neurocytol *32*, 685-696.

Maeda, M., Holder, E., Lowes, B., Valent, S., and Bies, R. D. (1997). Dilated cardiomyopathy associated with deficiency of the cytoskeletal protein metavinculin. Circulation *95*, 17-20.

Marangi, P. A., Wieland, S. T., and Fuhrer, C. (2002). Laminin-1 redistributes postsynaptic proteins and requires rapsyn, tyrosine phosphorylation, and Src and Fyn to stably cluster acetylcholine receptors. J Cell Biol *157*, 883-895.

Marfatia, S., Leu, R., Branton, D., and Chishti, A. (1995). Identification of the protein 4.1 binding interface on glycophorin C and p55, a homologue of the Drosophila discs-large tumor suppressor protein. JOURNAL OF BIOLOGICAL CHEMISTRY *270*, 715-719.

Marfatia, S., Lue, R., Branton, D., and Chishti, A. (1994). In vitro binding studies suggest a membrane-associated complex between erythroid p55, protein 4.1, and glycophorin C. JOURNAL OF BIOLOGICAL CHEMISTRY *269*, 8631-8634.

Marfatia, S., Morais, C. J., Lin, L., Hough, C., Bryant, P., Stolz, L., and Chishti, A. (1996). Modular organization of the PDZ domains in the human discs-large protein suggests a mechanism for coupling PDZ domain-binding proteins to ATP and the membrane cytoskeleton. JOURNAL OF CELL BIOLOGY *135*, 753-766.

Marfatia, S. M., Byron, O., Campbell, G., Liu, S. C., and Chishti, A. H. (2000). Human homologue of the Drosophila discs large tumor suppressor protein forms an oligomer in solution. Identification of the self-association site. J Biol Chem *275*, 13759-13770.

Martinez-Estrada, O. M., Villa, A., Breviario, F., Orsenigo, F., Dejana, E., and Bazzoni, G. (2001). Association of junctional adhesion molecule with calcium/calmodulin-dependent serine protein kinase (CASK/LIN-2) in human epithelial caco-2 cells. J Biol Chem *276*, 9291-9296. Epub 2000 Dec 9218.

Martin-Padura, I., Lostaglio, S., Schneemann, M., Williams, L., Romano, M., Fruscella, P., Panzeri, C., Stoppacciaro, A., Ruco, L., Villa, A.*, et al.* (1998). Junctional adhesion molecule, a novel member of the immunoglobulin superfamily that distributes at intercellular junctions and modulates monocyte transmigration. J Cell Biol *142*, 117-127.

Matsushita, T., Oyamada, M., Fujimoto, K., Yasuda, Y., Masuda, S., Wada, Y., Oka, T., and Takamatsu, T. (1999). Remodeling of cell-cell and cell-extracellular matrix interactions at the border zone of rat myocardial infarcts. Circ Res *85*, 1046-1055.

Matter, K., and Balda, M. S. (2003a). Functional analysis of tight junctions. Methods *30*, 228-234.

Matter, K., and Balda, M. S. (2003b). Holey barrier: claudins and the regulation of brain endothelial permeability. J Cell Biol *161*, 459-460.

Matter, K., and Balda, M. S. (2003c). Signalling to and from tight junctions. Nat Rev Mol Cell Biol *4*, 225-236.

Maximov, A., Sudhof, T. C., and Bezprozvanny, I. (1999). Association of neuronal calcium channels with modular adaptor proteins. J Biol Chem *274*, 24453-24456.

Mayer, B. J. (2001). SH3 domains: complexity in moderation. J Cell Sci *114*, 1253-1263.

McCarthy, K. M., Skare, I. B., Stankewich, M. C., Furuse, M., Tsukita, S., Rogers, R. A., Lynch, R. D., and Schneeberger, E. E. (1996). Occludin is a functional component of the tight junction. J Cell Sci *109 (Pt 9)*, 2287-2298.

McConville, J., and Vincent, A. (2002). Diseases of the neuromuscular junction. Curr Opin Pharmacol *2*, 296-301.

McGee, A., and Bredt, D. (1999). Identification of an intramolecular interaction between the SH3 and guanylate kinase domains of PSD-95. JOURNAL OF BIOLOGICAL CHEMISTRY *274*, 17431-17436.

McGee, A. W., Dakoji, S. R., Olsen, O., Bredt, D. S., Lim, W. A., and Prehoda, K. E. (2001). Structure of the SH3-guanylate kinase module from PSD-95 suggests a mechanism for regulated assembly of MAGUK scaffolding proteins. Mol Cell *8*, 1291-1301.

McLaughlin, M., Hale, R., Ellston, D., Gaudet, S., Lue, R. A., and Viel, A. (2002). The distribution and function of alternatively spliced insertions in hDlg. J Biol Chem *277*, 6406-6412. Epub 2001 Nov 6426.

McMahon, L., Legouis, R., Vonesch, J. L., and Labouesse, M. (2001). Assembly of C. elegans apical junctions involves positioning and compaction by LET-413 and protein aggregation by the MAGUK protein DLG-1. J Cell Sci *114*, 2265-2277.

Meier, T., Gesemann, M., Cavalli, V., Ruegg, M. A., and Wallace, B. G. (1996). AChR phosphorylation and aggregation induced by an agrin fragment that lacks the binding domain for alpha-dystroglycan. Embo J *15*, 2625-2631.

Meier, T., and Wallace, B. G. (1998). Formation of the neuromuscular junction: molecules and mechanisms. Bioessays *20*, 819-829.

Migaud, M., Charlesworth, P., Dempster, M., Webster, L., Watabe, A., Makhinson, M., He, Y., Ramsay, M., Morris, R., Morrison, J.*, et al.* (1998). Enhanced long-term potentiation and impaired learning in mice with mutant postsynaptic density-95 protein [see comments]. NATURE *396*, 433-439.

Minguillon, C., and Logan, M. (2003). The comparative genomics of T-box genes. Brief Funct Genomic Proteomic *2*, 224-233.

Mok, H., Shin, H., Kim, S., Lee, J. R., Yoon, J., and Kim, E. (2002). Association of the kinesin superfamily motor protein KIF1Balpha with postsynaptic density-95 (PSD-95), synapse-associated protein-97, and synaptic scaffolding molecule PSD-95/discs large/zona occludens-1 proteins. J Neurosci *22*, 5253-5258.

Montanaro, F., Gee, S. H., Jacobson, C., Lindenbaum, M. H., Froehner, S. C., and Carbonetto, S. (1998). Laminin and alpha-dystroglycan mediate acetylcholine receptor aggregation via a MuSK-independent pathway. J Neurosci *18*, 1250-1260.

Morais Cabral, J. H., Petosa, C., Sutcliffe, M. J., Raza, S., Byron, O., Poy, F., Marfatia, S. M., Chishti, A. H., and Liddington, R. C. (1996). Crystal structure of a PDZ domain. Nature *382*, 649-652.

Morita, K., Furuse, M., Fujimoto, K., and Tsukita, S. (1999a). Claudin multigene family encoding four-transmembrane domain protein components of tight junction strands. Proc Natl Acad Sci U S A *96*, 511-516.

Morita, K., Sasaki, H., Furuse, M., and Tsukita, S. (1999b). Endothelial claudin: claudin-5/TMVCF constitutes tight junction strands in endothelial cells. J Cell Biol *147*, 185-194.

Muller, B., Kistner, U., Kindler, S., Chung, W., Kuhlendahl, S., Fenster, S., Lau, L., Veh, R., Huganir, R., Gundelfinger, E., and Garner, C. (1996). SAP102, a novel postsynaptic protein that interacts with NMDA receptor complexes in vivo. NEURON *17*, 255-265.

Muller, B., Kistner, U., Veh, R., C., C.-L., Becker, B., Gundelfinger, E., and Garner, C. (1995). Molecular characterization and spatial distribution of SAP97, a novel presynaptic protein homologous to SAP90 and the Drosophila discs-large tumor suppressor protein. JOURNAL OF NEUROSCIENCE *15*, 2354-2366.

Muller, C. W., and Herrmann, B. G. (1997). Crystallographic structure of the T domain-DNA complex of the Brachyury transcription factor. Nature *389*, 884-888.

Nagano, T., Jourdi, H., and Nawa, H. (1998). Emerging roles of Dlg-like PDZ proteins in the organization of the NMDA-type glutamatergic synapse. JOURNAL OF BIOCHEMISTRY *124*, 869-875.

Nahirney, P. C., and Ovalle, W. K. (1993). Distribution of dystrophin and neurofilament protein in muscle spindles of normal and Mdx-dystrophic mice: an immunocytochemical study. Anat Rec *235*, 501-510.

Naisbitt, S., Kim, E., Weinberg, R. J., Rao, A., Yang, F. C., Craig, A. M., and Sheng, M. (1997). Characterization of guanylate kinase-associated protein, a postsynaptic density protein at excitatory synapses that interacts directly with postsynaptic density-95/synapse-associated protein 90. J Neurosci *17*, 5687-5696.

Nakagawa, T., Futai, K., Lashuel, H. A., Lo, I., Okamoto, K., Walz, T., Hayashi, Y., and Sheng, M. (2004). Quaternary structure, protein dynamics, and synaptic function of SAP97 controlled by L27 domain interactions. Neuron *44*, 453-467.

Nakamura, A., Harrod, G., and Davies, K. (2001). Activation of calcineurin and stress activated protein kinase/p38-mitogen activated protein kinase in hearts of utrophin-dystrophin knockout mice. Neuromusc Disord *11*, 251-259.

Nawrotzki, R., Loh, N. Y., Ruegg, M. A., Davies, K. E., and Blake, D. J. (1998). Characterisation of alpha-dystrobrevin in muscle. J Cell Sci *111*, 2595-2605.

Niethammer, M., Kim, E., and Sheng, M. (1996). Interaction between the C terminus of NMDA receptor subunits and multiple members of the PSD-95 family of membrane-associated guanylate kinases. J Neurosci *16*, 2157-2163.

Nitkin, R. M., Smith, M. A., Magill, C., Fallon, J. R., Yao, Y. M., Wallace, B. G., and McMahan, U. J. (1987). Identification of agrin, a synaptic organizing protein from Torpedo electric organ. J Cell Biol *105*, 2471-2478.

Nitta, T., Hata, M., Gotoh, S., Seo, Y., Sasaki, H., Hashimoto, N., Furuse, M., and Tsukita, S. (2003). Size-selective loosening of the blood-brain barrier in claudin-5-deficient mice. J Cell Biol *161*, 653-660.

Nix, S. L., Chishti, A. H., Anderson, J. M., and Walther, Z. (2000). hCASK and hDlg associate in epithelia, and their src homology 3 and guanylate kinase domains participate in both intramolecular and intermolecular interactions. J Biol Chem *275*, 41192-41200.

Ohlendieck, K., Ervasti, J. M., Snook, J. B., and Campbell, K. P. (1991). Dystrophin-glycoprotein complex is highly enriched in isolated skeletal muscle sarcolemma. J Cell Biol *112*, 135-148.

Okamoto, M., and Sudhof, T. C. (1997). Mints, Munc18-interacting proteins in synaptic vesicle exocytosis. J Biol Chem *272*, 31459-31464.

Olsen, O., and Bredt, D. S. (2003). Functional analysis of the nucleotide binding domain of membrane-associated guanylate kinases. J Biol Chem *278*, 6873-6878.

Olsen, O., Liu, H., Wade, J. B., Merot, J., and Welling, P. A. (2002). Basolateral membrane expression of the Kir 2.3 channel is coordinated by PDZ interaction with Lin-7/CASK complex. Am J Physiol Cell Physiol *282*, C183-195.

Osterweil, E., Wells, D. G., and Mooseker, M. S. (2005). A role for myosin VI in postsynaptic structure and glutamate receptor endocytosis. J Cell Biol *168*, 329-338.

Paarmann, I., Spangenberg, O., Lavie, A., and Konrad, M. (2002). Formation of complexes between Ca2+.calmodulin and the synapse-associated protein SAP97 requires the SH3 domain-guanylate kinase domain-connecting HOOK region. J Biol Chem *277*, 40832-40838.

Papaioannou, V. E. (2001). T-box genes in development: from hydra to humans. Int Rev Cytol *207*, 1-70.

Papaioannou, V. E., and Silver, L. M. (1998). The T-box gene family. Bioessays *20*, 9-19.

Patton, B. L. (2003). Basal lamina and the organization of neuromuscular synapses. J Neurocytol *32*, 883-903.

Pawson, T., and Scott, J. D. (1997). Signaling through scaffold, anchoring, and adaptor proteins. Science *278*, 2075-2080.

Perez-Moreno, M., Jamora, C., and Fuchs, E. (2003). Sticky business: orchestrating cellular signals at adherens junctions. Cell *112*, 535-548.

Perriard, J. C., Hirschy, A., and Ehler, E. (2003). Dilated cardiomyopathy: a disease of the intercalated disc? Trends Cardiovasc Med *13*, 30-38.

Petralia, R. S., Wang, Y. X., and Wenthold, R. J. (2002). NMDA receptors and PSD-95 are found in attachment plaques in cerebellar granular layer glomeruli. Eur J Neurosci *15*, 583-587.

Ponting, C. P., Phillips, C., Davies, K. E., and Blake, D. J. (1997). PDZ domains: targeting signalling molecules to sub-membranous sites. Bioessays *19*, 469-479.

Porter, J. D., Khanna, S., Kaminski, H. J., Rao, J. S., Merriam, A. P., Richmonds, C. R., Leahy, P., Li, J., Guo, W., and Andrade, F. H. (2002). A chronic inflammatory response dominates the skeletal muscle molecular signature in dystrophin-deficient mdx mice. Hum Mol Genet *11*, 263-272.

Porter, J. D., Merriam, A. P., Khanna, S., Andrade, F. H., Richmonds, C. R., Leahy, P., Cheng, G., Karathanasis, P., Zhou, X., Kusner, L. L.*, et al.* (2003a). Constitutive properties, not molecular adaptations, mediate extraocular muscle sparing in dystrophic mdx mice. Faseb J *17*, 893-895.

Porter, J. D., Merriam, A. P., Leahy, P., Gong, B., Feuerman, J., Cheng, G., and Khanna, S. (2004). Temporal gene expression profiling of dystrophin-deficient (mdx) mouse diaphragm identifies conserved and muscle group-specific mechanisms in the pathogenesis of muscular dystrophy. Hum Mol Genet *13*, 257-269.

Porter, J. D., Merriam, A. P., Leahy, P., Gong, B., and Khanna, S. (2003b). Dissection of temporal gene expression signatures of affected and spared muscle groups in dystrophin-deficient (mdx) mice. Hum Mol Genet *12*, 1813-1821.

Protonotarios, N. I., Tsatsopoulou, A. A., and Gatzoulis, K. A. (2002). Arrhythmogenic right ventricular cardiomyopathy caused by a deletion in plakoglobin (Naxos disease). Card Electrophysiol Rev *6*, 72-80.

Ptacek, L. J. (1997). Channelopathies: ion channel disorders of muscle as a paradigm for paroxysmal disorders of the nervous system. Neuromuscul Disord *7*, 250-255.

Rafael, J. A., Hutchinson, T. L., Lumeng, C. N., Marfatia, S. M., Chishti, A. H., and Chamberlain, J. S. (1998a). Localization of Dlg at the mammalian neuromuscular junction. Neuroreport *9*, 2121-2125.

Rafael, J. A., Tinsley, J. M., Potter, A. C., Deconinck, A. E., and Davies, K. E. (1998b). Skeletal muscle-specific expression of a utrophin transgene rescues utrophin-dystrophin deficient mice. Nat Genet *19*, 79-82.

Rafael, J. A., Townsend, E. R., Squire, S. E., Potter, A. C., Chamberlain, J. S., and Davies, K. E. (2000). Dystrophin and utrophin influence fiber-type composition and post-synaptic membrane structure. Hum Mol Genet *9*, 1357-1367.

Rapraeger, A. C. (2000). Syndecan-regulated receptor signaling. J Cell Biol *149*, 995-998.

Rivier, F., Robert, A., Royuela, M., Hugon, G., Bonet-Kerrache, A., and Mornet, D. (1999). Utrophin and dystrophin-associated glycoproteins in normal and dystrophin deficient cardiac muscle. J Muscle Res Cell Motil *20*, 305-314.

Rongo, C., Whitfield, C. W., Rodal, A., Kim, S. K., and Kaplan, J. M. (1998). LIN-10 is a shared component of the polarized protein localization pathways in neurons and epithelia. Cell *94*, 751-759.

Ruegg, M. A., and Bixby, J. L. (1998). Agrin orchestrates synaptic differentiation at the vertebrate neuromuscular junction. Trends Neurosci *21*, 22-27.

Rumbaugh, G., Sia, G. M., Garner, C. C., and Huganir, R. L. (2003). Synapse-associated protein-97 isoform-specific regulation of surface AMPA receptors and synaptic function in cultured neurons. J Neurosci *23*, 4567-4576.

Saitou, M., Fujimoto, K., Doi, Y., Itoh, M., Fujimoto, T., Furuse, M., Takano, H., Noda, T., and Tsukita, S. (1998). Occludin-deficient embryonic stem cells can differentiate into polarized epithelial cells bearing tight junctions. J Cell Biol *141*, 397-408.

Sanes, J. R., and Lichtman, J. W. (1999). Development of the vertebrate neuromuscular junction. Annu Rev Neurosci *22*, 389-442.

Sanford, J. L., Mays, T. A., and Rafael-Fortney, J. A. (2004). CASK and Dlg form a PDZ protein complex at the mammalian neuromuscular junction. Muscle Nerve *30*, 164-171.

Sangorrin, M. P., Martone, C. B., and Sanchez, J. J. (2000). Identification of a myofibril-bound serine protease and its endogenous inhibitor in mouse skeletal muscle. Int J Biochem Cell Biol *32*, 1213-1222.

Sans, N., Racca, C., Petralia, R. S., Wang, Y. X., McCallum, J., and Wenthold, R. J. (2001). Synapse-associated protein 97 selectively associates with a subset of AMPA receptors early in their biosynthetic pathway. J Neurosci *21*, 7506-7516.

Sanyal, S. K., Johnson, W. W., Thapar, M. K., and Pitner, S. E. (1978). An ultrastructural basis for electrocardiographic alterations associated with Duchenne's progressive muscular dystrophy. Circulation *57*, 1122-1129.

Sawada, N., Murata, M., Kikuchi, K., Osanai, M., Tobioka, H., Kojima, T., and Chiba, H. (2003). Tight junctions and human diseases. Med Electron Microsc *36*, 147-156.

Schuh, K., Uldrijan, S., Gambaryan, S., Roethlein, N., and Neyses, L. (2003). Interaction of the plasma membrane Ca2+ pump 4b/CI with the Ca2+/calmodulin-dependent membrane-associated kinase CASK. J Biol Chem *278*, 9778-9783. Epub 2003 Jan 9702.

Shin, H., Hsueh, Y. P., Yang, F. C., Kim, E., and Sheng, M. (2000). An intramolecular interaction between Src homology 3 domain and guanylate kinase-like domain required for channel clustering by postsynaptic density-95/SAP90. J Neurosci *20*, 3580-3587.

Shirataki, H., Kaibuchi, K., Sakoda, T., Kishida, S., Yamaguchi, T., Wada, K., Miyazaki, M., and Takai, Y. (1993). Rabphilin-3A, a putative target protein for smg p25A/rab3A p25 small GTP-binding protein related to synaptotagmin. Mol Cell Biol *13*, 2061-2068.

Si, J., Tanowitz, M., Won, S., and Mei, L. (1998). Regulation by ARIA/neuregulin of acetylcholine receptor gene transcription at the neuromuscular junction. Life Sci *62*, 1497-1502.

Simske, J. S., Kaech, S. M., Harp, S. A., and Kim, S. K. (1996). LET-23 receptor localization by the cell junction protein LIN-7 during C. elegans vulval induction. Cell *85*, 195-204.

Sirotkin, H., Morrow, B., Saint-Jore, B., Puech, A., Das Gupta, R., Patanjali, S. R., Skoultchi, A., Weissman, S. M., and Kucherlapati, R. (1997). Identification, characterization, and precise mapping of a human gene encoding a novel membrane-spanning protein from the 22q11 region deleted in velo-cardio-facial syndrome. Genomics *42*, 245-251.

Smith, C. L., Mittaud, P., Prescott, E. D., Fuhrer, C., and Burden, S. J. (2001). Src, Fyn, and Yes are not required for neuromuscular synapse formation but are necessary for stabilization of agrin-induced clusters of acetylcholine receptors. J Neurosci *21*, 3151-3160.

Smith, M. A., Yao, Y. M., Reist, N. E., Magill, C., Wallace, B. G., and McMahan, U. J. (1987). Identification of agrin in electric organ extracts and localization of agrin-like molecules in muscle and central nervous system. J Exp Biol *132*, 223-230.

Songyang, Z., Fanning, A., Fu, C., Xu, J., Marfatia, S., Chishti, A., Crompton, A., Chan, A., Anderson, J., and Cantley, L. (1997). Recognition of unique carboxyl-terminal motifs by distinct PDZ domains. SCIENCE *275*, 73-77.

Straub, V., and Campbell, K. P. (1997). Muscular dystrophies and the dystrophin-glycoprotein complex. Curr Opin Neurol *10*, 168-175.

Strochlic, L., Cartaud, A., Labas, V., Hoch, W., Rossier, J., and Cartaud, J. (2001). MAGI-1c: a synaptic MAGUK interacting with muSK at the vertebrate neuromuscular junction. J Cell Biol *153*, 1127-1132.

Sugiyama, J. E., Glass, D. J., Yancopoulos, G. D., and Hall, Z. W. (1997). Laminin-induced acetylcholine receptor clustering: an alternative pathway. J Cell Biol *139*, 181-191.

Tabuchi, K., Biederer, T., Butz, S., and Sudhof, T. C. (2002). CASK participates in alternative tripartite complexes in which Mint 1 competes for binding with caskin 1, a novel CASK-binding protein. J Neurosci *22*, 4264-4273.

Tada, M., and Smith, J. C. (2001). T-targets: clues to understanding the functions of T-box proteins. Dev Growth Differ *43*, 1-11.

Takai, Y., Kaibuchi, K., Kikuchi, A., Sasaki, T., and Shirataki, H. (1993). Regulators of small GTPases. Ciba Found Symp *176*, 128-138; discussion 138-146.

Tavalin, S. J., Colledge, M., Hell, J. W., Langeberg, L. K., Huganir, R. L., and Scott, J. D. (2002). Regulation of GluR1 by the A-kinase anchoring protein 79 (AKAP79) signaling complex shares properties with long-term depression. J Neurosci *22*, 3044-3051.

Tavares, G. A., Panepucci, E. H., and Brunger, A. T. (2001). Structural characterization of the intramolecular interaction between the SH3 and guanylate kinase domains of PSD-95. Mol Cell *8*, 1313-1325.

Tejedor, F., Bokhari, A., Rogero, O., Gorczyca, M., Zhang, J., Kim, E., Sheng, M., and Budnik, V. (1997). Essential role for dlg in synaptic clustering of Shaker K+ channels in vivo. JOURNAL OF NEUROSCIENCE *17*, 152-159.

Thomas, U., Ebitsch, S., Gorczyca, M., Koh, Y. H., Hough, C. D., Woods, D., Gundelfinger, E. D., and Budnik, V. (2000). Synaptic targeting and localization of discs-large is a stepwise process controlled by different domains of the protein. Curr Biol *10*, 1108-1117.

Thomas, U., Kim, E., Kuhlendahl, S., Koh, Y., Gundelfinger, E., Sheng, M., Garner, C., and Budnik, V. (1997). Synaptic clustering of the cell adhesion molecule fasciclin II by discs-large and its role in the regulation of presynaptic structure. NEURON *19*, 787-799.

Tiffany, A. M., Manganas, L. N., Kim, E., Hsueh, Y. P., Sheng, M., and Trimmer, J. S. (2000). PSD-95 and SAP97 exhibit distinct mechanisms for regulating K(+) channel surface expression and clustering. J Cell Biol *148*, 147-158.

Tinsley, J. M., Potter, A. C., Phelps, S. R., Fisher, R., Trickett, J. I., and Davies, K. E. (1996). Amelioration of the dystrophic phenotype of mdx mice using a truncated utrophin transgene. Nature *384*, 349-353.

Towbin, J. A. (1998). The role of cytoskeletal proteins in cardiomyopathies. Curr Opin Cell Biol *10*, 131-139.

Towbin, J. A., and Bowles, N. E. (2002). The failing heart. Nature *415*, 227-233.

Toyo-Oka, T., Kawada, T., Nakata, J., Xie, H., Urabe, M., Masui, F., Ebisawa, T., Tezuka, A., Iwasawa, K., Nakajima, T.*, et al.* (2004). Translocation and cleavage of

myocardial dystrophin as a common pathway to advanced heart failure: a scheme for the progression of cardiac dysfunction. Proc Natl Acad Sci U S A *101*, 7381-7385. Epub 2004 May 7385.

Tracey, I., Scott, R. B., Thompson, C. H., Dunn, J. F., Barnes, P. R., Styles, P., Kemp, G. J., Rae, C. D., Pike, M., and Radda, G. K. (1995). Brain abnormalities in Duchenne muscular dystrophy: phosphorus-31 magnetic resonance spectroscopy and neuropsychological study. Lancet *345*, 1260-1264.

Traweger, A., Fuchs, R., Krizbai, I. A., Weiger, T. M., Bauer, H. C., and Bauer, H. (2003). The tight junction protein ZO-2 localizes to the nucleus and interacts with the heterogeneous nuclear ribonucleoprotein scaffold attachment factor-B. J Biol Chem *278*, 2692-2700.

Trinidad, J. C., Fischbach, G. D., and Cohen, J. B. (2000). The Agrin/MuSK signaling pathway is spatially segregated from the neuregulin/ErbB receptor signaling pathway at the neuromuscular junction. J Neurosci *20*, 8762-8770.

Tsukita, S., and Furuse, M. (2000a). Pores in the wall: claudins constitute tight junction strands containing aqueous pores. J Cell Biol *149*, 13-16.

Tsukita, S., and Furuse, M. (2000b). The structure and function of claudins, cell adhesion molecules at tight junctions. Ann N Y Acad Sci *915*, 129-135.

Tsukita, S., Furuse, M., and Itoh, M. (1997). Molecular architecture of tight junctions: occludin and ZO-1. Soc Gen Physiol Ser *52*, 69-76.

Tsukita, S., Furuse, M., and Itoh, M. (2001). Multifunctional strands in tight junctions. Nat Rev Mol Cell Biol *2*, 285-293.

Ushkaryov, Y. A., Petrenko, A. G., Geppert, M., and Sudhof, T. C. (1992). Neurexins: synaptic cell surface proteins related to the alpha-latrotoxin receptor and laminin. Science *257*, 50-56.

Wagner, K. R., Cohen, J. B., and Huganir, R. L. (1993). The 87K postsynaptic membrane protein from Torpedo is a protein- tyrosine kinase substrate homologous to dystrophin. Neuron *10*, 511-522.

Wang, G. S., Hong, C. J., Yen, T. Y., Huang, H. Y., Ou, Y., Huang, T. N., Jung, W. G., Kuo, T. Y., Sheng, M., Wang, T. F., and Hsueh, Y. P. (2004a). Transcriptional modification by a CASK-interacting nucleosome assembly protein. Neuron *42*, 113-128.

Wang, T. F., Ding, C. N., Wang, G. S., Luo, S. C., Lin, Y. L., Ruan, Y., Hevner, R., Rubenstein, J. L., and Hsueh, Y. P. (2004b). Identification of Tbr-1/CASK complex target genes in neurons. J Neurochem *91*, 1483-1492.

Wei, C. J., Xu, X., and Lo, C. W. (2004). Connexins and cell signaling in development and disease. Annu Rev Cell Dev Biol *20*, 811-838.

Wheelock, M. J., and Johnson, K. R. (2003a). Cadherin-mediated cellular signaling. Curr Opin Cell Biol *15*, 509-514.

Wheelock, M. J., and Johnson, K. R. (2003b). Cadherins as modulators of cellular phenotype. Annu Rev Cell Dev Biol *19*, 207-235.

Woods, D., and Bryant, P. (1991a). The discs-large tumor suppressor gene of Drosophila encodes a guanylate kinase homolog localized at septate junctions. CELL *66*, 451-464.

Woods, D. F., and Bryant, P. J. (1991b). The discs-large tumor suppressor gene of Drosophila encodes a guanylate kinase homolog localized at septate junctions. Cell *66*, 451-464.

Woods, D. F., Hough, C., Peel, D., Callaini, G., and Bryant, P. J. (1996). Dlg protein is required for junction structure, cell polarity, and proliferation control in Drosophila epithelia. J Cell Biol *134*, 1469-1482.

Wu, H., Reissner, C., Kuhlendahl, S., Coblentz, B., Reuver, S., Kindler, S., Gundelfinger, E. D., and Garner, C. C. (2000). Intramolecular interactions regulate SAP97 binding to GKAP. Embo J *19*, 5740-5751.

Wyszynski, M., Kim, E., Yang, F., and Sheng, M. (1998). Biochemical and immunocytochemical characterization of GRIP, a putative AMPA receptor anchoring protein, in rat brain. NEUROPHARMACOLOGY *37*, 1335-1344.

Yamniuk, A. P., and Vogel, H. J. (2004). Calmodulin's flexibility allows for promiscuity in its interactions with target proteins and peptides. Mol Biotechnol *27*, 33-57.

Yang, L., Luo, J., and Petrof, B. J. (1998). Corticosteroid therapy does not alter the threshold for contraction- induced injury in dystrophic (mdx) mouse diaphragm. Muscle Nerve *21*, 394-397.

Zhang, Y., Luan, Z., Liu, A., and Hu, G. (2001). The scaffolding protein CASK mediates the interaction between rabphilin3a and beta-neurexins. FEBS Lett *497*, 99-102.

Zhou, H., Glass, D. J., Yancopoulos, G. D., and Sanes, J. R. (1999). Distinct domains of MuSK mediate its abilities to induce and to associate with postsynaptic specializations. J Cell Biol *146*, 1133-1146.